METAMATERIAL INSPIRED RECONFIGURABLE ANTENNA FOR COGNITIVE RADIO APPLICATIONS

Thesis

Submitted in partial fulfilment of the requirements for the degree of

DOCTOR OF PHILOSOPHY

by

NAVEEN JACOB

DEPARTMENT OF ELECTRONICS & COMMUNICATION ENGINEERING
NATIONAL INSTITUTE OF TECHNOLOGY KARNATAKA,
SURATHKAL, MANGALORE – 575025, INDIA
AUGUST 2022

DECLARATION

by the Ph.D. Research Scholar

I hereby *declare* that the Research Thesis entitled **METAMATERIAL INSPIRED RECONFIGURABLE ANTENNA FOR COGNITIVE RADIO APPLICATIONS**, which is being submitted to the **National Institute of Technology Karnataka, Surathkal** in partial fulfillment of the requirements for the award of the degree of **Doctor of Philosophy** in **Department of Electronics and Communication** is *a bonafide report of the research work carried out by me*. The material contained in this thesis has not been submitted to any University or Institution for the award of any degree.

Place: NITK, Surathkal

Date : 11-08-2022

Naveen Jacob

Register No.: 177143EC008

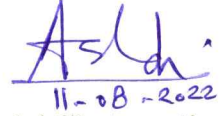Department of Electronics and Communication

CERTIFICATE

This is to *certify* that the Research Thesis entitled **METAMATERIAL INSPIRED RECONFIGURABLE ANTENNA FOR COGNITIVE RADIO APPLICATIONS**, submitted by **Naveen Jacob (Register Number: 177143EC008)** as the record of the research work carried out by him, is accepted as a *Research Thesis Submission* in partial fulfillment of the requirements for the award of degree of **Doctor of Philosophy**.

Dr. Muralidhar Kulkarni

Professor

(Research Guide)

Dept. of ECE

NITK, Surathkal

Dr. Krishnamoorthy K.

Assistant Professor

(Additional Research Guide)

Dept. of ECE

NITK, Surathkal

Dr. Ashvini Chaturvedi

11-08-2022

Professor

HOD

Dept. of ECE

NITK, Surathkal

ACKNOWLEDGEMENTS

ABSTRACT

The rapid development of electronics and wireless communication led to great demand for wireless devices that can operate at different standards, concurrently. These devices require low profile, compact, high gain antennas which can handle multiple functions simultaneously. Reconfigurable antennas integrated with electromagnetic metamaterial structures is a promising solution for the above requirement.

A miniaturized multiband reconfigurable Artificial Magnetic Conductor (AMC) unit cell, a zero phase reflection metasurface and a phase gradient metasurface are designed to integrate with the antenna for improving the gain and achieving beam steerability.

Antennas designed for Cognitive Radio (CR) services requires switching between Ultra-Wide Band (UWB) response and multiple Narrow Band (NB) responses for the purpose of "spectrum sensing" and "communicating" respectively. Focusing on this requirement a frequency reconfigurable circular monopole antenna is designed which can switch and fine tune between UWB response and several number of NB responses.

Modern wireless devices that operates on different communication standards requires, change in data rate, depending upon the requirement of application. This demands the antenna to be capable of tuning its bandwidth. Focusing on this requirement a bandwidth reconfigurable antenna is designed by integrating the metamaterial structure, complementary split ring (CSRR) with the antenna. Circular polarization with switchable polarization sense of LHCP and RHCP, is also implemented in the designed antenna. Radiation pattern reconfigurability, with a good beam steering angle is also achieved for the designed antenna by integrating phase gradient metasurface.

Designed antenna is fabricated and tested in an anechoic chamber. Its measured parameters are compared with existing designs in the literature to showcase the improved performance exhibited by the designed antenna.

Keywords: Reconfigurable Antenna, Metamaterial, Metasurface, Artificial Magnetic Conductor, Frequency Reconfigurable, Bandwidth Reconfigurable, Circular Polarization, Beam Steering, Split Ring Resonator, Inter-digital Capacitor.

TABLE OF CONTENTS

LIST OF FIGURES

LIST OF TABLES

ABBREVIATIONS

MPA	Microstrip Patch Antenna
MTM	Metamaterial
PEC	Perfect Electric Conductor
PMC	Perfect Magnetic Conductor
AMC	Artificial Magnetic Conductor
EBG	Electromagnetic Band Gap
FSS	Frequency Selective Surface
HIS	High Impedance Surface
UWB	Ultra Wide Band
NB	Narrow Band
IDC	Inter-Digital Capacitor
CP	Circular Polarization
LHCP	Left Hand Circular Polarization
RHCP	Right Hand Circular Polarization
ARBW	Axial Ratio Band Width
SRR	Split Ring Resonator
CSRR	Complementary Split Ring Resonator

CHAPTER 1

INTRODUCTION

It is stated that "any communication system is as good as its antenna". The rapid development of electronics and wireless communication led to great demand for wireless devices that can operate at different standards including, GSM, WiFi, Long Term Evolution (LTE), WiMAX, Cognitive Radio Networks, WLAN, Satellite communication etc. An antenna being an integral part of these devices plays an important role in defining their performance. Among various kinds of antennas, printed antennas like Microstrip Patch Antenna (MPA), received considerable attention due to their low profile nature, small size, ease of fabrication and integration with associated electronics. Various methods for MPA miniaturization and performance improvement have been reported in literature out of which, the method of using metamaterial structures gained major attention, due its better performance. The word "Meta" is taken from Greek, meaning "beyond". Metamaterial are artificial materials synthesized by embedding periodic metallic patterns on dielectric substrate of the MPA, thereby obtaining properties beyond the natural occurring materials. MPA design using metamaterial structures along with reconfigurability features, will provide additional control over frequency, bandwidth, polarization, gain, radiation performance and miniaturization of antenna.

1.1 Wireless Communication & Cognitive Radio

The term wireless communication was introduced in the 19th century. Later it has developed as a technology, in which the data or information can be transmitted from one point to other, without using any connection like wires, cables or any other physical medium. Transmission and reception of information signals without any physical medium are realized using antennas. Antennas are electrical devices that transform the electrical signals to radio signals in the form of Electromagnetic (EM) Waves and vice

versa. These electromagnetic waves propagates through space. Hence, both transmitter and receiver requires an antenna. The primary and important benefit of wireless communication is mobility. Also, the infrastructure for wireless communication can be installed easily and low cost. In emergency situations and remote locations, where the setup of wired communication is difficult, wireless communication is a feasible option.

Even though antenna plays a key role in the wireless communication scenario, one of its limitation is that, the characteristics of an antenna designed for a particular application is fixed and cannot be used for another application standard. There is a continuous demand for wireless devices that can adapt to different channel characteristics and can be tuned to operate at different communication standards with varying data rates, depending upon the requirement. Devices designed for applications such as cognitive radio, satellite / space communication, biomedical application, etc., requires low profile, compact, high gain antennas which can handle multiple functions simultaneously. Reconfigurable antenna is a promising solution for the above requirement [[37], Hamid Boudaghi et al. (2012)].

Due to the exploding demand of smart phones, the information and communication technology industry is today facing global challenge related to scarcity in spectral domain. This will affect other wireless devices also in near future. In this scenario, Cognitive Radio (CR) concept is anticipated to improve the spectrum usage efficiency.
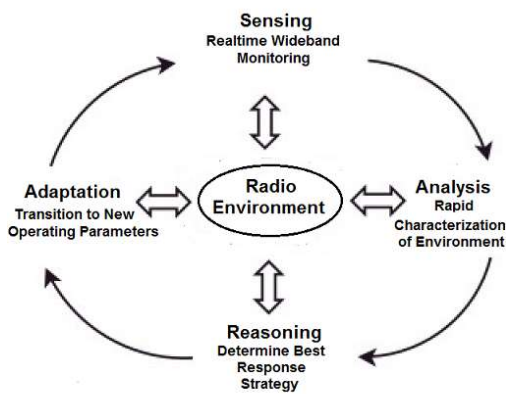
Fig. 1.1. Functions of Cognitive Radio
(S. Parvin et al. (2012))
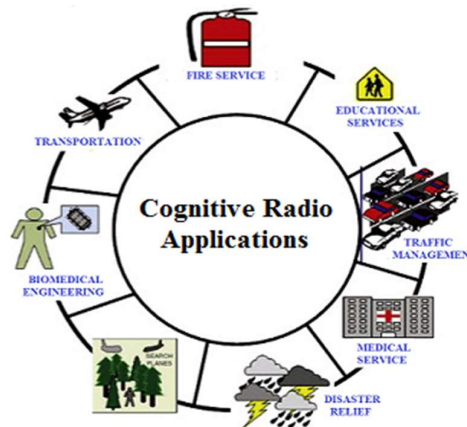
Fig. 1.2. Applications of Cognitive Radio
(S. Parvin et al. (2012))

The term cognitive radio is derived from "cognition", which refers to the mental process involved in thinking, understanding, remembering, judging and problem-solving. CR have features like estimation of channel interference, channel capacity prediction, dynamic frequency allocation, adaptive modulation, transmit power control, location awareness, frequency agility etc. CR, intelligently identifies unused radio spectrum and deploys dynamic resource sharing between primary and secondary users through frequency hopping, facilitated by the attached tunable antenna, resulting in reduced congestion and efficient utilization of the spectrum. Cognitive Radio can determine its location, change frequency, adjust output power or even alter transmission parameters and characteristics, resulting in efficient and comprehensive use of the spectrum [[32], G. P. Jin et al. (2011)].

1.2 Motivation & Problem Definition

In modern wireless communication system, different applications with pre-assigned operating frequency bands are integrated to a single system. This requires design and integration of multiple antennas with different operating bands, polarization and radiation pattern diversity on the same device, which results in the increase of complexity, size and cost. Hence the design of single antenna with multi-functional capability which can exhibit different characteristics, as per the requirement, has received lot of research attention.

From the literature review, we understood that, reconfigurable microstrip antennas are highly accredited solution for this problem and are extensively investigated during last decade. One of the major application of reconfigurable antenna is in Cognitive Radio (CR) system, which provides a prospective solution for spectrum underutilization problem. A CR requires a "sensing antenna", which must have wide band response to scan full spectrum in order to identify the unused frequency bands and should be able to select and switch over to numerous narrow band "communicating antennas", on the fly, to operate at specific frequency bands. Hence, the antenna design requires the integration of all the above features into a single compact microstrip antenna.

The existing literature presents various designs in line with these demands, but our extensive survey shows that certain gaps need to be filled. There still exists a

requirement for simple and compact antenna structures, having considerable gain and radiation diversity that could provide these features and those that could be easily reconfigured as per need. In view of this, we try to use the current state of art technology for optimization and fabrication of various designs that can meet these demands appropriately

1.3 Research Gaps

1) Artificial Magnetic Conductor (AMC) structures, having multiple zero phase-frequency reflections, can be used along with multiband antenna, for improving the antenna performance. Miniaturized AMC unit cell with more than three closely spaced, zero phase-frequency reflections within the S and C bands are not reported in the literature. The reason is that, as more no. of resonant frequencies in higher frequency region are shifted to low frequency region, size of the unit cell increases. In addition to this, independent electrical reconfigurability of the individual reflection phase bands also has to be achieved, in order to use the unit cell with the antenna designed for cognitive radio applications.

2) Conventional cognitive radio services uses multiple antenna or multiport antenna to switch between Ultra Wide Band (UWB) and Narrow Band (NB) responses for the purpose of "spectrum sensing" and "communicating" respectively, which results in increase of size and complexity of antenna. To reduce the size and complexity, single port reconfigurable antennas have to be designed and switched, to achieve both UWB as well as NB response. The single port antennas mentioned in literature are not compact and also has limited range of tuning for NB responses.

3) Bandwidth tuning capability of individual NB responses is essential for the antennas used for cognitive radio services. This is because, when there is a need to adjust the data rate due to a change in application or communication environment, the bandwidth of the antenna has to be varied on the fly, without altering the center frequency. Bandwidth reconfigurable antennas given in the literature has limited tunability, since tuning is carried out on either upper band limit or lower band limit.

1.4 Research Objectives

The objectives of the research work formulated after rigorous literature review and identifying the research gaps, are presented below:

1. Design and fabricate a miniaturized reconfigurable Artificial Magnetic Conductor (AMC) unit cell, which can provide zero reflection phase at multi band resonant frequencies.

2. Design and fabricate a low profile frequency reconfigurable microstrip patch antenna, which can switch between ultra-wide band and narrow band frequencies, with minimum number of switching elements, suitable for cognitive radio services.

3. Design and fabricate a bandwidth reconfigurable microstrip patch antenna which can tune the bandwidth of individual narrow band frequencies used for communication in cognitive radio services.

4. Integrate the AMC structure with the microstrip antenna used for cognitive radio services and study the performance improvement in gain and radiation characteristics of antenna.

1.5 Methodology

Looking towards the best possible means for realization of our objectives, it could be found that the upcoming technology of metamaterials / metasurfaces, artificial magnetic conductors, interdigital capacitors etc. can be integrated with the already existent antenna technology, could prove to be the most appropriate solution for developing designs that meet our aforementioned demands. In addition to this, PIN diodes and discrete capacitors/varactor diodes can be incorporated with antenna to achieve reconfigurability. The preliminary works are carried out using CST Studio Suite 2016.

1.6 Organization of the Thesis

The aim of this thesis is to design and implement an electronically reconfigurable microstrip patch antenna using the magical properties of metamaterials and metasurfaces. The thesis is organized in to several chapters, beginning in the first

chapter with an introduction, which comprises of motivation of this research work, problem definition and research objectives based on the research gaps identified from the extensive literature survey.

The beginning of second chapter discusses the basic concepts on microstrip patch antenna, its characteristics and parameters. It also elaborates on the basics of metamaterial/metasurfaces, and its application in antenna engineering. This is followed by an extensive literature survey on different types of antennas, metamaterial designs and various techniques introduced for its performance enhancement.

In the third chapter, design of multiband, AMC unit cell and metasurfaces are discussed, which can be integrated with patch antenna to improve its performance.

The fourth chapter discusses the design, fabrication and testing of an electronically tunable frequency reconfigurable patch antenna.

The fifth chapter provides the details on the design, fabrication and testing of an electronically tunable bandwidth and polarization reconfigurable patch antenna.

Sixth chapter, demonstrates the gain enhancement and beam steering capability of antenna using phase gradient metasurface.

Seventh chapter concludes the thesis by providing brief description on the research contributions and scope for the future research work.

CHAPTER 2

BACKGROUND AND LITERATURE SURVEY

2.1 Microstrip Patch Antenna

Microstrip patch antennas are low profile, simple and inexpensive to manufacture using modern printed-circuit technology. In addition to this, by integrating PIN and varactor diodes, frequency, polarization, and pattern reconfigurability can be achieved. Major operational disadvantages of microstrip antennas are their low efficiency, low power, high Q, poor polarization purity, poor scan performance, spurious feed radiation and very narrow bandwidth. However, there are methods, such as increasing the height of the substrate, which can be used to extend the efficiency and bandwidth. However, as the height increases, surface waves are introduced, which travel within the substrate, and are not desirable because they extract power from the total available radiation and degrade the antenna pattern and polarization performance.

Another very important aspect in microstrip antenna designs is to miniaturize the size of the antenna. This can be achieved simply by increasing the dielectric constant of the substrate. But this will result in excitation of strong surface waves in the substrate. The antennas on the high dielectric constant substrates exhibit lower directivities and higher back radiation lobes because the surface waves diffract at the edges of the ground plane resulting in end-fire radiation and back scattering, and hence performing poor radiation efficiency. Surface waves can be eliminated, while maintaining large bandwidths, by inserting artificial magnetic conductors (AMC) or otherwise called electromagnetic band gap structures (EBG). Microstrip patch antenna with patch width (W), patch length (L), is shown in Fig. 2.1. [[18], Constantine A. Balanis (2005)]
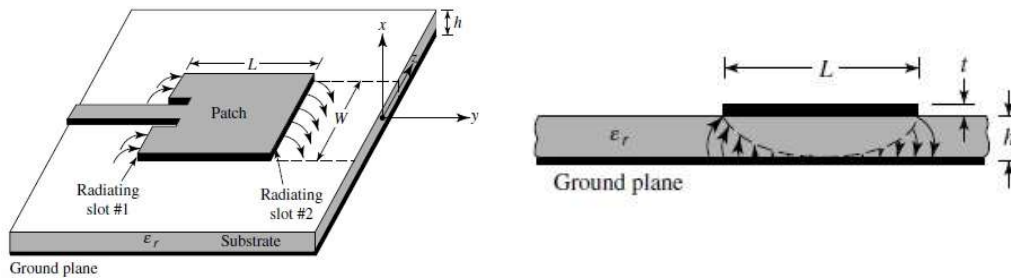
Fig. 2.1. Microstrip Patch Antenna – a) Top view b) Side View (C. A. Balanis (2005))

2.2 Reconfigurable Antenna

Rapid development in the area of modern wireless communication systems has led to demand for reconfigurable antennas to be used in various wireless services. Reconfigurability of an antenna refers to the capacity to adapt to the antenna characteristics in terms of resonant frequency, bandwidth, radiation pattern, polarization etc. A frequency reconfigurable antenna is the most practically feasible option for switching its operation to the desired frequency, instead of utilizing a number of antennas operating in different frequencies for signal transmission or reception, which reduces space and cost. Bandwidth reconfigurable antennas are useful in applications which needs a change in bandwidth according to the varying data rate. Pattern reconfigurable antennas is useful in applications such as surveillance and tracking because they produce more than one radiation pattern with different directivity at the same operating frequency. In addition, manipulation of patterns is useful in avoiding noise sources, mitigating electronic jamming, improving security and increasing energy efficiency. The polarization reconfigurable antennas can switch the polarization characteristics of the antenna between various linear polarizations, right-hand circular polarization (RHCP), left-hand circular polarization (LHCP) etc. Different types of switching techniques used in implementing reconfigurable antennas are classified as below:

- ❖ **Electrical reconfiguration:**- uses active elements such as PIN diodes, varactor diodes, Radio Frequency Micro-Electro-Mechanical System (RFMEMS) switches, etc.
- ❖ **Optical reconfiguration:**- relies on photoconductive switching elements.

8

- ❖ **Mechanical reconfiguration:-** by altering the structure of the antenna, physically.
- ❖ **Reconfigurable antennas with smart materials:-** using smart substrate materials in the antenna configuration, whose permittivity and permeability can be varied by applied voltage, induced magnetic field, optical excitation, and even thermal change, for tuning the antenna characteristics.

Metamaterials (MTMs) have emerged out as a nice solution for the miniaturization of these traditional planar antennas. It is proved that, Split Ring Resonators (SRR), Complementary Split Ring Resonators (CSRR), Inter-digital Capacitors (IDC), etc. have showed similar properties as that of MTMs. Currently, these novel MTM structures are being widely used with microstrip antennas to alter their natural characteristics.

2.3 Metamaterials

Metamaterials (MTM) are artificially structured materials, with properties not found in nature that are designed to interact with and control electromagnetic waves. It is well known that the response of a system to the presence of an electromagnetic field is determined to a large extent by permittivity ε and permeability μ of these materials. This allows for the classification of a medium as shown in Fig. 2.2. [[67], Nader Engheta et al. (2006)].
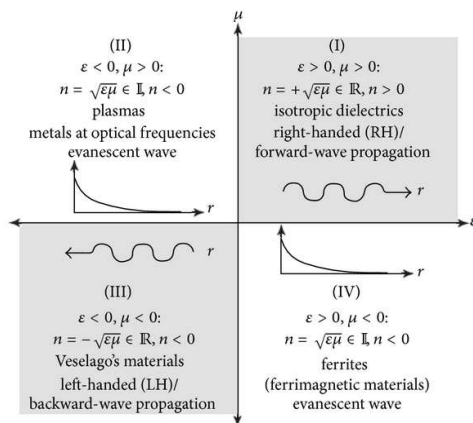
Fig. 2.2. Material Classification (Caloz & Itoh (2005))
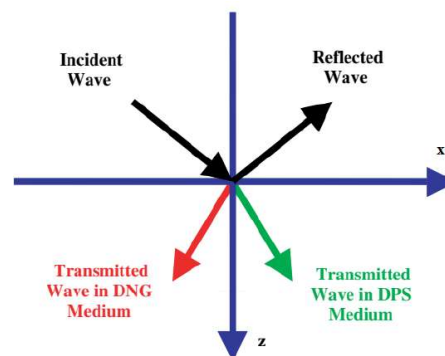
Fig. 2.3. Scattering of a wave on a DPS–DNG interface (N. Engheta & R. W. Ziolkowski (2006))

It is to be noted that, depending upon the value of ε and μ the materials are classified into Double-Positive (DPS), Epsilon-Negative (ENG), Double-Negative (DNG) and Mu-Negative (MNG) medium. DNG medium, is not found in nature and hence, this class of materials has only been demonstrated with artificial constructs. In optics and microwave engineering, metamaterials are often called as "Artificial magnetic Conductors" (AMC) or "Electromagnetic Band Gap" (EBG). Geometry of the scattering of a wave obliquely incident upon a DPS–DNG interface is shown in Fig. 2.3. The index of refraction of a DNG metamaterial has been shown theoretically to be negative by several researchers. Note that if the index of refraction of a medium is negative, then the refracted angle, according to Snell's law, should also become "negative." This suggests that the refraction is anomalous, and the refracted angle is on the same side of the interface normal, as the incident angle is. This shows that the DNG medium has a backward nature of wave propagation.

2.4 Split Ring Resonators & Complementary Split Ring Resonators

The Split Ring Resonator (SRR) is a metamaterial whose electrical performance can be well-reproduced by an LC circuit. SRR behaves as a resonant magnetic dipole that can be excited by an axial magnetic field, which in turn induce currents oscillating between the two rings of the SRR, resulting in resonance and prohibits signal propagation to obtain stop band at that frequency. It is also possible to synthesize the electrical counterpart of the SRR, called Complementary Split Ring Resonator (CSRR), by etching its negative image on a substrate.
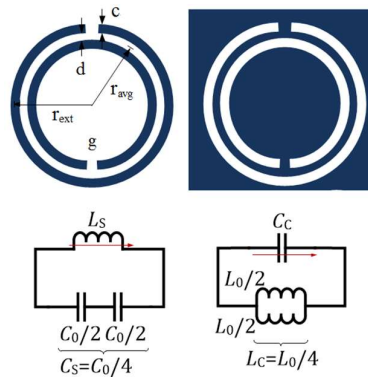
Fig. 2.4. Circular SRR and CSRR, with their equivalent circuits

(J. D. Baena et al. (2005))

The CSRR behaves as an electric dipole that can be excited by an axial electric field to obtain stop band at designed frequency. Circular SRR and CSRR along with their equivalent circuits are shown in Fig. 2.4 [[40], J. D. Baena et al. 2005].

The resonant frequency of SRR is given by : $f_{SRR} = 1 / 2\pi\sqrt{Ls\,Cs}$ (2.1)

It follows from duality that, equivalent values of inductance and capacitance of CSRR can be calculated using the design equations of SRR of same dimensions.

The resonant frequency of SRR is given by : $f_{CSRR} = 1 / 2\pi\sqrt{Lc\,Cc}$ (2.2)

2.5 Inter-digital Capacitors (IDC)

The interdigital capacitor (IDC) is a multi-finger periodic structure and it uses lumped circuit elements for RF/microwave development. The interdigital capacitors use the capacitance that occurs across a narrow gap between copper conductors. These gaps are essentially very long and folded to use a small amount of area.
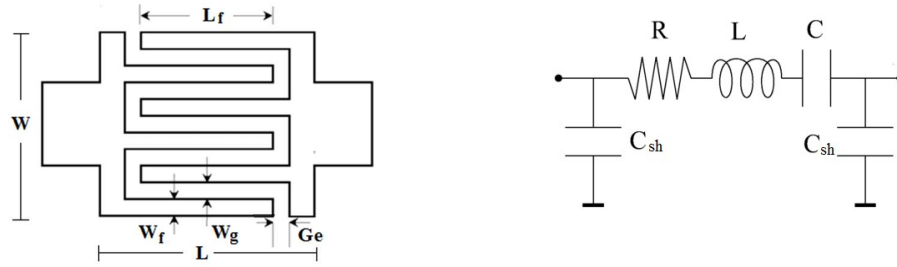
Fig. 2.5. Structure of inter-digital capacitor with equivalent circuit
(Francisco P. Casares-Miranda et al.(2005))

The structure of an interdigital capacitor is designed using copper as conducting material, along with its equivalent circuit is shown in Fig. 2.5. The length of the finger (L_f), width of the finger (w_f), gap width between the fingers (w_g) and gap at the end finger (Ge) are specified and the conductor is mounted on a substrate. The overall length of the IDC is L and width is W. The characteristic of substrate will also affect the performance of IDC.

The equation for capacitance of interdigital capacitor shown in Fig. 2.5, is given by,

$$C = \left[\frac{\varepsilon_r + 1}{W}\right] L[(N-3)A_1 + A_2)] \text{ pF/unit length}$$ (2.3)

where, ε_r is the dielectric constant of the material, N is the no. of fingers, L is the length of the finger and W is the width of the interdigital capacitor. [Gary D. Alley (1979)]

11

A1 and A2 are given by,

$$A_1 = 4.409 \tanh\left[0.55\left(\frac{h}{w_f}\right)^{-0.45} \right] \times 10^{-6} \text{ (pF/}\mu\text{m)} \tag{2.4}$$

$$A_2 = 9.92 \tanh\left[0.52\left(\frac{h}{w_f}\right)^{-0.5} \right] \times 10^{-6} \text{ (pF/}\mu\text{m)} \tag{2.5}$$

where, h is the height of substrate and w_f is the finger width of interdigital capacitor. [Beeresha R. S. et al. (2016)].

2.6 Artificial Magnetic Conductors or Electromagnetic Band Gap Structures

The design of Artificial Magnetic Conductor (AMC) or otherwise known as Electromagnetic Band Gap (EBG) metasurface, has become an area of interest over the past few years. They are periodically patterned, tailored conducting patches, placed on the top of a dielectric substrate backed by conducting ground plane. They can assist or prohibit the propagation of electromagnetic waves for specific bands of frequency of the incident plane wave, and hence they are also called Frequency Selective Surfaces (FSS). [Dan Sievenpiper et al. (1999)]

AMC structures can be designed with or without conducting via to ground. Since perfect magnetic conductors are not available in nature, we go for AMC. When AMC is illuminated by a normal plane wave, its reflection phase crosses through 0° at resonant frequency thereby exhibiting a reflection coefficient $\Gamma = +1$, as opposed to that of a perfect electric conductor which has $\Gamma = -1$. This leads to constructive interference of incident and reflected wave, causing increase in radiation intensity for low profile antennas. The bandwidth is defined over a frequency range corresponding to reflection coefficient for which phase is between $\pm 90^o$. In addition to the above property, the surface impedance of AMC structure is very high in the operating band which prohibits unwanted surface wave, thereby achieving better radiation pattern. Due to this property they are also called High Impedance Surfaces (HIS).

One of the major operational disadvantages of microstrip antenna is the use of metallic sheets as reflectors or conventional ground planes for increasing the gain of antennas

by pre-directing half of the radiation into the opposite direction and partially shield objects located on the other side. Unfortunately, reflectors as good conducting surfaces reverse the phase of impinging electromagnetic waves. If a plane wave is normally impinged upon a ground plane which is a perfect electric conductor (PEC), then the PEC will give 180^0 phase shift. Hence, in order to get 0^0 phase shift for constructive interference, the antenna needs to be placed at the distance one-quarter wavelength ($\lambda/4$) from the reflector, as shown in Fig. 2.6. This increases the size of the antenna.

Solution for the above problem is to use a perfect magnetic conductor (PMC) as reflection plane so that the reflection phase is 0^0 resulting in constructive interference. Research on EBG structures reveals that they can realize the PMC condition in a certain frequency band to ensure the constructive interference between the incident and reflected waves. This allows the antenna to be placed at a distance $\ll \lambda/4$ from the reflector, resulting in reduction of overall size of the antenna. Thus, they are sometimes referred to as artificial magnetic conductors (AMC), as shown in Fig. 2.7.
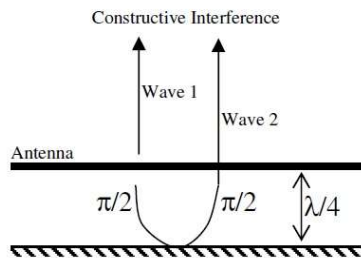
Fig. 2.6. Antenna backed by PEC ground
(D. F. Sievenpiper (1999))
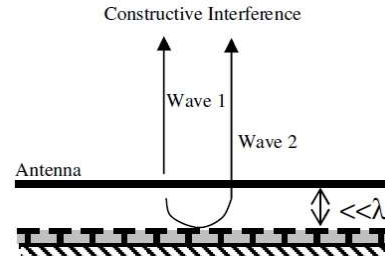
Fig. 2.7. Antenna backed by AMC surface
(D. F. Sievenpiper (1999))

The second disadvantage is that, if an antenna is placed near a conductive sheet, surface wave will propagates along the sheet resulting in reduction of antenna efficiency. The problem can be mitigated by incorporating the EBG structures which inhibits the passage of electromagnetic wave at certain angles of incidence at some specific frequency band.

2.6.1 Sievenpiper EBG Model with lumped LC elements

The Sievenpiper mushroom structure EBG has been widely studied in the microwave engineering field due to its unique properties. It basically consists of a metallic patch

connected to ground with a shorting post, as shown in Fig. 2.8 and the equivalent LC model is shown in Fig. 2.9. [Dan Sievenpiper et al. (1999)].
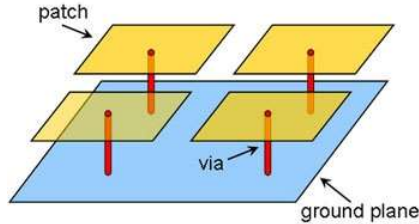
Fig. 2.8. 2X2 array of mushroom type EBG unit cells
(O. Borazjani et al. (2020))
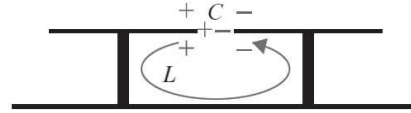
Fig. 2.9. EBG – Equivalent LC Model
(N. Engheta (2006))

The capacitor results from the gap between the patches and the inductor results from the current along adjacent patches. The impedance of a parallel resonant LC circuit is given by:

$$Z = \frac{j\omega L}{1 - \omega^2 LC} \tag{2.6}$$

The resonant frequency of the circuit is calculated as following:

$$\omega_0 = \frac{1}{\sqrt{LC}} \tag{2.7}$$

At low frequencies, the impedance is inductive and supports TM surface waves. It becomes capacitive at high frequencies and TE surface waves are supported. Near the resonance frequency ω_0, high impedance is obtained and the EBG does not support any surface waves, resulting in a frequency band gap.

2.6.2 EBG Reflection Phase: Normal incidence

Reflection coefficient is defined as the ratio of the reflected field over the incident field at the reflecting surface. The reflection phase of an EBG structure is a function of frequency, as shown in Fig.2.10. It varies continuously from 180◦ to −180◦ as frequency increases. [Fan Yang & Rahmat Samii (2009)].
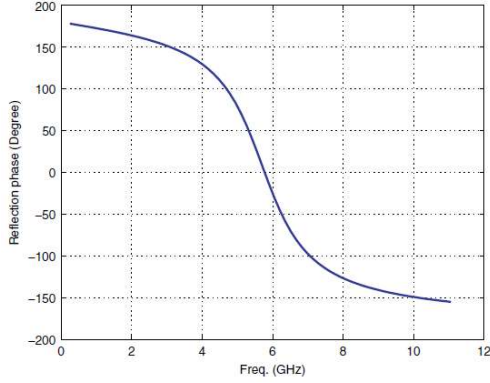
Fig. 2.10. Reflection phase plot of the mushroom-like EBG

(D. Sievenpiper (1999)

As shown in the figure, at frequencies around 5.74 GHz, the EBG surface exhibits a reflection phase close to 0^0, which resembles a PMC surface. Bandwidth of AMC unit cell is defined as rage of frequencies between $+90^0$ to -90^0 reflection phase.

2.6.3 AMC Metasurface

Metasurfaces are two-dimensional (2D) metamaterials, which have extraordinary flexibility in tailoring the electromagnetic (EM) waves. If the 2D metamaterial array is formed by employing the AMC unit cell elements with zero reflection phase at a selected frequency, then a zero phase metasurface is obtained. This metasurface can be used as a reflecting surface for the antenna radiation to increase the gain of the antenna. If the AMC unit cell is arranged in an array and its reflection phase is programmed as a function of position across the surface, then a phase gradient metasurface is obtained. A linear phase gradient $(\mathrm{d}\phi/\mathrm{dx})$ will reflect a normally incident microwave beam to an angle θr that depends on the magnitude of the gradient, given by the equation 2.8.

$$\theta_r = \mathrm{Sin}^{-1}\left(\frac{\lambda}{2\pi}\frac{\mathrm{d}\phi}{\mathrm{dx}}\right) \tag{2.8}$$

where, θr is reflected angel of beam, λ is the wavelength and $(\mathrm{d}\phi/\mathrm{dx})$ is the linear phase gradient along the metasurface in x direction. Among the above mentioned types of metasurfaces, phase gradient metasurface have drawn substantial attentions for the excellent capability of beam steering.

An electrically tunable impedance surface can be built by connecting neighboring cells with PIN diodes or varactor diodes. By individually addressing each cell, the reflection

15

phase can be programmed as a function of position across the surface, which will result in tilting of beam at an angle θr, as shown in Fig. 2.11 and Fig. 2.12 [Engheta and Ziolkowski (2006)].
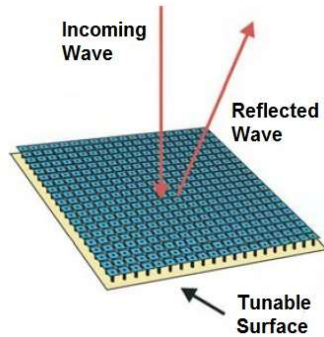
Fig. 2.11. Phase Gradient Metasurface

(N. Engheta (2006))
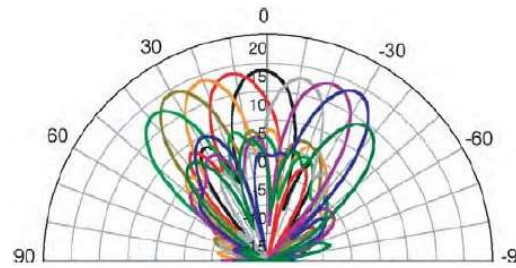
Fig. 2.12. Beam Steering

(N. Engheta (2006))

2.7 Circular Polarization

The polarization of an antenna refers to the orientation of the electric field with respect to the wave propagation direction and is determined by the structure and orientation of the antenna. Polarization may be classified into linear, circular and elliptical polarization. A wave is linearly polarized (LP) if its electric-field (or magnetic-field) vector is always oriented along the same straight line at every instant of time. This is accomplished if the field vector (electric or magnetic) possesses only one component or two orthogonal linear components, which are in-phase.

A wave is circularly polarized if the electric (or magnetic) field vector traces a circle as a function of time, shown in Fig. 2.13. The necessary and sufficient conditions to accomplish this are,

a) The field must have two orthogonal linear components, and
b) The two components must have the same magnitude, and
c) The two components must have a time-phase difference of odd multiples of 90^0.

The sense of rotation is always determined by observing the field rotation as the wave is viewed as it travels away from the observer. If the rotation is clockwise, the wave is

right-hand circularly polarized (RHCP) and if the rotation is counterclockwise, the wave is left-hand circularly polarized (LHCP).
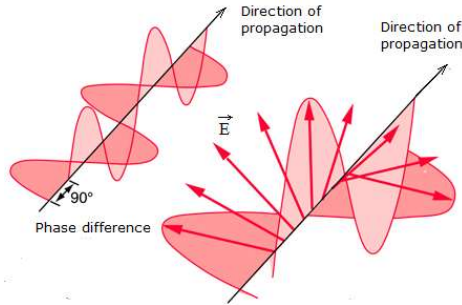
Fig. 2.13. Circular Polarization   **Fig. 2.14.** Polarization Ellipse
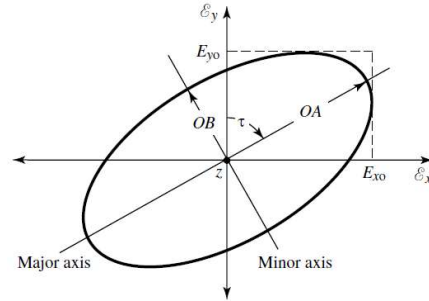
A wave is elliptically polarized if the tip of the field vector (electric or magnetic) traces an elliptical locus in space. For this, the necessary and sufficient conditions to be possessed by the field vector (electric or magnetic) are given below:

a) The field must have two orthogonal linear components, and

b) The two components can be of the same or different magnitude. If the two components are of different magnitude, the time-phase difference between the two components must not be 0^0 or multiples of 180^0 (otherwise it will become linear). If the two components are of the same magnitude, the time-phase difference between the two components must not be odd multiples of 90^0 (otherwise it will become circular).

Axial Ratio (AR) is the parameter used to measure polarization. It is the ratio of the major axis to the minor axis, shown in Fig. 2.14.

$$AR = \frac{\text{Major Axis}}{\text{Minor Axis}} = \frac{OA}{OB} \quad ; \qquad 1 \leq AR \leq \infty \qquad (2.9)$$

AR is between 1 to ∞, and it is also expressed in dB scale. A perfectly circularly polarized wave have a 0 dB axial ratio. Since it is impractical to achieve 0 dB circular polarization, the range of frequencies over which the AR < 3 dB is considered for the radiation to be circularly polarized.

The polarization of each antenna in a system should be properly aligned. Maximum signal strength between stations occurs when both stations are using identical polarization. Circularly polarized antennas shows better performance in reducing signal loss due to polarization mismatch.

17

2.8 PIN Diode Switches

A PIN diode is a diode with a wide, undoped intrinsic semiconductor region between heavily doped p-type and n-type semiconductor region. When the diode is forward biased, the injected carrier concentration is typically several orders of magnitude higher than the intrinsic carrier concentration, resulting in faster operation, suitable at high frequencies. Under reverse-bias (the "OFF" state), a PIN diode has a low capacitance which will not pass much of an RF signal. Under a forward bias (the "ON" state), a typical PIN diode will have an RF resistance of about 2 to 5 ohms, making it a good RF conductor, along with high switching speed. PIN diodes are useful as RF switches, attenuators, photodetectors, and phase shifters. A typical surface mount PIN diode is MADP-000907-14020W (Solderable AlGaAs Flip Chip PIN Diode), supplied by MACOM Technology Solutions, and is shown in Fig. 2.15 and equivalent circuit model is shown in Fig. 2.16.
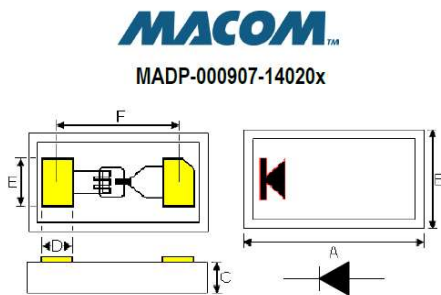
Fig. 2.15. PIN Diode - MADP-000907-14020x
(MACOM PIN Diode Datasheet)
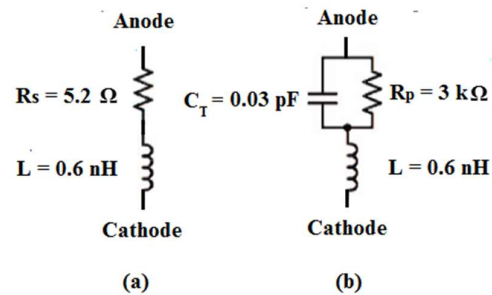
Fig. 2.16. Equivalent Circuit of PIN Diode
(B. Majumder et al. (2017)

Features:

- Lower Series resistance : 5.2 Ω
- Lower Capacitance : 0.03 pF
- Switching Speed : 2 ns
- Frequency Range : Up to 70 GHz
- Forward voltage : 1.3 V

All the antenna designs are fabricated using LPKF S103 Protomat Fabrication machine. The S-parameters are measured and analyzed using E8363C PNA Microwave Network Analyzer. The radiation pattern, axial ratio and gain parameters are measured using

measurement set-up, placed inside the anechoic chamber in the RF Circuits & Systems Laboratory.

2.9 Literature Survey

In the first section, we review the previous works carried out in the area of metamaterial based antennas. Second section details on recent works carried out in Artificial Magnetic Conductors (AMC) and the different techniques used to achieve multiband zero-phase reflection responses, their advantages and setbacks and how the designs have evolved over time. In the third and fourth sections, we discuss the previous works carried out in the implementation of frequency and bandwidth reconfigurable antennas that can switch between ultra-wide band (UWB) and multiple narrow-band (NB) frequencies, used for cognitive radio applications. Also, some earlier work are discussed, related to reconfigurable antennas integrated with metamaterial/AMC cells to obtain considerable gain and radiation diversity for the antenna depending upon the applications.

2.9.1 Metamaterial Based Antennas

This section discusses some techniques to design a Microstrip Patch Antenna using metamaterial for better performances, offered by various researchers.

- ❖ *N. Engheta and R.W. Ziolkowski* [2006] presented the research advances associated with diverse set of metamaterials in their book titled, "Metamaterials : Physics and Engineering"
- ❖ *Yahya Rahmat-Samii* [2006] presented classification, design and applications of metamaterials in Antenna applications.
- ❖ *Georgina Roses* et al. [2010] proposed a Smart Antenna using Metamaterial and MEMS. It is shown that the antenna can be tuned to frequency range from 5.3 GHz to 5.8 GHz by using MEMS capacitor.
- ❖ *Yuandan Dong* et al. [2012] presented a detailed review on the recent research efforts to develop small antennas based on metamaterials. Some practical limitations in their development are pointed out and possible solutions to the problems are illustrated.

❖ *K. K. A. Devi* et al. [2013] had presented a design of patch antenna using metamaterials at GSM-1800. An array of squared dual split ring resonators (SRR) on FR4 substrate and strip conductors are used and showed to be resonating at 1846 MHz.

❖ *Sarin V. Pushpakaran* et al. [2014] had proposed a Metaresonator Inspired Dual Band Antenna for 2.4/5.2 GHz. Dual band operation in 2.4/5.2 GHz is achieved by utilizing stacking technique on a dog bone shaped dipole antenna made on FR4 substrate with a total dimension of 38x40x3.2 mm^3 .

❖ *Weiping Cao* et al. [2015] had presented a Smart Antenna based on Metamaterial, consisting of cut wire metal rods which are used to form a circle. The antenna gain reaches 14 dBi in the range of 1.8 GHz -1.9 GHz.

❖ *Pratap N. Shinde* et al. [2015] had proposed a compact Pentagonal Slot Antenna with wide bandwidth of 4.21 GHz (3.24 – 7.45 GHz) with a size reduction of 84% than the reference antenna.

❖ *K. Kandasamy* et al. [2016] had proposed a Low Radar Cross Section (RCS) and polarization Reconfigurable Antenna using an asymmetric cross shaped metasurface. Design was simulated, fabricated and measured which showed good performance at 4.4 GHz.

❖ *Y. M. Pan* et al. [2016] had proposed a low profile, high gain wide band filtering antenna using Metasurface consisting of non-uniform metallic patch cells, fed by two separated microstrip, coupled slot from bottom. The gain obtained was 8.2 dBi at 5 GHz.

❖ *Bushra Farooq* et al. [2016] had presented a comparative study of the performance of a 2.4 GHz MPA, using various metamaterial surfaces like, Frequency Selective Surface (FSS) and Artificial Magnetic Conductor (AMC). It is found that AMC based micro strip patch antenna without via gave higher gain than AMC with via.

❖ *K. Krishnamoorthy* et al. [2016] had proposed a reconfigurable slot antenna enabled by the anisotropic metasurface layer composed of periodic arrangements of I-shaped metallic inclusion which can be tuned by rotating the metasurface with respect to the center of slot antenna. It is shown that operating frequency can be tuned from 2.55 to 3.45 GHz, with a gain of 5.3 dBi

- *Ankit Kumar Singh* et al. [2018] proposed an optimal multiband MIMO antenna suitable for fifth generation (5G) wireless communication using the capabilities of metamaterials split ring resonators (SRR). The designed structure achieves multiple bands at 2.61 GHz and 7.1 GHz

- *Haiyang Zhang and Lianrong Lv* [2018], proposed a novel metamaterial structure that can be used with the microstrip antenna for increasing bandwidth.

2.9.2 Multi-band Artificial Magnetic Conductor

This section discusses literature survey on characteristics of Artificial Magnetic Conductor (AMC). It also discusses some techniques to design multiband AMC unit cell and to integrate with reconfigurable antennas in order to improve the performance of antenna.

- *Dan Sievenpiper* et al. [1999] had proposed a new type of electromagnetic structure by incorporating a special texture on a conducting surface and thereby altering its electromagnetic properties. Unlike normal conductors, the new surface prohibit surface waves and reflects electromagnetic waves with no phase reversal, behaving as a kind of Artificial Magnetic Conductor

- *Y. Rahmat-Samii and H. Mosallaei* [2001] presented the classification, characterization and application of Electromagnetic Band Gap structures.

- *Fan Yang and Y. Rahmat-Samii* [2002] presented the different applications of Electromagneic Band Gap structures in microwave engineering

- *Fan Yang and Y. Rahmat-Samii* [2003] presented the reflection phase characteristics of EBG ground plane for low profile antenna applications

- *Douglas J. Kern* et al. [2005] had presented different designs such as, fractal unit cell geometries and methodologies for multiband artificial magnetic conducting surfaces for operation at GPS and cellular frequencies.

- *D. Hamzaoui* et al. [2014] had proposed a 3 types of hexagonal loop type AMC unit cell for Wi-Fi application. All 3 types of unit cell provided dual band phase-frequency responses.

- *Basudev Majumdar* et al. [2015] presented a frequency reconfigurable slot antenna using mechanical rotation of metasurface unit cell.

- *Amin Tayebi* et al. [2015] had proposed a dual band reconfigurable double square loop AMC which uses varactor diode to dynamically tune and alter the phase of the scattered field.

- *Ning Liu Xianjun* et al. [2017], *Mahmoud Niroo-Jazi* et al. [2011] *and H. Zahra* et al. [2015] had proposed different types of electronically reconfigurable modified Jerusalem – type unit cell having multiband tunable responses.

- *Z. Fneish* et al. [2017] had proposed a miniaturized modified double square loop AMC unit cell to obtain dual band response. A modified version, having tri-band phase-frequency response is also presented.

- *Pramod P. Bhavarthe* et al. [2018] presented a compact two via double slot type dual band gap EBG structure. Compactness is achieved because of two via per unit cell, square slot, and inverse C-type slot on EBG patch.

- *Constantine A. Balanis* et al. [2018] presented different applications of AMC – based impedance surfaces. AMCs can be used for realizing low profile antennas, RCS reduction, beam scanning, reduction in surface wave and increasing directivity and gain.

Table 2.1 Comparative analysis of literature survey on multi-band AMC unit cell

References	Parameters			
	Type and Dimension of Unit Cell (mm)	**Mechanism for Tuning**	**No. of Bands & Zero Reflection Phase frequencies (GHz)**	**Independent Tuning of Single band Reflection Phase**
M. Abu et. al [2011]	Square loop Size : 64 x 32	No	Dual band (0.92 and 5.5)	No
Adeel Afridi et al. [2014]	Square loop Size : 20 x 20	PIN diode	Dual band (2.4 and 5.2)	No
Amin Tayebi et al. [2015]	Square loop Size : 22 x 22	Varactor diode.	Dual band (3.49 and 5.3)	No
D. Hamzaoui et al. [2015]	Double Hexagonal loop Size : 15 x 15	No	Dual band (2.5 and 5.5)	No
H. Zahra et al. [2015]	Modified Jerusalem Cross Size : 11.5 x 11.5	PIN diode.	Tri band (2.45, 4.5 and 5)	No
Basudev Majumder et al. [2016]	"I"shaped Size : 10 x 2	Rotation of Metasurface layer.	Tuning range – (2.55 to 3.45)	No
D. J Kern et al. [2016]	Jerusalem Cross Size : 20 x 20	PIN diode.	Dual band (2.5 and 4)	No

Table 2.1 Comparative analysis of literature survey on multi-band AMC unit cell

References	Parameters			
	Type and Dimension of Unit Cell (mm)	Mechanism for Tuning	No. of Bands & Zero Reflection Phase frequencies (GHz)	Independent Tuning of Single band Reflection Phase
Vivek kumar et al. [2016]	Modified Double Square loop Size : 19 x19	No	Dual band (2.4 and 5.5)	No
Adil Zaman Babar et al. [2017]	Double Circular loop Size : 16 x 16	No	Dual band (2.4 and 5.6)	No
Ning Liu et al. [2017]	Spiral Slot Size : 20 x 20	PIN diode.	Tri band (1.2, 2.6 and 4.1)	No
Mahmoud Nroo-Jazi et al. [2017]	Elliptical Ring Size : 58 x 30	PIN diode.	Dual band (1.8 and 2.5)	No
Ameni Mersani et al. [2018]	Square loop Size : 25 x 25	No	Dual band (2.45 and 5.8)	No

2.9.3 Frequency Reconfigurable Antenna

This section discusses a review on the previous research works on reconfigurable antenna which can switch between UWB and NB frequencies for cognitive radio services.

- ❖ *James R. Kelly* et al. [2010] had proposed a small rectangular patch electrically connected to ground plane of rectangular monopole antenna using PIN diode, for the purpose of switching between UWB and NB frequencies. But the result consists of band notches in UWB response and also they could realize only single narrow band response.

- ❖ *Eko Tjipto Rahardjo* et al. [2011] had proposed two monopole sharing a common ground plane, where one antenna is used for "sensing" and other for "communication". Here switching is done between antennas, which increases size and cost.

- ❖ *G. P. Jin* et al. [2011] had proposed optically controlled reconfigurable antenna, controlled by four photoconductive switches made up of silicon. One UWB and three narrow band responses are obtained.

- *Y Tawk* et al. [2011] had proposed a mechanically reconfigurable antenna for cognitive radio services. Frequency agility is achieved by rotation motion of antenna patch using stepper motor, mounted on the back of antenna, which increases the size and complexity of the antenna structure.

- *Hamid Boudaghi* et al. [2012] had proposed monopole antenna which uses slots connected by PIN diodes, in ground plane to achieve reconfigurability.

- *Mohsen Gholamrezaei* et al. [2014] presented a frequency reconfigurable antenna to switch between UWB and NB frequencies, with individual tuning of NB frequencies.

- *K. Kandasamy* et al. [2015] had utilized the negative permeability of split ring resonators to switch between UWB and NB frequencies. At resonant frequency of SRR, except that frequency, all other frequencies are stopped.

- *Minakshi Tewari* et al. [2016] had proposed frequency reconfigurable antenna using pixel ground plane. The ground plane is removed partially and equipped with pixel patches connected by PIN diodes, to achieve reconfigurability.

- *Sonu Jain* et al. [2017] proposed a circular monopole antenna with partial ground plane to realize UWB response. By embedding metamaterial periodic structures on the partial ground plane and electrically connecting with partial ground plane, NB frequency responses are obtained.

- *Saffrine Kingsly* et al. [2018] proposed a multiband reconfigurable filtenna for cognitive radio applications to provide 1.8 GHz, 2.4 GHz, 3.5 GHz and 5.2 GHz tunable responses.

- *Chinmoy Saha* et al. [2018] presented a coplanar waveguide fed monopole antenna that can provide reconfigurable UWB notched / NB responses, depending on status of the switches and position of SRR in the feed region.

- *Mansour Nejatijahromi* et al. [2018] had proposed a UWB to NB frequency switchable monopole antenna using variable discrete capacitors. 0.1 pF to 0.8 pF values of capacitance are used for switching.

Table 2.2: Comparative analysis of literature survey on frequency reconfigurable antennas

References	Parameters			
	Antenna dimension (mm)	Mechanism for switching	UWB Response (GHz)	No. of Narrow Bands
James R. Kelly et al. [2010]	110 x 30	PIN diodes	(3.1 – 10.6)	1
Eko Tjipto et al. [2011]	140 x 80	PIN diodes	(1.35 – 11.7)	2
G. P Jin et al. [2011]	49 x 33.5	Photoconductive switches	(2.65 – 10.3)	3
Y. Tawk et al. [2011]	70 x 50	Mechanical switching	(2 – 10)	5
Hamid Boudaghi et al. [2011]	40 x 40	PIN diodes	(3.1 – 10.6)	4
K. Kandasamy et al. [2015]	40 x 40	PIN diodes	(3 – 10)	1
G. P Jin et al. [2011]	49 x 33.5	Photoconductive switches	(2.65 – 10.3)	3
Y. Tawk et al. [2011]	70 x 50	Mechanical switching	(2 – 10)	5
Hamid Boudaghi et al. [2011]	40 x 40	PIN diodes	(3.1 – 10.6)	4
A. Mansoul et al. [2014]	68 x 51	PIN diodes	(2.63 – 3.7)	4
I. H. Idris et al. [2014]	88 x 83	PIN diodes	(2 – 6)	3
Mansour Nejatijahromi et al. [2018]	24 x 30.5	Variable capacitor	(3.1 – 10.6)	2
Chinmoy Saha et al. [2018]	50 x 50	PIN diodes	(2.6 – 10.8)	3
Bei-Jia Liu et al. [2018]	23.5 x 31.5	PIN and varactor diodes	(3.82 – 8.94)	1

2.9.4 Bandwidth Reconfigurable Antenna

This section discusses a review on the previous research works on bandwidth reconfigurable antenna which can switch between UWB and NB frequency along with the capability of tuning the bandwidth of the narrow band for cognitive radio services.

❖ *Ali Mansoul* et al. [2016] presented bandwidth reconfigurable monopole antenna in which bandwidth is varied by switching PIN diode placed across slots on the ground plane. But, in this work, only upper band limit can be varied by keeping lower band limit constant.

❖ *Mohamed Alibakshi-Kenari* et al. [2015] had proposed two types of bandwidth reconfigurable monopole antennas, with/without loading a split ring resonator

on to the ground plane. But in this case separate antennas are needed, which increases size and cost.

❖ *Sasmita Pahadsingh* et al. [2017] had proposed a coplanar waveguide fed bandwidth reconfigurable antenna. A hair pin resonator and PIN diodes are used to tune bandwidth as well as frequency. This design requires separate antennas for UWB and narrow band response, which will lead to increase in size and cost.

❖ *D. E. Anagnostou* et al. [2017] had presented a bandwidth reconfigurable antenna, in which, Vanadium Dioxide (VO2) strips are placed and heated/cooled, for tuning the bandwidth.

❖ *Linglong Meng* et al. [2017] had proposed a slot loaded planar dipole antenna. In this case, bandwidth is varied by switching PIN diodes placed across the slots.

❖ *K. Kandasamy* et al. [2016] had proposed a dual band circularly polarized split ring resonators loaded square slot antenna in which the two bands can be tuned independently. Moreover, the polarization sense of the two bands can be controlled independently.

❖ *Chinmoy Saha* et al. [2011] presented a theoretical model for estimation of resonance frequency of rotational circular split ring resonators.

❖ *J. D. Baena* et al. [2015] had presented equivalent circuit models for split ring resonators and complementary split ring resonators coupled to planar transmission lines.

Table 2.3: Comparative analysis of literature survey on bandwidth reconfigurable antennas

References	Parameters				
	Antenna Dimensions (mm) and technique used	**Bandwidth ranges and percentage bandwidth variation [($F_h - F_l$) / F_c] x 100**	**Switchable Polarization Sense**	**Beam Steering ability**	**Factor by which percentage bandwidth increased**
Ali Mansoul et al. [2016]	Electronically reconfigurable antenna. Size:56 x 54	810 MHz to 1870 MHz (43% – 76%)	Nil	Nil	1.77
Mohamed Alibakshi-Kenari et al. [2015]	"F" and "T" shaped monopole antennas loaded with/without SRR. Size:30 x 22	"F"antenna – 1.5GHz and 3.5GHz (31.5% – 75.4%)	Nil	Nil	2.39

Table 2.3: Comparative analysis of literature survey on bandwidth reconfigurable antennas

References	Parameters				
	Antenna Dimensions (mm) and technique used	Bandwidth ranges and percentage bandwidth variation $[(F_h - F_l) / F_c]$ x 100	Switchable Polarization Sense	Beam Steering ability	Factor by which percentage bandwidth increased
Sasmitha Pahadsingh et al. [2017]	Electronically reconfigurable monopole antenna. Size:20 x 25.32	700 MHZ and 1200 MHz (7.2 % – 12.2%)	Nil	Nil	1.69
D. E. Anagnostou et al. [2017]	Chemically reconfigurable antenna loaded with VO_2 strips	380 MHz and 470 MHz (8% – 10%)	Nil	Nil	1.25
Linglong Meng et al. [2017]	Electronically reconfigurable planar dipole antenna. Size:70 x 30	600 MHz, 690 MHz and 1030 MHz (30.9% – 47.6%)	Nil	Nil	1.54

2.9.5 Polarization Reconfigurable Antenna

This section discusses a review on the previous research works on circularly polarized antenna with different senses of polarization and its applications.

❖ *Fan Yang and Yahya Rahmat-Samii* [2002] had proposed a microstrip probe feed patch antenna, in which two orthogonal slots are incorporated into the patch and two pin diodes are utilized to switch the slots ON or OFF to obtain LHCP and RHCP at 4.64 GHz, with 3 dB axial ratio bandwidth (ARBW) of 3% .

❖ *Kin-Fai Tong and Ting-Pong Wong* [2007] had presented a circularly polarized probe feed microstrip patch antenna loaded with an asymmetrical U-slot which can generate two orthogonal modes to obtain circular polarization without cutting any corner of the patch antenna. The antenna operated at 2.3 GHz and the measured ARBW is about 4%, from 2.27 to 2.36 GHz.

❖ *Boyon Kim* et al. [2008] had proposed a circular microstrip antenna with polarization reconfigurability. This antenna consists of a circular patch, with an "arc" slot loaded with five PIN diodes. It can be switched between LP, LHCP and RHCP radiations. In addition to this, two open circuit stubs and a short

circuit stub are connected to feed line through PIN diodes for tuning the impedance matching. Antenna deliver CP between 2.445 and 2.450 GHz.

❖ *Pei-Yuan Qin* et al. [2010] had presented a patch antenna with reconfigurable polarization in which the length of the arms of a U-slot is varied by switching PIN diode, which alters the antenna's polarization state. Circular polarization is achieved from 5.725 GHz to 5.85 GHz, with ARBW greater than 2.8%.

❖ *Venkateshwar V. Reddy and N. V. S. N. Sarma* [2015] had proposed a probe feed frequency reconfigurable CP antenna using two Koch fractal patch, in which smaller one is embedded in the middle portion of larger one. These patches are connected with PIN diodes. Asymmetrical Koch curves are used as boundaries of the two patches to generate CP. The obtained 3-dB AR bandwidths at 1.8 GHz and 2.48 GHz are 1.1% and 1.6%, respectively.

❖ *Krishnamoorthy Kandasamy* et al. [2016] proposed a dual-band circularly polarized microstrip line fed slot antenna using a set of split ring resonators. The proposed antenna is designed to operate at 3.1 and 4.7 GHz. Resonance frequencies of the two bands can be tuned independently. Moreover, the polarization sense of the two bands can be controlled independently.

❖ *Puneeth Kumar* et al. [2019] had proposed a coplanar waveguide (CPW) fed triband circularly polarized planar slot antenna loaded with split ring resonators, in which the truncated slot antenna resonates at 4.15 GHz. The second and third band resonances are achieved at 4.77 GHz and 5.1 GHz respectively due to the loading of SRRs. The axial ratio bandwidths obtained are 11.76%, 1.9%, and 3.87% for the first, second and third band, respectively.

❖ *Tu Tuan Le and Tae-Yeoul Yun* [2019] had presented a quad-band dual-sense circularly-polarized (CP) antenna. The corner-fed square-ring radiator is designed excites dual-band, dual-sense CP radiation with RHCP at one frequency band and a LHCP at the other band. Later, a rhombic-shaped slot and an inverted V-shaped parasitic element, excites two additional LHCP bands. The measured results yield 3-dB axial ratio ARBW of 7.3% (2.38-2.56 GHz), 9.0% (2.75-3.03 GHz), 3.7% (3.42-3.53 GHz), and 7.1% (5.16-5.54 GHz).

❖ *Princy M. Paul* et al. [2019] had presented a dual-band circularly polarized, line fed square slot antenna with pair of symmetric rectangular extensions on

opposite corners and loaded with an array of inclined and truncated rectangular copper strips. The lower band resonates between 2.24 to 2.62 GHz with a 3 dB ARBW of 15.7% and higher band resonates between 3.26 and 5.18 GHz, having ARBW of 45.5%. The polarization sense and resonant frequency of the proposed antenna can be independently tuned depending on the position and dimensions of the slot and strips, respectively.

❖ *Reshmi Dhara* [2021] proposed a single feed dual-band dual-polarized (DBDP) patch antenna having an inverted Y-shaped radiating patch and a rectangular open-loop positioned near its right corner to create CP. To achieve enhanced axial ratio bandwidth (ARBW), a semi-rectangular ground plane with two asymmetric truncated L-shaped slots has been used. The two ARBW bands span over 7.22 GHz–10.99 GHz and 11.67 GHz–12.25 GHz.

2.9.6 Antenna Beam Steering using Phase Gradient Metasurface

This section discusses a review on the previous research works on beam steering antenna using phase gradient metasurface placed as reflector to the radiation.

❖ *Daniel F. Sievenpiper* et al. [2003] had proposed an electronically steerable reflector, based on a resonant textured surface loaded with varactor diodes. By varying the bias voltage across the varactor diodes, the reflection phase of the surface can be tuned as a function of frequency to produce a tunable phase gradient, which can steer a reflected microwave beam, resulting in 2-D beam steering over a range of +/- 40^0.

❖ *Fan Yang* et al. [2003] had presented a detailed characteristic study of the properties mushroom-like electromagnetic band-gap structures. For normal incidence of plane wave n EBG surface, the phase of the reflected field changes continuously from $+180^0$ to -180^0, with respect to frequency. Important application of this feature is that the conventional perfect electric conductor (PEC) ground plane can be replaced with an EBG ground plane for low profile antenna design, resulting in good return loss in the input-match frequency band, which can be identified from the reflection phase curve.

❖ *N.A. Abbasi & R.J. Langley* [2010] proposed an artificial magnetic conductor based multiband antenna. The AMC is a simple dual band structure, with the reflection phase in the 2.0 GHz and 5.8 GHz ranges. A wideband circular disc monopole antenna is placed over the metasurface formed by dual band AMC, which converts it to multiband antenna covering 1.58 GHz, 1.8 GHz, 1.92 GHz, 1.95 GHz, 2.45 GHz, 5.5 GHz and 5.8 GHz, with considerably high gain.

❖ *K.Kandasamy* et al. [2015] proposed a method for steering the antenna beam to a specific direction by varying the position of via in electromagnetic band gap structure. The maximum tilt angle of 34^0 and 29^0 is achieved in E-plane and H-plane respectively.

❖ *Chao Gu* et al. [2017] presented a cylindrical active frequency selective surface (AFSS)-based electronically beam-switching antenna, which can operate at two different frequency bands (2.5 GHz and 5.3 GHz). By controlling the dc bias voltages to different columns of p-i-n diodes, the directive beams of the antenna can be swept to cover the whole azimuth plane.

❖ *B. Majumder* et al. [2017] proposed a continuously beam steerable dipole antenna using a tunable metasurface as phase varying reflector. The top layer of the metasurface based unit cell consists of three small gap loaded vertical stubs. RF switches can be connected at the gap of those vertical stubs to control the surface impedance and thereby reflection phase. By this technique, the antenna beam can be steered from $+30^0$ to -30^0 in the broadside direction.

❖ *Yun Fei Cao & Xiu Yin Zhang* [2018] proposed a beam-steerable slot antenna consisting of, one cross-shaped main radiating slot, two parasitic slots with two p-i-n diodes as the reflectors, and an AMC surface. By switching the p-i-n diodes ON/OFF, the main lobe of the radiation pattern can be steered between 0^0, -36^0, and $+36^0$. Presence of AMC metasurface increases gain, to more than 7 dBi, from 4.9 to 5.5 GHz.

❖ *Liping Han* et al. [2019] presented a beam-sweeping antenna using an active frequency-selective surface (FSS). It consists of a dipole and a cylindrical FSS formed by six columns of four unit cells each. The radiation pattern of the antenna could be reconfigured by controlling the states of the PIN diodes in the

FSS. Beam-steering antenna can operate at 2.45 GHz and the main beam can be swept across the whole azimuth plane with a peak gain of 8.15 dBi.

❖ *M. Ameen, O. Ahmad & R.K. Chaudhary* [2019] proposed the design of a two-element polarization diversity antenna, mainly consists of two monopole radiators loaded with metasurface reflector as a ground plane. The antenna has an impedance bandwidth of (2.23 GHz–2.91 GHz) and wider ARBW of (2.16 GHz–2.92 GHz) with a fractional ARBW of 26.45%. A maximum gain of 7.02 dBic is observed along with the operating frequency range. The antenna provides LHCP radiation at port-1 and provides RHCP radiation at port-2.

❖ *Huy Hung Tran* et al. [2021] had presented a low-profile circularly polarized antenna with a truncated corner patch, having wideband and polarization-reconfigurable characteristics. The antenna alone produce a narrow CP band around 4.8 GHz. When it is backed by a uniform metasurface, additional CP bands are generated and the ARBW become 1.2 GHz (4.6 GHz - 5.8 GHz). When non-uniform metasurface is used, the ARBW significantly increases to 1.6 GHz (4.6 GHz - 6.2 GHz).

CHAPTER 3

RECONFIGURABLE MULTI-BAND AMC AND PHASE GRADIENT METASURFACE

Multiband antennas are used in many modern applications where selection of multiple frequency bands simultaneously is required. Hence, Artificial Magnetic Conductor (AMC) surface used along with antennas, require multiband resonance, matching to antenna operating frequencies. In this scenario, reconfigurable/tunable AMC structures will offer extra versatility to antenna design. Reconfigurability is achieved by either electrically or mechanically. Electrical tuning is preferred over mechanical tuning due to its reduced size and flexibility. Electrical tuning can be achieved by incorporating PIN diodes and varactor diodes on the unit cell.

In this work, a miniaturized, multiband reconfigurable AMC is designed. For miniaturization procedure, a modified design is employed for conventional square loop dual-band AMC. Modified unit cell resonates more number of zero reflection phase-frequency bands inside S and C bands. Phase gradient metasurface is designed using the array of unit cell, keeping 6 GHz as center frequency, which can be used for designing beam steering antenna.

3.1 Conventional Dual Band AMC Unit Cell

The AMC unit cell can be considered as equivalent to a parallel LC resonant circuit, whose dimensions and geometry determines the resonant frequency, f_o given by equation (3.1).

$$f_o = 1 / 2\pi\sqrt{LC} \qquad\qquad (3.1)$$

where, L and C are the effective inductance and capacitance of unit cell. N. A. Abbasi & R. J. Langley [2010] presented a square loop dual band tunable AMC which resonates in S and C band region, having a size of 22mm x 22mm x 3.2mm on FR4 substrate.

In this work, for the purpose of miniaturization, we have designed a conventional, dual band square loop AMC unit cell having, 11mm x 11mm x 3.2mm, compact size, as shown in Fig. 3.1. Ground plane is a conducting patch of dimensions Ws=Ls=11mm. The reflection phase-frequency diagram is shown in Fig. 3.2.
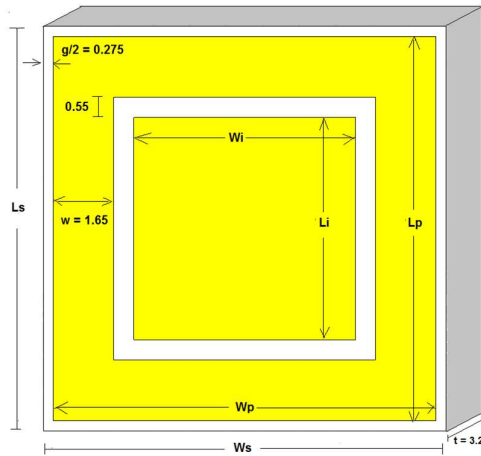
Fig. 3.1. Top view of conventional dual-band AMC unit cell. (All dimensions are in mm).
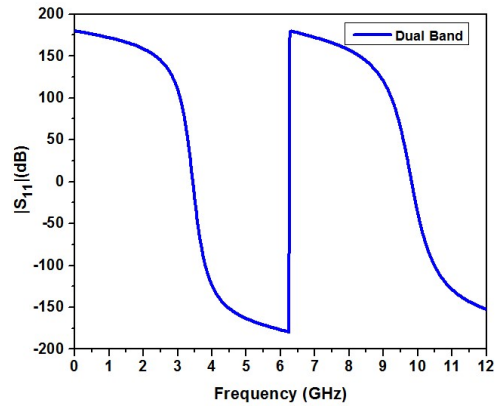
Fig. 3.2. Reflection phase diagram of conventional square loop dual-band AMC

Height of the unit cell is 3.2mm and substrate used is FR4 with a relative permittivity of 4.3. The dimensions, Wp=Lp=10.45mm and Wi=Li=6.05mm. Wp and Lp are width and length of conducting patch outside the square loop whereas, Wi and Li are width and length of conducting patch inside the square loop. Here, g/2= 0.275, where g is the gap between patches of adjacent unit cells (when placed in an array).

The zero reflection phase, shown in Fig. 4.2, are occurring at frequencies, 3.45 GHz and 9.8 GHz for first and second band respectively. The reflection phase throttles between ±180^0. The frequency region within which phase falls between ±90° is the bandwidth of each band, given by 640 MHz and 1 GHz respectively.

In order to achieve miniaturization along with multiband resonances, inside the same S and C bands, the unit cell patch geometry has to be modified. Also, for achieving reconfigurability, PIN diodes are to be used. This is presented in the next section.

3.2 Modified Reconfigurable Multiband AMC Unit Cell Design

Modified compact multi band reconfigurable AMC unit cell is proposed in this section as shown in Fig. 3.3. The modified unit cell is on FR4 substrate and kept at the same

size, 11mm x 11mm x 3.2mm. Ground plane is conducting patch of size 11mm x 11mm. The value of L and C in equation (3.1), are given by (3.2) and (3.3).

$$L = \mu\, t \tag{3.2}$$

$$C = \frac{W_p\, \varepsilon_o\, (1 + \varepsilon_r)}{\pi} \cosh^{-1}\left(\frac{a + g}{g}\right) \tag{3.3}$$

where, "ε_r" is the relative permittivity and "t" is the thickness of the substrate. "W_p" is the width of the outer patch, "Wi" is the width of the inner patch and "g" is the gap between patches of adjacent unit cells, as shown in Fig.3.1. The parameter "(a + g)" is called "array period" and can take values, a=W_p or a=Wi, which influences the in-phase reflection of lower resonance and higher resonance bands respectively.

For shifting the reflection phase-frequency band to lower frequency region, the value of L or C should be increased. In order to increase the value of L thickness of substrate has to be increased which will increase the size of the unit cell. In order to increase the value of C, effective length of W_p and Wi has to be varied [Adeel Afridi et al. [2014]].

Fig. 3.3. Modified AMC unit cell with PIN diodes (All dimensions in mm.)

For this, the square loop is meandered, which increases the circumference of the inner patch, thereby increasing effective length of Wi, without altering overall size of unit cell. In addition to this, two long horizontal slits named, T_{hr} and B_{hr} are made at the top and bottom of the outer patch, so that effective length of W_p is increased. Additionally, 4 slots named, L_{tp}=R_{bt}=2.75mm, L_{bt}=R_{tp}=3.575mm are made and connected to the 4

35

corners of outer side of the meandered loop using PIN diodes for tuning the patch capacitance. For tuning, six PIN diodes D1, D2, D3, D4, D5 and D6 are employed.

3.3   Simulation Results

The simulated reflection phase coefficients for 5 different diode switching configurations are tabulated, as shown in Table 3.1. Diode ON condition is represented by "1" and OFF condition by "0".

Table 3.1: Diode switching conditions for tuning reflection phase of AMC unit cell
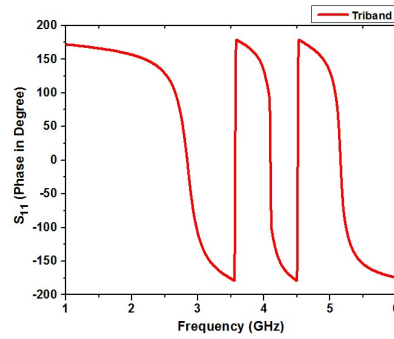
Cases	Diode switching conditions						No. of Bands (GHz)	Frequency at 0^0 Reflection Phase (GHz)	Band Width (MHz)
	D1	D2	D3	D4	D5	D6			
Case I	1	1	1	1	1	1	Dual-band	3, 5.2	412, 127
Case II	1	1	0	0	1	1	Tri-band	2.8, 4.1, 5.2	250, 50, 150
Case III	0	1	1	1	1	0	Tetra-band	2.6, 4.3, 5.2, 6.5	210, 40, 100, 380
Case IV	0	1	1	0	1	0	Penta-band	2.6, 4.2, 5.2, 6, 7.2	170, 100, 35, 230, 40
Case V	0	0	0	0	0	0	Hexa-band	2.4, 3.6, 5.1, 6.0, 8.1, 9.9	140, 30, 80, 210, 30, 690

> **Case I:** Here all diodes are in ON condition. Length of outer patch, W_p will influence lower reflection phase-frequency band and length of inner patch width Wi will influence higher reflection phase-frequency band. Here, since all diodes are ON, W_p does not vary. Hence unit cell will give a dual-band response similar to the case of conventional "single square loop" unit cell, as shown in Fig. 3.4. But, since the inner loop is meandered the value of Wi will be more than that of conventional unit cell, resulting in the increase of effective capacitance and hence the dual band response will occur at lower frequency region, than that of conventional unit cell.

> **Case II:** Since D3 and D4 are OFF, the effective inner patch width Wi increases, thereby increasing capacitance. Hence the higher resonance band gets shifted to lower frequency region and hence tri-band response results, as shown in Fig. 3.5.

> **Case III:** Here D1 and D6 are OFF. Hence effective outer patch width, W_p increases, thereby increasing the effective capacitance. This will influence the lower resonant frequency band which gets shifted to further low frequency region and hence tetra-band response results, as shown in Fig. 3.6.

➢ **Case IV:** Here D1, D4 and D6 are OFF. Hence both W_p and Wi are increased. Hence both lower and higher frequency bands gets shifted to further lower frequency region and hence penta-band results, as shown in Fig. 3.7.

➢ **Case V:** Here all the diodes are OFF. This will result in further increase of Wi, compared to Case IV, and thereby effective capacitance increases. Hence, both lower and higher resonance band gets shifted to lower frequency region and hence hexa-band results, as shown in Fig. 3.8.
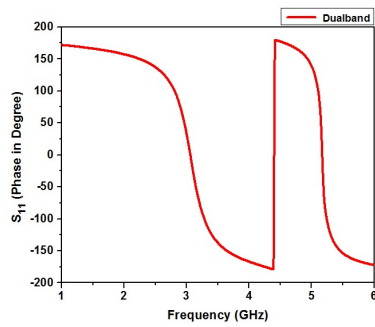
Fig. 3.4. Reflection phase for Case I – Dual-band
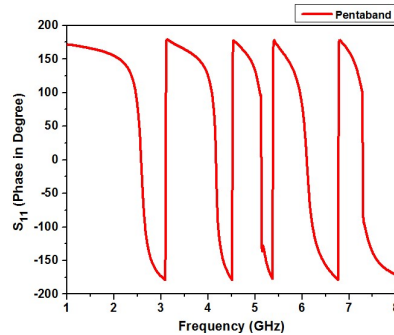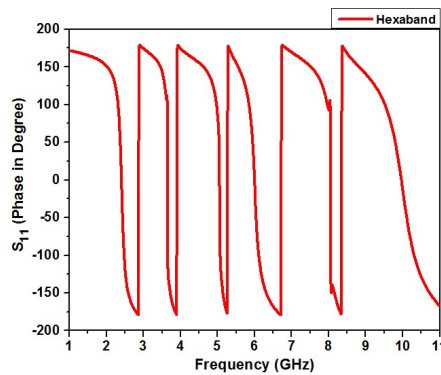

Fig. 3.5. Reflection phase for Case II – Tri-band
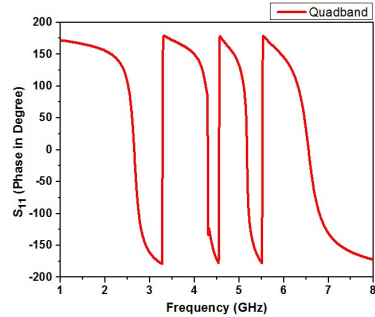
Fig. 3.6. Reflection phase for Case III – Tetra-band

Fig. 3.7. Reflection phase for Case IV – Penta-band

Fig. 3.8. Reflection phase for Case V – Hexa-band

Depending upon different PIN diode switching conditions, the unit cell exhibits dual-band, tri-band, tetra-band, penta-band and hexa-band resonances, with zero reflection phase at frequencies of 2.4, 2.6, 3, 3.6, 4.2, 5.2, 6, 6.5, 7.2, 8.1 and 9.9 GHz, as shown in Fig.3.4, Fig.3.5, Fig.3.6 Fig.3.7 and Fig.3.8. A comparative study of this work with similar previous works is shown in Table 3.2.

Table 3.2 Comparative study of this work with similar previous works on multiband AMC unit cell

References	Parameters			
	Type and Dimension of Unit Cell (mm)	Mechanism for Tuning	No. of Bands & Zero Reflection Phase frequencies (GHz)	Independent Tuning of Single band Reflection Phase
M. Abu et. al [2011]	Square loop. Size : 64 x 32	No	Dual band (0.92 and 5.5)	No
Adeel Afridi et al. [2014]	Square loop. Size : 20 x 20	Electrical switching using PIN diode	Dual band (2.4 and 5.2)	No
Amin Tayebi et al. [2015]	Square loop. Size : 22 x 22	Electrical tuning using Varactor diode.	Dual band (3.49 and 5.3)	No
D. Hamzaoui et al. [2015]	Double Hexagonal loop. Size : 15 x 15	No	Dual band (2.5 and 5.5)	No
H. Zahra et al. [2015]	Modified Jerusalem Cross. Size : 11.55 x 11.55	PIN diode.	Tri band (2.45, 4.5 and 5)	No
Basudev Majumder et al. [2016]	"I"shaped. Size : 10 x 2	Rotation of Metasurface layer.	Tuning range – (2.55 to 3.45)	No
D. J Kern et al. [2016]	Jerusalem Cross. Size : 20 x 20	PIN diode.	Dual band (2.5 and 4)	No
Vivek kumar et al. [2016]	Modified Double Square loop. Size : 19 x19	No	Dual band (2.4 and 5.5)	No
Adil Zaman Babar et al. [2017]	Double Circular loop. Size : 16 x 16	No	Dual band (2.4 and 5.6)	No
Ning Liu et al. [2017]	Spiral Slot. Size : 20 x 20	PIN diode.	Tri band (1.2, 2.6 and 4.1)	No
Mahmoud Nroo-Jazi et al. [2017]	Elliptical Ring. Size : 58 x 30	PIN diode.	Dual band (1.8 and 2.5)	No
Ameni Mersani et al. [2018]	Square loop Size : 25 x 25	No	Dual band (2.45 and 5.8)	No
This Work	**Modified Square Loop. Size : 11 x 11**	**Electrical switching using PIN diode.**	**Dual, Tri, Tetra, Penta & Hexa-band (2.4, 2.6, 3, 3.6, 4.2, 5.2, 6, 6.5, 7.2, 8.1 and 9.9)**	**Yes**

3.4 Design of AMC Metasurface

The unit cell can be arranged in the form of an array to form a 2 dimensional metasurface. If the array is formed by employing the unit cell elements with zero reflection phase at a selected frequency, then a zero phase metasurface is obtained. This metasurface can be used as a reflecting surface for the antenna radiation to increase the gain of the antenna.

If the unit cell elements in the array have varying reflection phase along the length or width of the array, then a phase gradient metasurface can be obtained. This type of metasurface can be used for deflecting the antenna radiation in a designed direction and thereby beam steering can be achieved.

3.4.1 Zero Phase Reflection Metasurface

The unit cell shown in Fig. 3.3, with Ltp=Rbt=2.75mm, Lbt=Rtp=3.575mm, with all diodes "OFF" condition (Case V) has 0^0 degree reflection phase at 6 GHz, as shown in Fig. 3.9.
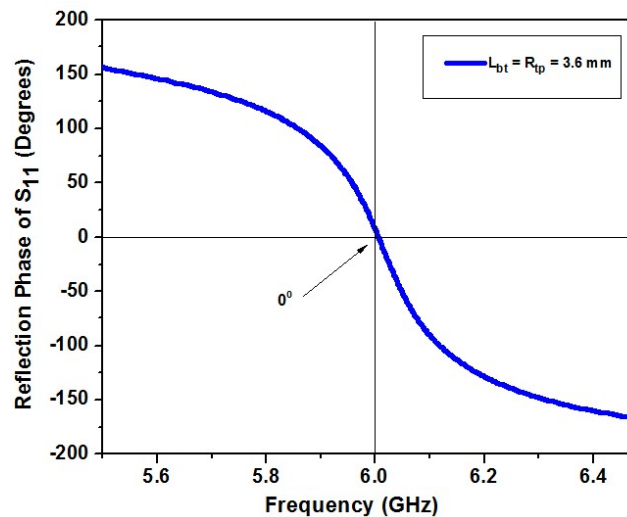
Fig. 3.9. Zero phase reflection at 6GHz for switching case-V

This unit cell is used to form a 5x5 array of zero reflection phase metasurface as shown in Fig. 3.10. The overall size of metasurface is 55mm x 55mm x 3.2mm. Fabricated prototype of Zero Reflection Phase Metasurface at 6 GHz is shown in Fig. 3.11.

39

Fig. 3.10. Zero Reflection Phase Metasurface at 6 GHz
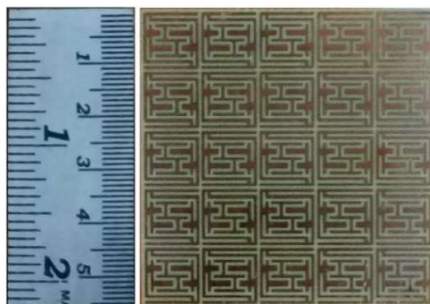
Fig. 3.11. Fabricated prototype of Zero Reflection Phase Metasurface at 6 GHz

3.4.2   Phase Gradient Metasurface – A Parametric Analysis

The reflection phase at 6 GHz alone can be varied from -180^0 to $+180^0$, without shifting the reflection phase at other frequencies. For varying the reflection phase of higher bands, capacitance of meandered loop has to be varied as given in equation 3.3. For this, the length of slots, L_{bt} and R_{tp} are varied equally, by keeping all other dimensions constant.
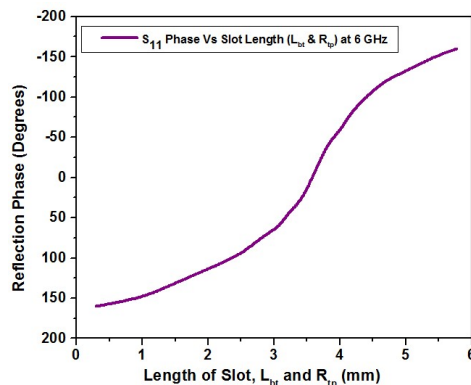
Fig. 3.12. Reflection phase **Vs** Slot Length (L_{bt} and R_{tp}) at 6 GHz

40

The variation of reflection phase at 6GHz, with respect to the variation in length of the slots, L_{bt} and R_{tp} is plotted in Fig.3.12. It can be seen that, the phase variation is approximately linear from -180^0 to $+180^0$. Fig.3.13 and Fig.3.14 shows the variation of reflection phase at 6GHz through -120^0, -60^0, 0^0, $+60^0$ and $+120^0$ with respect to the length f slots L_{bt} and R_{tp}, by keeping the reflection phase of all other frequencies almost constant.
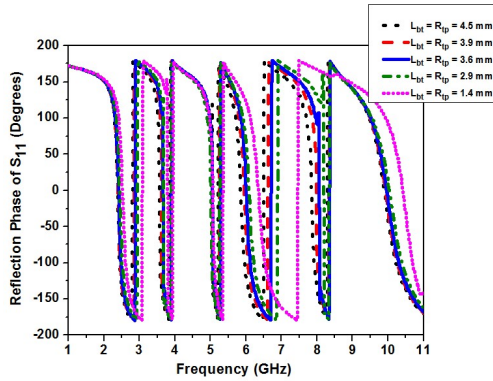
Fig. 3.13. Reflection phase (Case V) for varying values of L_{bt} and R_{tp}
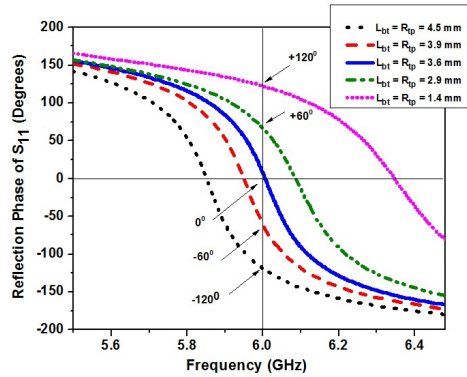
Fig. 3.14. Reflection phase at 6GHz (Case V) for varying values of L_{bt} and R_{tp}
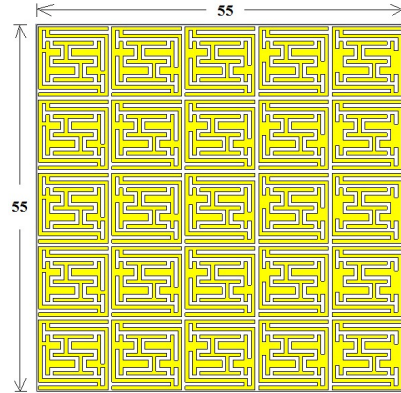
Fig. 3.15. Phase Gradient Metasurface at 6GHz
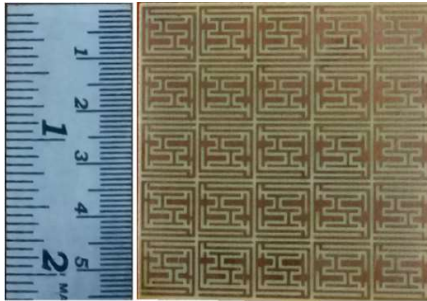
Fig. 3.16. Fabricated prototype of Phase Gradient Metasurface at 6 GHz

41

This Unit cells with different values of L_{bt} and R_{tp}, given by 4.5, 3.9, 3.6, 2.9 and 1.4 mm, are designed to obtain 5 different reflection phases, -120^0, -60^0, 0^0, $+60^0$ and $+120^0$. They are arranged in a 5x5 array, as shown in Fig. 3.15, for the design of phase gradient metasurface. The overall size of metasurface is 55mm x 55mm x 3.2mm. Fabricated prototype o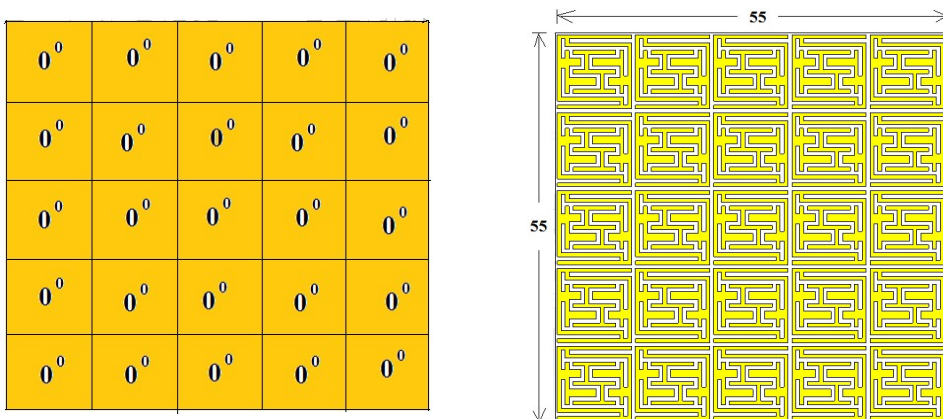f Phase Gradient Metasurface at 6 GHz is shown in Fig. 3.16. Metasurface design is suitable for using with multiband antennas also, because, beam of a single band can be steered without affecting other radiating bands.

3.5 Summary

A 75% reduction in the area of unit cell is achieved when compared to N. A. Abbasi & R. J. Langley [2015]. Depending upon different PIN diode switching conditions, the unit cell exhibits resonance for dual-band, tri-band, tetra-band, penta-band and hexa-band, with zero reflection phase at frequencies of 2.4, 2.6, 3, 3.6, 4.2, 5.2, 6, 6.5, 7.2, 8.1 and 9.9 GHz. Using this miniaturized multiband unit cell, zero phase reflection metasurface and phase gradient metasurface are designed which can be integrated with the antenna for improving the gain and steering the beam.

CHAPTER 4

FREQUENCY RECONFIGURABLE ANTENNA

One of the major application of reconfigurable antennas is in the Cognitive Radio (CR) system, which provides a prospective solution for spectrum underutilization problems. In CR system, the primary users are assigned to specific frequency bands of the channel while secondary users are allowed to use the unoccupied parts of the spectrum by spectrum sensing process, resulting in efficient utilization of the spectrum. Therefore, a CR requires a "sensing antenna", which must have wide band response to scan full spectrum, in order to identify the unused frequency bands and numerous NB "communicating antennas" to operate at specific frequency bands. Conventional CR uses multiple/multiport antennas for sensing and communicating.

In this work we propose an antenna to switch between UWB and NB frequency responses by electrically connecting interdigital capacitors to the ground plane as well as the feed line using PIN diodes.

4.1   Theory and Design Approach

Conventional monopole antennas will inherently deliver the narrowband response. Removal of the ground plane will result in wideband response due to the reduction in patch capacitance. If we represent patch antenna in terms of parallel resonant L-C-G network, the quality factor, Q and bandwidth are given by the equations [K. C. Gupta (1988)],

$$Q = \frac{\omega C}{G} \tag{4.1}$$

where, C is the patch capacitance and G is the patch conductance. Q is related to bandwidth by the following equation,

$$BW = \frac{S-1}{Q\sqrt{S}} \tag{4.2}$$

where, S represents VSWR.

Thus it is clear that the removal of the ground plane partially will result in a reduction of capacitance, which will reduce the quality factor Q, resulting in an increase of bandwidth. Hence if we can tune the capacitance using interdigital capacitor, then the wide band to narrowband conversion can be realized.

4.2 Antenna Geometry and Design

Circular disc monopole patch antenna with a partial ground plane is selected for the design of UWB antenna. The schematic of the proposed antenna is shown in Fig. 4.1 (a) and (b). The substrate material used is FR4 with ε_r = 4.3 with loss tangent = 0.025. The height of the substrate is 1.6mm. Radius of circular patch is 9mm. The overall size of the antenna is 40 mm x 40 mm. The thickness of the copper is 35μm.

This monopole antenna with full ground plane will deliver narrow band response at 4.6 GHz. For obtaining UWB response, the ground plane is partially removed. The idea of switching between UWB and narrow band can be implemented through tuning the patch capacitance by electrically connecting a piece of conducting patch to the partial ground plane as well as feed line, using PIN diodes. The conducting patch connected to antenna is modified to form interdigital capacitor (IDC) in order to utilize its self-resonating nature for obtaining more number of narrow band responses.
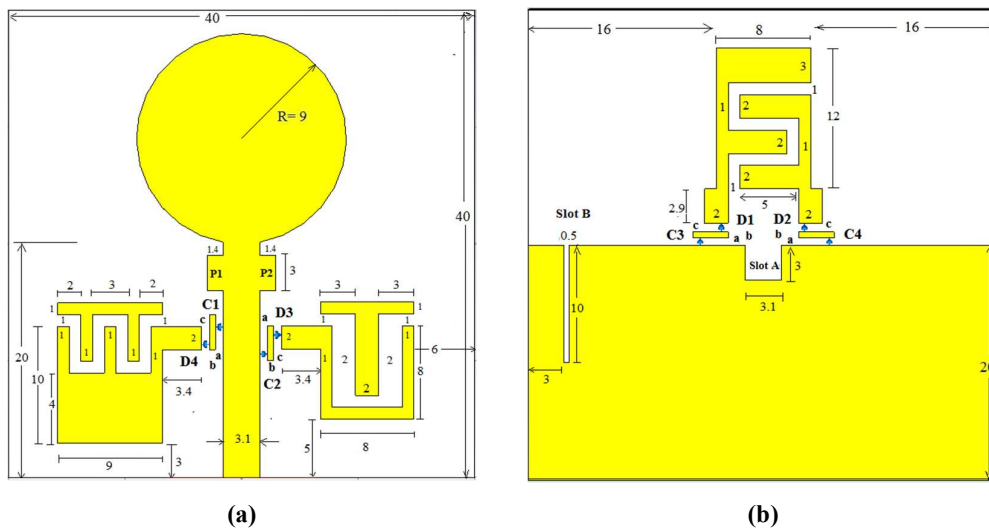
Fig. 4.1. Schematic of Antenna – (a) Front View (b) Back View (All dimensions are in mm)

The structure of IDC and its equivalent circuit are shown in Fig.4.2 and Fig.4.3 respectively. The equation for the series capacitance is given by,

$$C = \left[\frac{\varepsilon_r + 1}{W}\right] L_f \left[(N-3) A_1 + A_2\right] \quad \text{pF/unit length} \qquad (4.3)$$

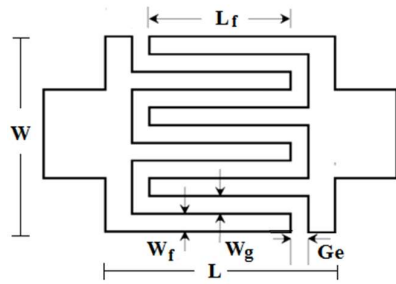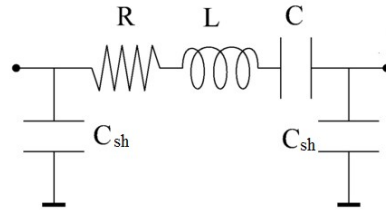where ε_r is the dielectric constant of the material, N is the no. of fingers, L_f is the length of the finger, w_f is width of the finger, w_g is width of the gap between the fingers, L is the overall length and W is the overall width of the interdigital capacitor. A1 and A2 are capacitance values contributed by inner and outer fingers respectively.

Fig. 4.2. Structure of interdigital capacitor   **Fig. 4.3.** Equivalent circuit of IDC

The equivalent circuit of IDC, shown in Fig. 4.3, consists of series inductance (L), series resistance (R) series capacitance (C) and shunt capacitance (C_s). The series capacitance and inductance are responsible for its self-resonant nature. The series capacitance, given by equation 4.3, is contributed by the total length of the gap between the fingers, from one end to other end of IDC. When the IDC is excited by the electric field, due to its self-resonant nature, it will generate more resonances, in addition to the original $\lambda/2$ resonance of monopole antenna. These additional resonances, excited by IDC exists at frequencies for which the total length of the gap between the fingers is a multiple of $\lambda/2$. The total length of the gap between the fingers depends upon the physical parameters such as N, L_f, w_f, and w_g.

Three interdigital capacitors, each with different values of physical parameters are electrically connected to partial ground as well as feed line using four PIN diodes, D1, D2, D3 and D4. C1, C2, C3 and C4 are DC blocking capacitors of 100 pF each. "a" and "c" represents the width of the gap, 0.3 mm, provided for placing the blocking capacitor and PIN diode respectively. "b" is the width of the conducting pad, 0.5 mm, kept between antenna and IDCs. The length of the pad is 3 mm.

Slot A is used for impedance matching of UWB response before modeling of the diode. After modelling the diode and simulating, impedance mismatch occurs due to the parasitic capacitance of diode during OFF condition. In order to compensate for this impedance mismatch, Slot B is included in the ground plane and in addition to that, two patches P1 and P2 are placed on the feed line. (1 mm below the circular disc).

4.3 Simulation Study

CST Microwave Studio Suite environment, is employed for the simulation of the antenna with different switching configurations of PIN diodes. Four PIN diodes are used for switching between UWB and narrow band responses. When all diodes are in OFF condition, all interdigital capacitors are electrically isolated from the antenna which results in UWB response. When one or more diodes are in ON condition, the patch capacitance will be varied by IDC resulting in multiple narrowband frequency responses.

In this work, the PIN diode, MADP-000907-14020W (MACOM Technology Solutions Inc.) was used for switching due to its low, total capacitance (0.03pF), 5.2Ω series resistance, 2ns switching speed and up to 70 GHz operating band. The equivalent circuit of the diode is shown in Fig. 4.4.

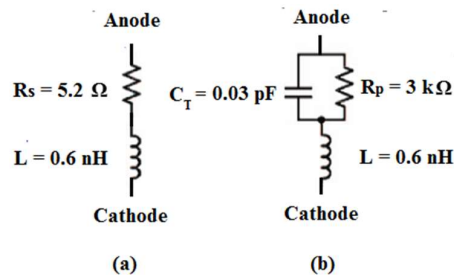**Fig. 4.4.** Equivalent circuit of PIN diode as Switch (a) ON (b) OFF

In CST, the diode is modeled as lumped elements and the values shown in the figure are used for simulating ON and OFF condition of the diode. During the simulation, capacitors having value 100 pF is modelled using lumped elements and placed between antenna and diode for the purpose of DC blocking while fabrication and testing.

4.4 Parametric Analysis of Interdigital Capacitor

Parametric analysis has been performed to study the variation of reflection coefficient of antenna with respect to the variation of different physical parameters of interdigital capacitor. The IDC structure, which is connected using PIN diodes to the ground plane of the antenna, as shown in Fig. 4.1 (b), is selected for this analysis. Simulations are carried out by switching ON the diodes, D1, D2 and switching OFF the diodes, D3, D4.

In this analysis, each physical parameters shown in the Fig.4.2, such as number of fingers (N), length of the finger (L_f), width of the finger (w_f), and gap width between the fingers (w_g) are varied by keeping the value of others parameters, constant. Based upon this analyses five different cases are deduced, as given below:

- **Case (i):** Number of fingers (N) is varied by keeping other parameters like L_f, w_f and w_g, constant. Fig.4.5 shows that, as N increases, the resonant frequency gets shifted to lower end.

- **Case (ii):** Width of the finger (w_f) is varied by keeping other parameters like N, L_f and w_g, constant. Fig.4.6 shows that, as the w_f increases, the resonant frequency gets shifted to lower end.

- **Case (iii):** Length of the finger (L_f) is varied by keeping other parameters like, N, w_f and w_g, constant. Fig.4.7 shows that, as the L_f of each finger increases, the resonant frequency gets shifted to lower end.

  In the above three cases, increase in the value of either N, w_f or L_f will increase the total length of the gap between the fingers, which causes an increase of series capacitance value, resulting in lowering the frequency of resonance. A frequency shift of 1 GHz is achieved for the lowest resonant band, in all the three cases.

- **Case (iv):** Gap width between the fingers (w_g) is varied by keeping other parameters like N, L_f and w_f, constant. Increasing the w_g, will surely reduce the value of series capacitance. But here, since the value of w_f is kept constant, increasing the value of w_g, results in increase of the length of the gap between the alternate fingers. This will increase the value of capacitance, resulting in lowering the frequency of resonance, as shown in Fig.4.8. Since there is a trade-off between

the variations of capacitance, the lower band has got only a marginal frequency shift of approximately 200 MHz.

- **Case (v):** Gap width between the fingers (w_g) and finger width (w_f) are varied without varying the overall width (W) and length (L) of the IDC. The other parameters like N and L_f are kept constant. Increasing the w_g will reduce the value of series capacitance. Also, as the w_g increases, the w_f reduces, in order to keep the overall area of structure, constant. This will reduce the conducting area which will further reduces capacitance value, resulting in shifting of resonant frequency to higher band, as shown in Fig.4.9. A frequency shift of 300 MHz is achieved for the lowest resonant band.
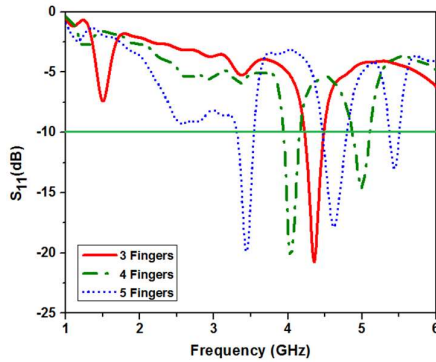

Fig. 4.5. Simulated S_{11} for Case (i)
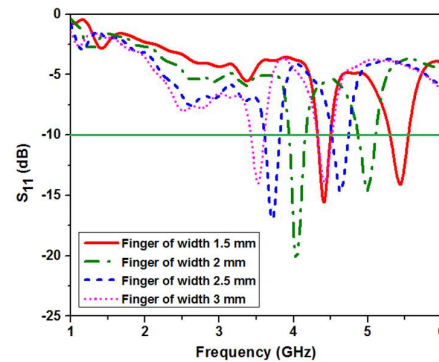
Fig. 4.6. Simulated S_{11} for Case (ii)
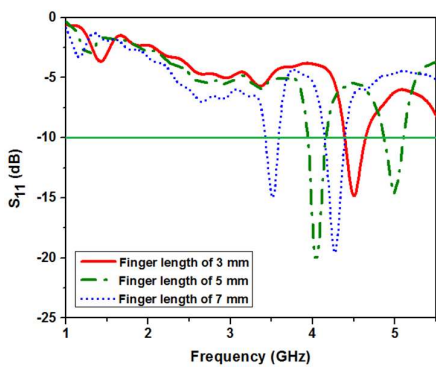
Fig. 4.7. Simulated S_{11} for Case (iii)
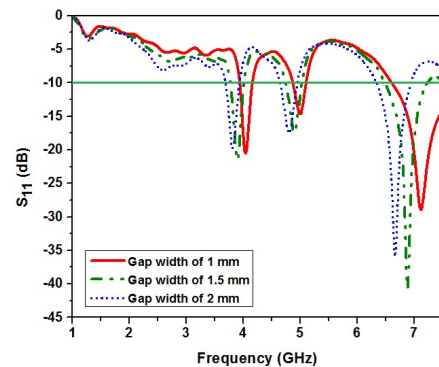
Fig. 4.8. Simulated S_{11} for Case (iv)
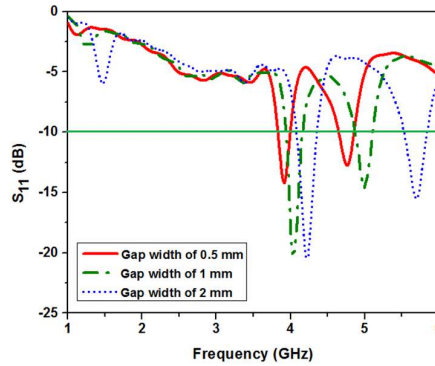
Fig. 4.9. Simulated S_{11} for Case (v)

From the above parametric analysis, it is clearly shown that, by tuning various parameters of IDC, the resonant frequency can be fine-tuned to any frequency inside the band of interest. This is demonstrated in next section, through simulation study, by incorporating a varactor diode between the fingers of IDC.

4.5 Fine tuning of Narrow-Band Responses

The capability of the antenna to fine-tune the frequency response is demonstrated in this section. For achieving tunability, a varactor diode with a dynamic range of 0.1-0.7pF is placed between the fingers of, one of the IDC, which is connected to ground plane by PIN diodes, D1 and D2, as shown in Fig. 4.10. Both the diodes are switched ON and simulations are carried out with and without the varactor diode.
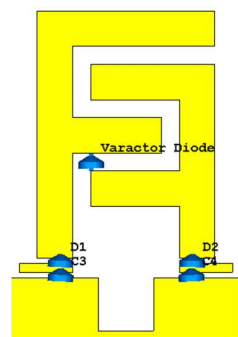
Fig. 4.10. IDC with Varactor diode
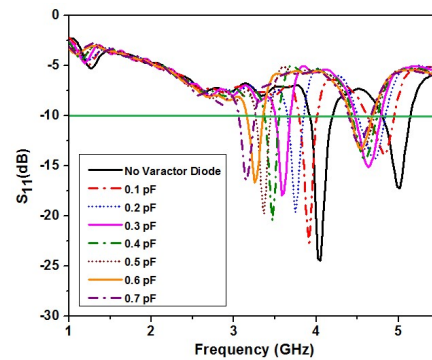
Fig. 4.11. S_{11} for different values of varactor capacitance

The simulated reflection coefficient plot is shown in Fig. 4.11. The antenna resonate at 4 GHz and 5 GHz, without varactor diode. As the varactor capacitance value increases stepwise, from 0.1-0.7pF, the resonant frequency at 4 GHz gets tuned through 3.9, 3.76,

49

3.6, 3.47, 3.37, 3.26 and 3.15 GHz. Thus, it is clearly shown that, as the capacitance value increases, the resonant frequency gets shifted to lower band.

It is to be noted that, when the capacitance value varies from 0.2-0.7pF, only lower band is shifted by keeping higher band resonance, constant at 4.5 GHz. Thus the antenna resonance can be switched using PIN diodes and each resonant frequency can be fine-tuned independently, to any frequency, with in the band of interest.

4.6 Antenna Biasing and Fabrication

The antenna is fabricated using substrate material FR4 with $\varepsilon_r = 4.3$ and thickness 1.6 mm. To avoid coupling of the RF signal and the DC bias current, a proper biasing circuit is provided, as shown in Fig. 4.12.
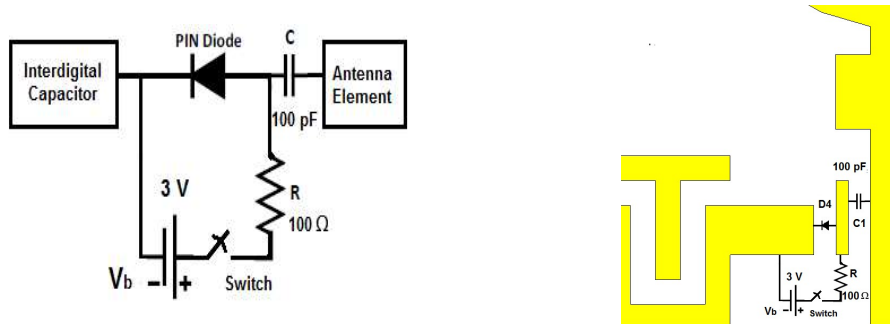
Fig. 4.12. Biasing circuit for PIN diode
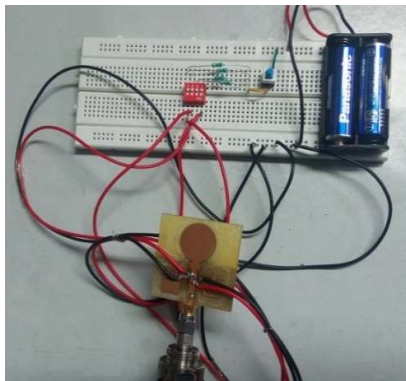
Fig. 4.13. Fabricated antenna
with biasing circuit and switch module.
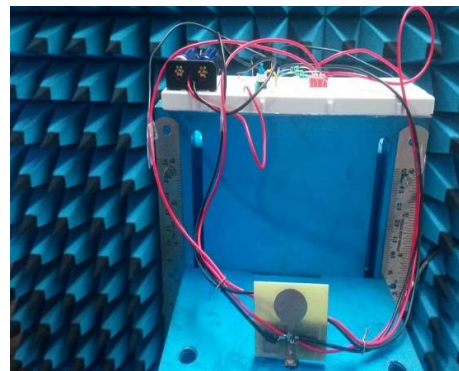
Fig. 4.14. Antenna parameter
measurement setup inside anechoic chamber

Fabricated antenna along with biasing circuit and switch module is shown in Fig.4.13. Surface mount capacitors of 100pF, provided by Murata Manufacturing, were used for blocking DC bias current. Series resistance of 100Ω was used to limit the maximum

bias current through diode. The biasing voltage of 3V is provided by a series combination of two AA batteries of 1.5V each. Slide type switch module is used for switching diode.

For biasing, a small piece of copper patch is placed between antenna feed line and interdigital capacitor, as shown in Fig. 4.12. Surface mount capacitor C1 of 100 pf is placed between small copper patch and feed line for blocking DC current from battery to flow into antenna. PIN diode D4 is connected from small copper patch to interdigital capacitor. Positive of the battery is connected through a switch and current limiting resistor of 100 Ω to the anode of PIN diode. Negative of battery is connected to interdigital capacitor, where cathode of diode is connected. Same circuit is used for other diodes also. Fig.4.14 shows the measurement setup for the fabricated antenna parameters in an anechoic chamber.

4.7 Simulated and Measured Results

The values of simulated and measured reflection coefficients, corresponding to 16 different cases of diode switching configurations are tabulated in Table 4.1. and are shown in Fig.4.15 to Fig.4.30. The diode ON condition is represented by "1" and OFF condition by "0".

Table 4.1: Diode switching conditions for tuning frequency responses of the reconfigurable antenna

Cases	Diode switching conditions				Frequency Response (GHz)	Impedance Bandwidth Range (GHz)
	D1	D2	D3	D4		
Case 1	0	0	0	0	UWB	(2.8 – 10.6)
Case 2	1	0	0	0	2.8, 5.8, 8.7	(2.5 – 3.1), (4.8 – 6.8), (7.8 – 8.8)
Case 3	1	1	0	0	3.8, 4.6, 7	(3.7 – 4.1), (4.2 – 5.4), (6.5 – 7.7)
Case 4	0	0	1	0	3.3, 6.5, 8.8	(2.8 – 3.6), (5.6 – 7.5), (8.5 – 10.5)
Case 5	1	1	1	0	3.9, 5.2	(3.6 – 4.1), (5.1 – 5.5)
Case 6	1	0	1	1	3.3, 4, 6.3	(3 – 3.6), (3.8 – 4.2), (6.1 – 6.6)
Case 7	0	1	1	1	3.4, 4.3, 5.2, 7.3, 9	(3.3 – 3.7), (4.2 – 4.5), (4.9 – 5.5), (7 – 7.5), (8.7 – 9.3)
Case 8	1	1	1	1	3.3, 4, 5.1, 7.4	(3.1 – 3.7), (3.8 – 4.2), (5 – 5.3), (7.3 – 7.6)
Case 9	0	0	0	1	3.3, 5.3, 6.1, 7.5, 8.5, 10.3	(3 – 3.5), (4.5 – 5.5), (5.6 – 6.3), (7.3 – 7.6), (8.2 – 9), (9.6 – 10.6)

Case 10	0	0	1	1	3.4, 4.4, 7.4	(3.2 – 3.8), (4.2 – 4.5), (7.2 – 7.5)
Case 11	0	1	0	1	3.3, 4.5, 5.9, 7.7	(2.6 – 3.6), (4.2 – 5), (5.8 – 6.2), (7.2 – 8.4)
Case 12	0	1	1	0	3.1, 4.4, 5.6, 7.4, 9.2	(2.6 – 3.5), (4.1 – 4.5), (5.1 – 6.1), (7 – 7.6), (8.1 – 9.8)
Case 13	0	1	0	0	2.8, 4.5, 7.1	(2.2 – 3.4), (4.1 – 5), (6.5 – 7.5)
Case 14	1	0	0	1	3.1, 6.1, 7.1, 9.5	(2.6 – 3.6), (5.6 – 6.6), (7 – 7.5), (9 – 10.2)
Case 15	1	0	1	0	3.3, 6.4	(2.7 – 3.7), (5.8 – 7.4)
Case 16	1	1	0	1	3.3, 4.8	(3 – 3.6), (4.3 – 5.3)
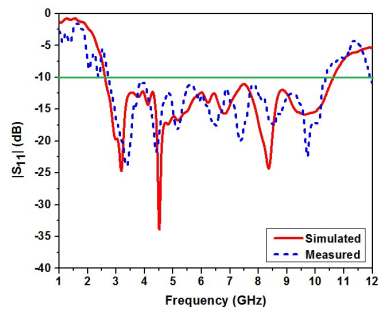
Fig. 4.15. Simulated and measured **S$_{11}$** for Case 1
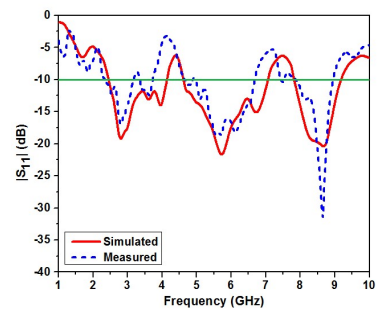
Fig. 4.16. Simulated and measured **S$_{11}$** for Case 2
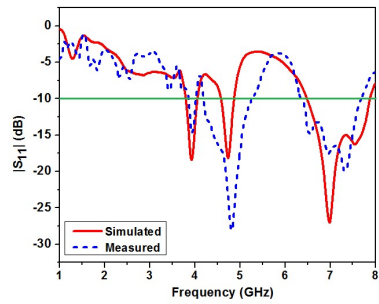
Fig. 4.17. Simulated and measured **S$_{11}$** for Case 3
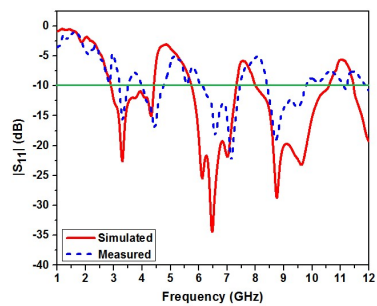
Fig. 4.18. Simulated and measured **S$_{11}$** for Case 4
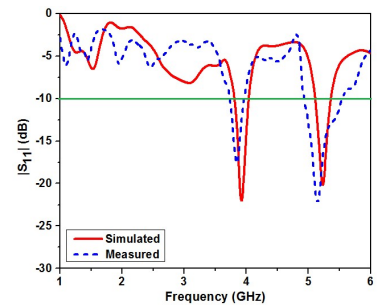
Fig. 4.19. Simulated and measured **S$_{11}$** for Case 5
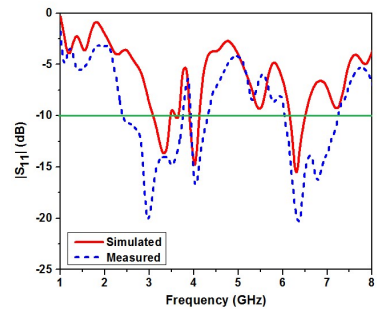
Fig. 4.20. Simulated and measured **S$_{11}$** for Case 6
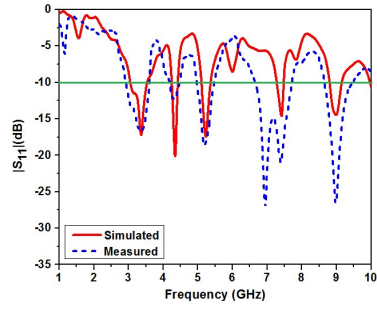
Fig. 4.21. Simulated and measured S_{11} for Case 7
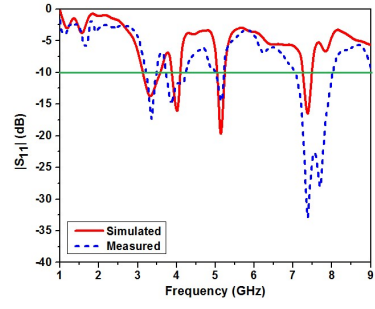
Fig. 4.22. Simulated and measured S_{11} for Case 8
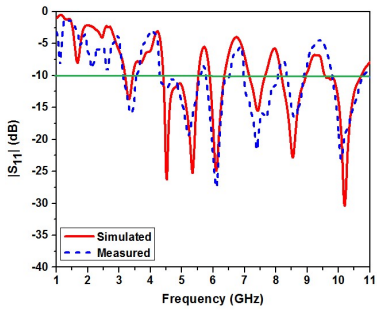
Fig. 4.23. Simulated and measured S_{11} for Case 9
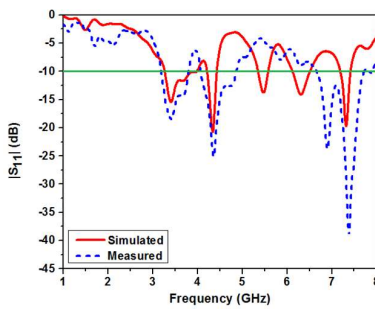
Fig. 4.24. Simulated and measured S_{11} for Case 10
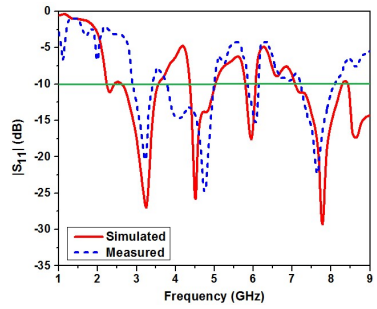
Fig. 4.25. Simulated and measured S_{11} for Case 11
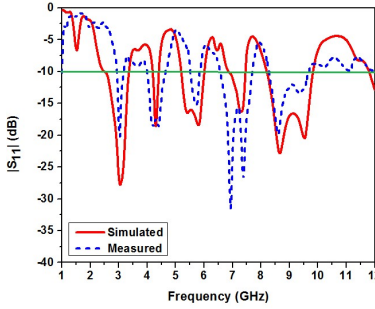
Fig. 4.26. Simulated and measured S_{11} for Case 12
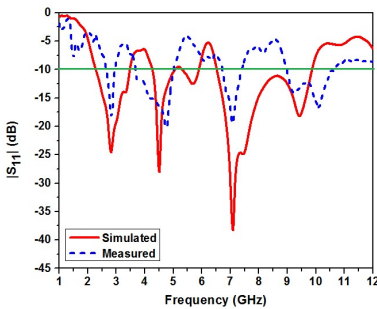
Fig. 4.27. Simulated and measured S_{11} for Case 13
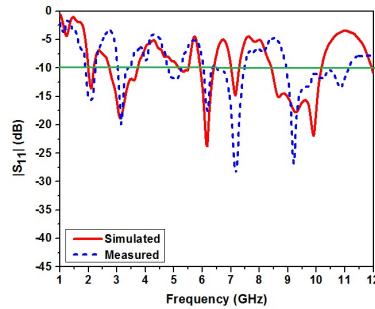
Fig. 4.28. Simulated and measured S_{11} for Case 14
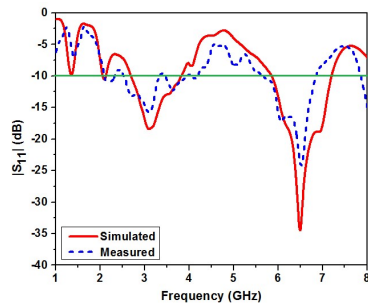
Fig. 4.29. Simulated and
measured S_{11} for Case 15
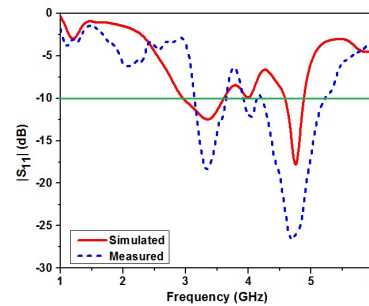
Fig. 4.30. Simulated and
measured S_{11} for Case 16

From the simulation results it is to be noted that, by using 16 diode switching conditions, the antenna can be switched between UWB and 36 different narrow-band frequencies, with in the band, spanning from 3.1 to 10.6 GHz. Since this is a reconfigurable antenna, random switching of PIN diode is carried out to show the capability of switching between UWB and any number of narrow band frequencies, within the band of interest. Depending upon the requirement of application, any specific resonant frequency can be obtained by varying the dimension of the physical parameters of IDC or by tuning its capacitance using varactor diodes.

The difference in the simulated and measured result of the prototype is mainly attributed to the inaccuracy of the substrate parameter, selection of ideal environment for simulation, fabrication error and assembly error due to the inclusion of the biasing circuit along with external power supply etc. Since we have designed electronically reconfigurable antenna, in additions to the above mentioned factors, there are some exceptional factors which may be adversely affect the measured result of our work:-

i) PIN diodes (length 0.3 mm) and DC blocking RF capacitors (length 1.6 mm) are manually soldered, which resulted in uneven accumulation of solder on the patch. Hence for better accuracy of result, soldering quality has to be improved.

ii) The internal parasitic capacitance of PIN diode will result in leakage of RF current during OFF condition and thereby variation in result. Hence to get better result, PIN diode with lower value of parasitic capacitance has to be selected during fabrication.

iii) Interference of the RF signal with the biasing circuit and its power supply may also result in variation of measured values.
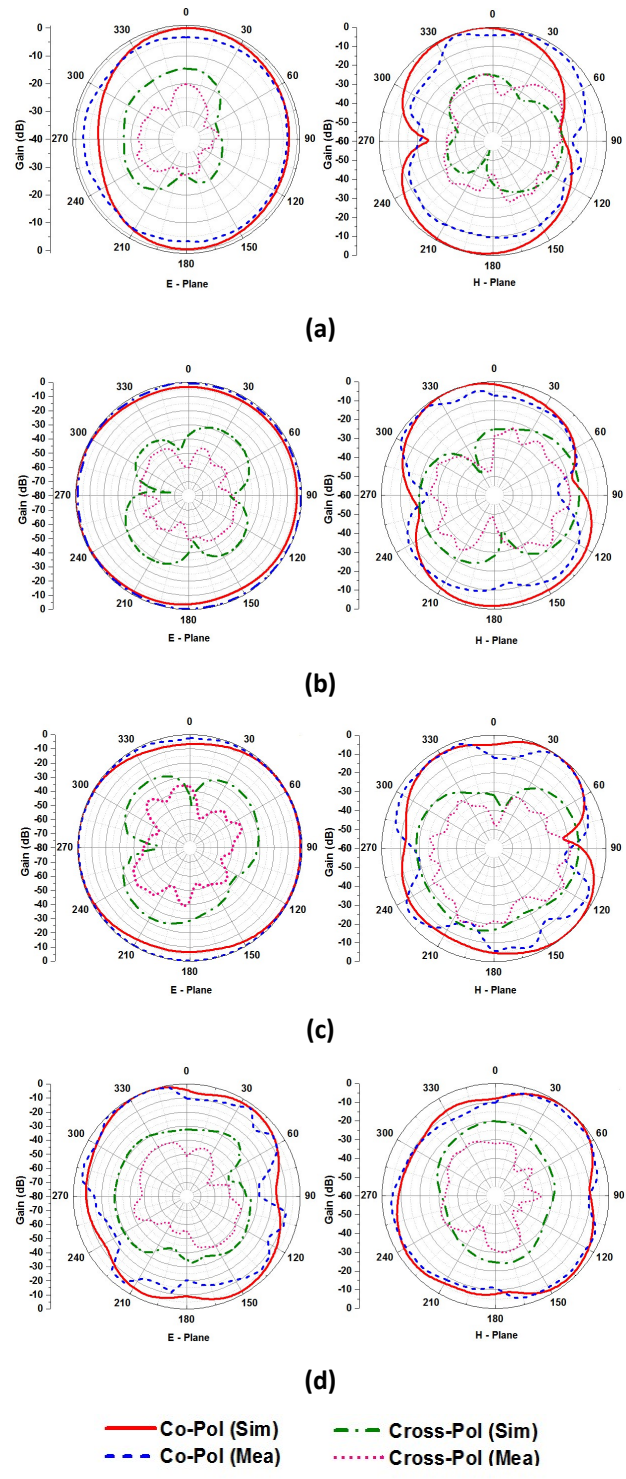
Fig. 4.31. Simulated and Measured E-plane and H-plane radiation patterns for the UWB response at frequencies, (a) 4.5 GHz (b) 6.5 GHz (c) 7.5 GHz (d) 9.5 GHz.

The E-plane and H-plane radiation patterns for UWB response are shown in Fig.4.31. Co-pol as well as cross-pol measurements are also shown. The E-plane and H-plane radiation patterns for narrow band response at 4 GHz for case 6 (D1, D3 and D4 - ON) is shown in Fig.4.32. The surface current distributions for various diode conditions are shown in Fig.4.33.
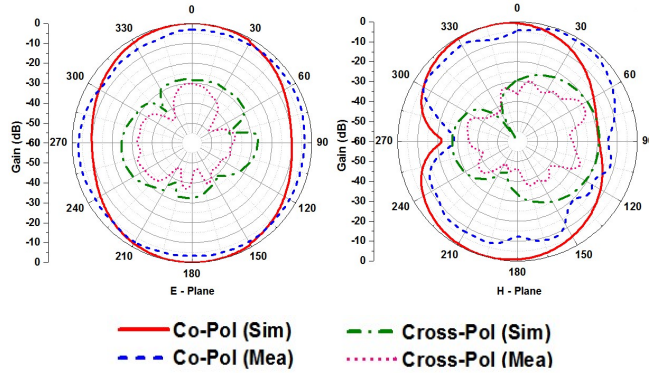
Fig. 4.32. Simulated and Measured E-plane and H-plane radiation patterns for the narrow band response of case 6 (D1, D3 and D4 – ON) at 4 GHz.
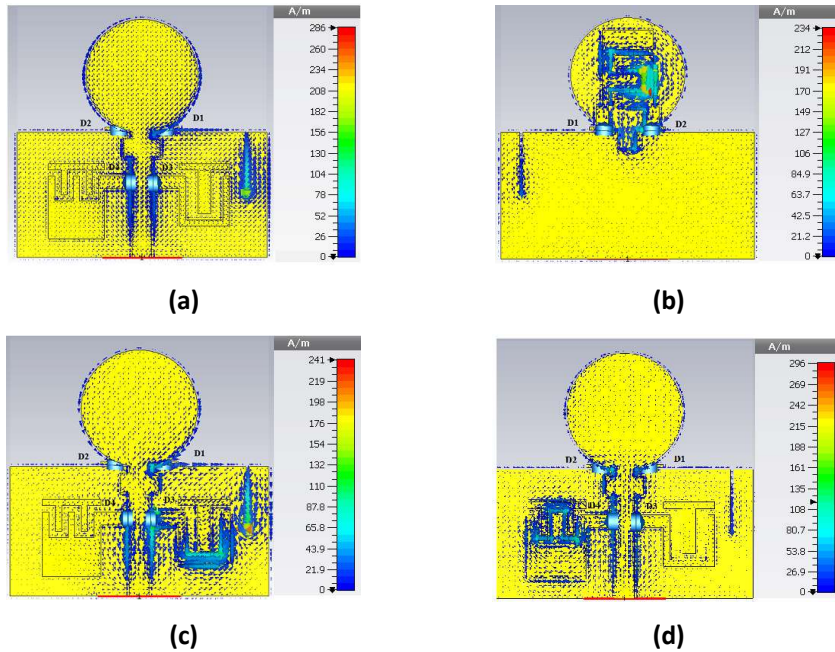
Fig. 4.33. Surface current distribution for different diode switching cases:
(a) All diodes OFF – UWB response (b) D1 and D2 – ON (c) D3 – ON (d) D4 – ON

Table 4.2 represents a detailed comparative study of this work with similar previous works. It shows that proposed antenna exhibits better performance than other works.

Table 4.2: Comparative study of this work with similar previous works works on frequency reconfigurable antennas

References	Parameters			
	Antenna dimension (mm)	Mechanism for switching and tuning	UWB Response (GHz)	No. of Narrow Bands
James R. Kelly et al. [2010]	110 x 30	PIN diodes	(3.1 – 10.6)	1
Eko Tjipto et al. [2011]	140 x 80	PIN diodes	(1.35 – 11.7)	2
K. Kandasamy et al. [2015]	40 x 40	PIN diodes	(3 – 10)	1
G. P Jin et al. [2011]	49 x 33.5	Photoconductive switches	(2.65 – 10.3)	3
Y. Tawk et al. [2011]	70 x 50	Mechanical switching	(2 – 10)	5
Hamid Boudaghi et al. [2011]	40 x 40	PIN diodes	(3.1 – 10.6)	4
A. Mansoul et al. [2014]	68 x 51	PIN diodes	(2.64 – 3.7)	4
I. H. Idris et al. [2014]	88 x 83	PIN diodes	(2 – 6)	3
M. Nejatijahromi et al. [2018]	24 x 30.5	Variable capacitor	(3.1 – 10.6)	2
Chinmoy Saha et al. [2018]	50 x 50	PIN diodes	(2.6 – 10.8)	3
Bei-Jia Liu et al. [2018]	23.5 x 31.5	PIN and varactor diodes	(3.82 – 8.94)	1
This Work	**40 x 40**	**PIN and varactor diodes**	**(2.8 – 10.6)**	**36**

4.8 Summary

A frequency reconfigurable antenna is presented, which can be tuned to UWB as well as many narrow band frequencies. It comprises of a compact monopole antenna with a partial ground plane. Three interdigital capacitors are electrically connected to the ground plane and feed line using PIN diodes. The antenna can be used in CR application, in the "sensing mode" which needs the UWB response. The same antenna can be operated in "communicating mode" by switching and selecting any band, out of the 36 narrow bands. A parametric analysis of IDC is carried out, through which it has been clearly shown that, the resonant frequency can be independently fine-tuned to any frequency inside the band, 2.8 to 10.6 GHz. This can be considered as a unique feature of the proposed antenna. Simulated and measured results show that the proposed antenna is a promising candidate for cognitive radio based IoT applications in 5G wireless communication networks.

CHAPTER 5

BANDWIDTH AND POLARIZATION SWITCHABLE ANTENNA

The fast growing desires in the field of wireless communication, demands the reduction in size of antenna, along with its ability to support multiple standards and multiple operations handled by single antenna. Cognitive Radio (CR) service is one such application that requires adaptability to the change in communication environment, standards, application and data rates. In case of a change in data rate, would require a change in system bandwidth to match with signal bandwidth, in order to maintain desired performance. Antenna having wider bandwidth than signal bandwidth, requires separate RF filters in order to filter out the out-of-band signal. If the antenna itself is capable of reconfiguring the bandwidth, then the RF filters at the front end can be avoided. The smart inclusion of resonant metamaterial structures into the antenna is a widely used method to improve the performance of antenna. Inclusion of the metamaterial structure, Split Ring Resonator (SRR) or its complementary part, Complementary Split Ring Resonator (CSRR), will exhibit negative permeability (μ) or negative permittivity (ε), respectively, which will alter the normal resonant condition of antenna.

This work presents a bandwidth reconfigurable, circularly polarized monopole antenna loaded with omega shaped complementary split ring resonator (omega-CSRR). The antenna can switch between UWB and narrow-band response at 6GHz.

5.1   Theory and Design Approach

Negative Index Metamaterials (NIMs) can be realized using artificial structures like SRR or CSRR, which will result in negative permeability or negative permittivity in the medium to obtain a stop band at the frequency of interest. Circular SRR and CSRR along with their equivalent circuits are shown in Fig. 5.1 [J. D. Baena et al. 2005]. SRR

can be excited by an axial magnetic field which in turn induce currents oscillating between the two rings of the SRR, which yield a resonance and prohibits signal propagation at that frequency. Similarly, CSRR can be excited by axial electric field to obtain stop band. A circular CSRR is designed and placed in the ground plane of antenna to produce stop band response at desired frequency. This stop band is tuned in order to control the bandwidth of narrow-band response.

Equivalent values of inductance and capacitance of CSRR are calculated using the design equations of SRR of same dimensions.
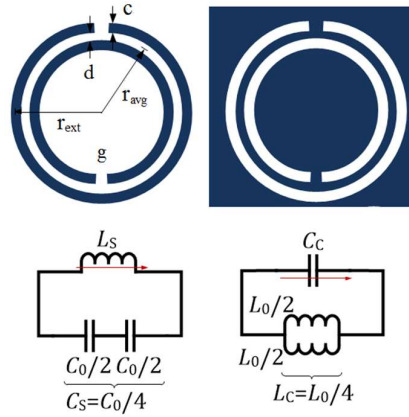
Fig. 5.1. Circular SRR and CSRR along with their equivalent circuits

The resonant frequency of SRR (f_{SRR}) with specified dimensions, is given by the following equation [Chinmoy Saha et al. 2012]:

$$f_{SRR} = 1 / 2\pi\sqrt{L_s\, C_s} \tag{5-1}$$

where, L_s and C_s are the effective inductance and capacitance.

$$L_s = 0.0002\, l\, (2.303 \log_{10}\left[\frac{4l}{c}\right] - 2.451)\ \mu H \quad \text{and} \quad C_s = \left[\frac{\pi\, r_{avg}\, C_{pul}}{2} + \frac{\varepsilon_0\, ch}{2g}\right] \tag{5-2}$$

where, c is the width of the ring and l is the length of the outer ring given by,

$$l = 2\pi\, r_{ext} - g,$$

$C_{pul} = \dfrac{\sqrt{\varepsilon_e}}{c_0\, Z_0}$ is the capacitance per unit length between the inner and outer rings of SRR, r_{ext} is the external ring radius, r_{avg} is the average ring radius, g is the split gap dimension of the ring, h is the thickness of the substrate, c_0 is the velocity of light, Z_0 is the characteristic impedance and ε_e is the effective permittivity.

It follows from duality that the parameters of the circuit models for the SRRs and CSRRs are related by the following equations:

$$C_c = 4\left[\frac{\varepsilon_0}{\mu_0}\right]L_s, \qquad C_s = C_o/4, \qquad C_o = 4\left[\frac{\varepsilon_0}{\mu_0}\right]L_o \quad \text{and} \qquad L_c = L_o/4 \qquad (5\text{-}3)$$

From the above equations, value of effective L_c and C_c of CSRR can be calculated. Resonant frequency of CSRR (f_{CSRR}) is given by the following equation:

$$f_{CSRR} = 1/2\pi\sqrt{L_c\,C_c} \qquad (5\text{-}5)$$

5.2 Antenna Geometry and Design

A circular monopole patch with partial ground plane is selected for the design of antenna. The top view and bottom view of the proposed antenna are shown in Fig.5.2 (a) and (b). All dimensions shown are in mm. The substrate material used is FR4 with ε_r=4.3 and loss tangent=0.025. The height of the substrate is 1.6mm. Thickness of the copper is 35 μm. Radius of the circular monopole is 9mm. W=L=40mm and width of all slots=0.2mm.

An Omega (Ω) shaped CSRR is designed for a resonant frequency of 4.16 GHz and its dimensions are shown in Fig.5.1. Here, "r_o=2.6mm" is outer ring radius, "r_i=2.2mm" is the inner ring radius and "g=0.2mm" is the split gap dimension. The width of both rings, c=0.2mm and separation between the rings, d=0.2mm. Four PIN diodes, D1, D2, D3 and D4 are used for tuning the bandwidth, as shown in Fig.5.2 (b).

(a)   (b)
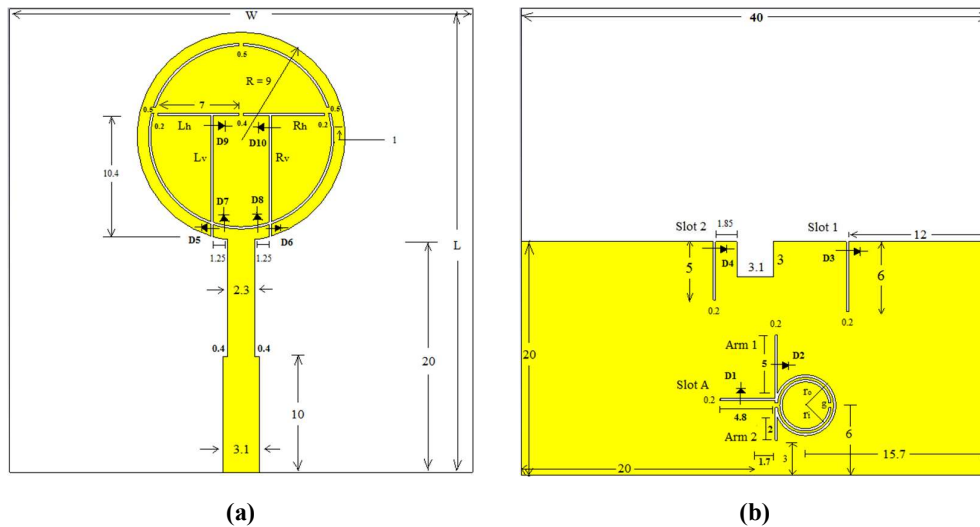
Fig. 5.2. Antenna with diode – (a) Top View, (b) Bottom View (All dimensions are in mm)

CSRR is loaded on the ground plane close to the feed line and Slot A is connected to CSRR using PIN diode D1, whose length extends to cross the feed line from underneath to obtain maximum coupling. Switching on the diode D1, which is placed on Slot A, below the feed line, will result in UWB response. Hence for all other switching cases of narrow band response, D1 should be OFF. Arm 1 and Arm 2 are two slots connected to CSRR, which forms the Ω shape. Arm 1is connected to CSRR using PIN diode D2. This slot when connected to CSRR, by switching OFF the diode D2, will increase the effective capacitance Cc, resulting in shifting of notch band towards the lower frequency band, thereby varying the impedance bandwidth.

In addition to this, two slots, Slot1 and Slot2 are cut on the ground plane and loaded using PIN diodes D3 and D4 respectively, to control the lower and upper band limit of the impedance bandwidth. 6 PIN diodes, D5, D6, D7, D8, D9 and D10 are placed across the slots on the disc of the monopole antenna for switching the sense of circular polarization (CP), as shown in Fig.5.2 (a).

5.3 Circular Polarization

Circularly polarized antennas shows better performance in reducing signal loss due to polarization mismatch. On the disc of the monopole antenna, 4 slots, L_h, L_v, R_h and R_v are connected to a semicircle slot to obtain switchable circular polarization, Left Hand Circular Polarization (LHCP) and Right Hand Circular Polarization (RHCP), at 6 GHz. These T-shaped slots excites the two orthogonal modes in phase quadrature for circular polarization. The slots L_v and R_v are designed of length $\lambda/4$, All four slot lengths are optimized to obtain CP centered at 6GHz with CP bandwidth of 1 GHz and a fractional axial ratio bandwidth of 16.7%.

Switching conditions of 6 PIN diodes, D5, D6, D7, D8, D9 and D10, determines the LHCP/RHCP state of the radiation pattern of antenna. When the left vertical slot, L_v is connected to circumference of the circular patch of the monopole antenna, by switching OFF the diode D5, then RHCP is obtained and when the right vertical slot, R_v is connected to the circumference of the circular patch, by switching OFF diode D6, then LHCP is obtained.

62

5.4 Antenna Biasing and Simulation Study

The simulation of antenna is carried out in CST Microwave Studio environment. In CST, PIN diode can be modelled using lumped elements. During simulation, the ON condition of diode can be realized by a series resistance of 1 Ω and OFF condition can be modelled by series resistance of 10^6 Ω. For fabrication, the actual internal parasitic component values of the PIN diode has to be taken into consideration. The equivalent circuit of the PIN diode, MADP-000907-14020W (MACOM Technology Solutions Inc.), used in this design is shown in the Fig.4.4 in section 4.3. During the simulation, the diode has to be re-modelled using these lumped element values, before fabrication. Capacitors having value 100 pF is modeled using lumped elements, for the purpose of DC blocking.
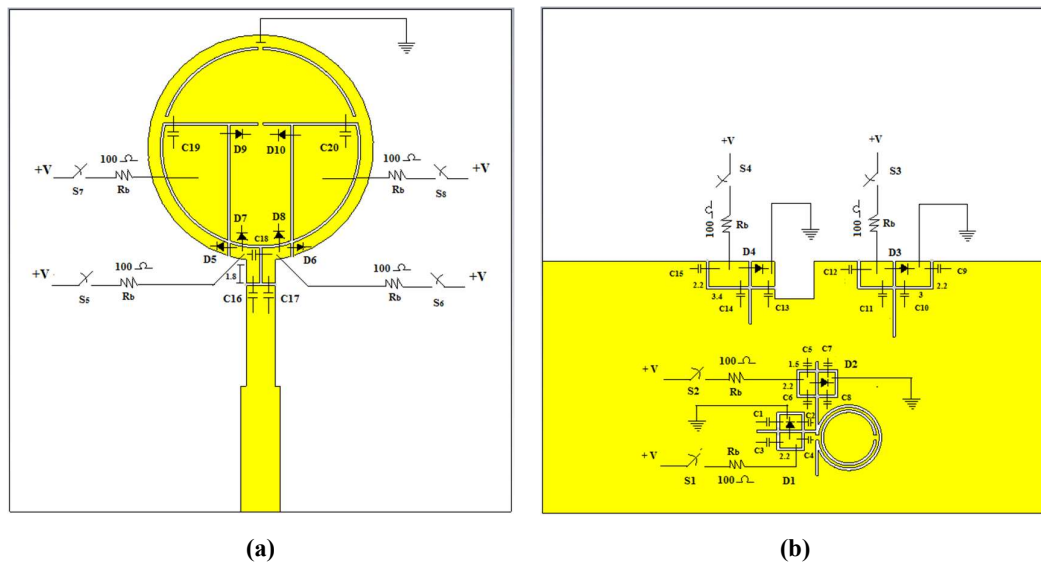
Fig. 5.3. Antenna with biasing circuit – (a) Top View, (b) Bottom View.

The biasing circuit for antenna is shown in Fig. 5.3(a) and Fig. 5.3(b). For biasing, surface mount capacitors (C1, C2, ..… C20) of 100 pF each, were used for blocking DC bias current and series resistance (R_b) of 100 Ω was used to limit the maximum bias current through diode. S1, S2, ….. , S8 are switches connected to DC power supply (battery), for controlling PIN diodes, ON/OFF conditions.

5.5 Simulated and Measured Results

The simulated and measured results of reflection coefficients obtained, based on the different cases of diode switching are given in Table 5.1:

Table 5.1: Diode switching conditions for tuning bandwidth and polarization of the reconfigurable antenna

Cases	Diode switching conditions										Polarization sense at 6GHz	Axial Ratio Bandwidth (GHz) & (%)	Impedance Bandwidth (GHz) & (%)
	D1	D2	D3	D4	D5	D6	D7	D8	D9	D10			
Case I	1	1	1	1	1	0	1	0	0	1	LHCP	0.9 (15 %)	UWB (2.6 – 12)
					0	1	0	1	1	0	RHCP	1.36 (22.7 %)	
Case II	0	1	0	1	1	0	1	0	0	1	LHCP	1 (16.7 %)	1 (16 %)
					0	1	0	1	1	0	RHCP	1 (16.7 %)	
Case III	0	1	1	1	1	0	1	0	0	1	LHCP	1 (16.7 %)	2.6 (48.8 %)
					0	1	0	1	1	0	RHCP	1 (16.7 %)	
Case IV	0	0	1	1	1	0	1	0	0	1	LHCP	1 (16.7 %)	3.2 (61 %)
					0	1	0	1	1	0	RHCP	1 (16.7 %)	
Case V	0	0	1	0	1	0	1	0	0	1	LHCP	1 (16.7 %)	4.4 (73.3 %)
					0	1	0	1	1	0	RHCP	1 (16.7 %)	

> **Case I:** Since the diode D1 is ON, the CSRR loses its coupling with feed line and hence, UWB response results. Fig. 5.4 shows, the UWB response from 2.6GHz to 12GHz, with an impedance bandwidth, more than 9GHz. Each switching case have two sub-conditions for diodes D5, D6, D7, D8, D9 and D10, which determines the sense of circular polarization (LHCP/RHCP). 3 dB AR (Axial Ratio) band width of 900 MHz (Fractional AR band width=15%) and 1.36 GHz (Fractional AR band width=22.7%) are obtained for LHCP and RHCP respectively.

> **Case II:** Here, since the diode D1 is OFF, "Slot A" on the ground plane which is crossing the feed line from beneath, changes the current distribution, resulting in narrowband response centered at 6 GHz. Ω-CSRR resonates, resulting in a notch frequency band at 4GHz. This is lower than the designed value of 4.16 GHz, due to the presence of Slot A, which will increase the effective value of capacitance, Cc of CSRR, given in the equation (5-5), resulting in lowering the notch frequency. Since diode D3 is OFF, the Slot 1 will produce another notch band at 5GHz resulting in limiting the impedance bandwidth to 1GHz, centered at 6GHz. This is shown in Fig.5.5 and Fig.5.6. A percentage impedance bandwidth (fractional impedance bandwidth) of 16% is obtained, given by the equation, **[(F_h – F_l) / F_c] x 100**, where F_h is the upper band limit, F_l is the lower band limit and F_c is the center frequency. 3dB AR bandwidth of 1GHz is obtained for both LHCP and RHCP.

> **Case III:** Here, since diode D3 is ON, the notch band at 5GHz disappear, which will shift the notch band at 4 GHz to a lower value of 3.75 GHz. Hence the impedance bandwidth is increased to 2.6GHz, centered at 6GHz, as shown in Fig.5.5 and Fig.5.6. A fractional impedance bandwidth of 48.8% is obtained. 3dB AR bandwidth of 1GHz is obtained for both LHCP and RHCP.

> **Case IV:** Since diode D2 is OFF, length of the slot, Arm1 connected to Ω-CSRR, increases, which will increase the effective value of Cc. Hence stop band again shifts to lower frequency of 3.53GHz resulting in the increase of impedance bandwidth to 3.2GHz, centered at 6GHz. This is shown in Fig.5.5 and Fig.5.6. A fractional impedance bandwidth of 61% is obtained. 3dB AR bandwidth of 1GHz is obtained for both LHCP and RHCP.

> **Case V:** Since diode D4 is OFF, the current distribution through Slot 2 will shift the upper band limit of the narrow band from 6.9GHz to 8.1GHz and hence the impedance bandwidth further increases to 4.4GHz, centered at 6GHz, as shown in Fig.5.5 and Fig.5.6. A fractional impedance bandwidth of 73.3% is obtained. 3dB AR band width of 1GHz is obtained for both LHCP and RHCP.
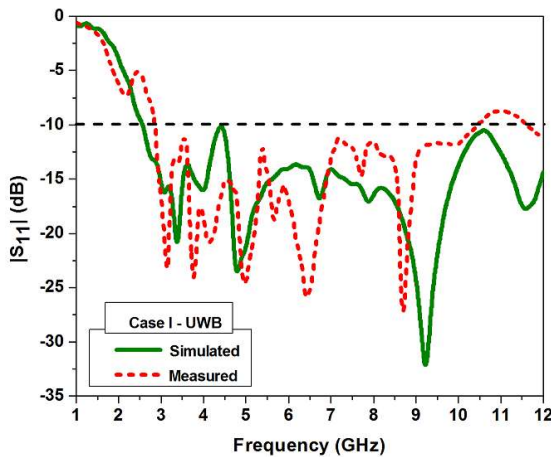
Fig. 5.4. S_{11} for Case I – UWB
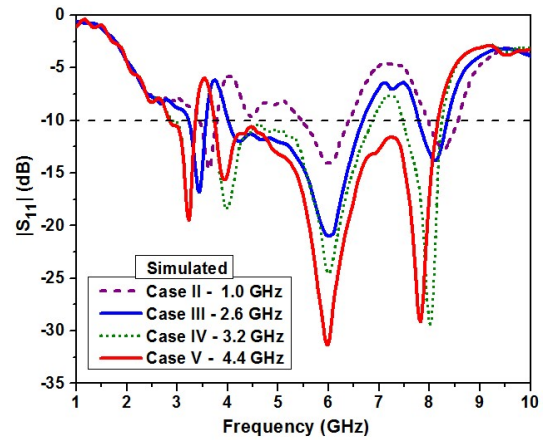
Fig. 5.5. Simulated S_{11} for Case II, III, IV & V

65
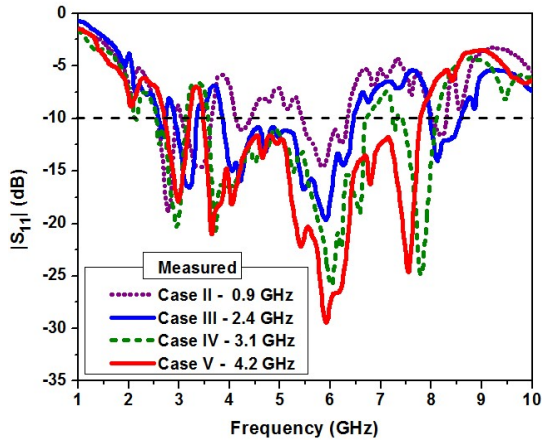
Fig. 5.6. Measured S_{11} for Case II, III, IV & V
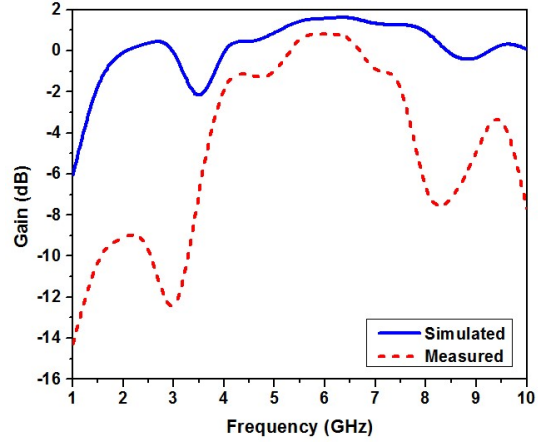
Fig. 5.7. Gain of the CP antenna
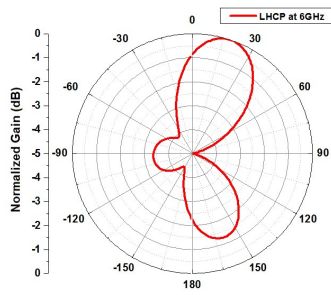
Fig. 5.8. Simulated LHCP pattern at 6 GHz
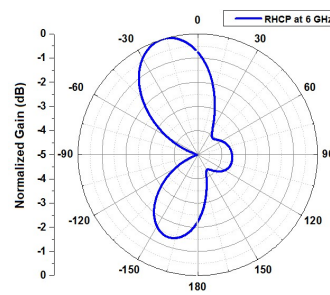
Fig. 5.9. Simulated RHCP pattern at 6 GHz
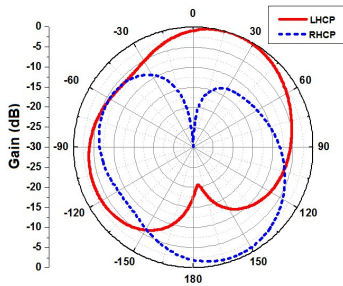
Fig. 5.10. E-Plane pattern at 6 GHz (LHCP)
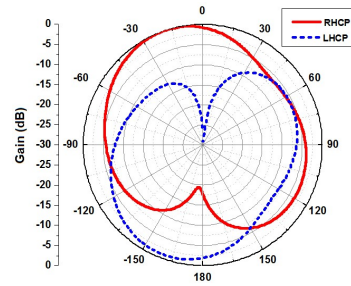
Fig. 5.11. E-Plane pattern at 6 GHz (RHCP)
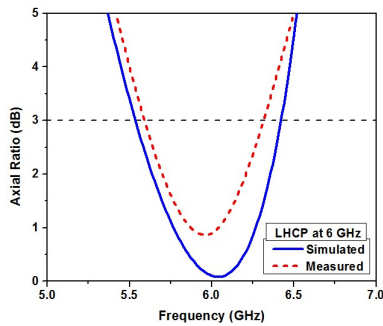
Fig. 5.12. Axial Ratio for LHCP at 6 GHz
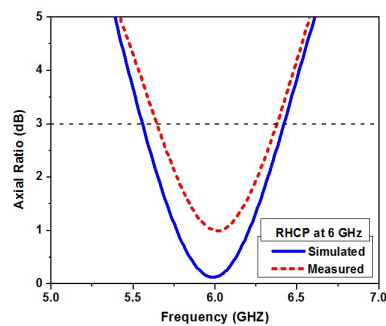
Fig. 5.13. Axial Ratio for RHCP at 6 GHz
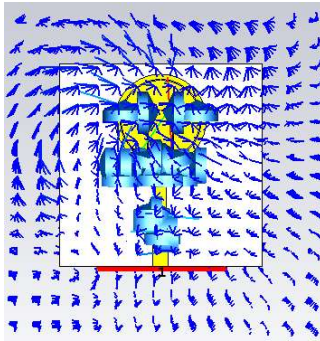
Fig. 5.14. E-Field distribution of LHCP at 6 GHz   **Fig. 5.15.** E-Field distribution of RHCP at 6 GHz
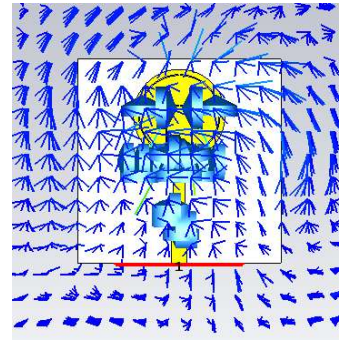
Fig.5.7 shows the gain (maximum gain of 1.5 dB) of the CP antenna. It is observed that the gain reduces at the stop band. Fig.5.8 and Fig.5.9 shows the simulated LHCP and RHCP field patterns of narrow band response at 6 GHz. Fig.5.10 and Fig.5.11 shows the E-Plane patterns of LHCP and RHCP radiation pattern at 6 GHz. Fig.5.12 and Fig.5.13 shows the axial ratio for LHCP and RHCP at 6 GHz, with an axial ratio bandwidth of 1 GHz, obtained as per the diode switching conditions shown in Table 5.1. Fig.5.14 and Fig.5.15 are the E-field distributions of LHCP and RHCP switching conditions. Thus, the antenna radiation exhibits both LHCP and RHCP, depending upon the switching conditions, without affecting the tuning of bandwidth.

(a)

(b)

(c)

(d)
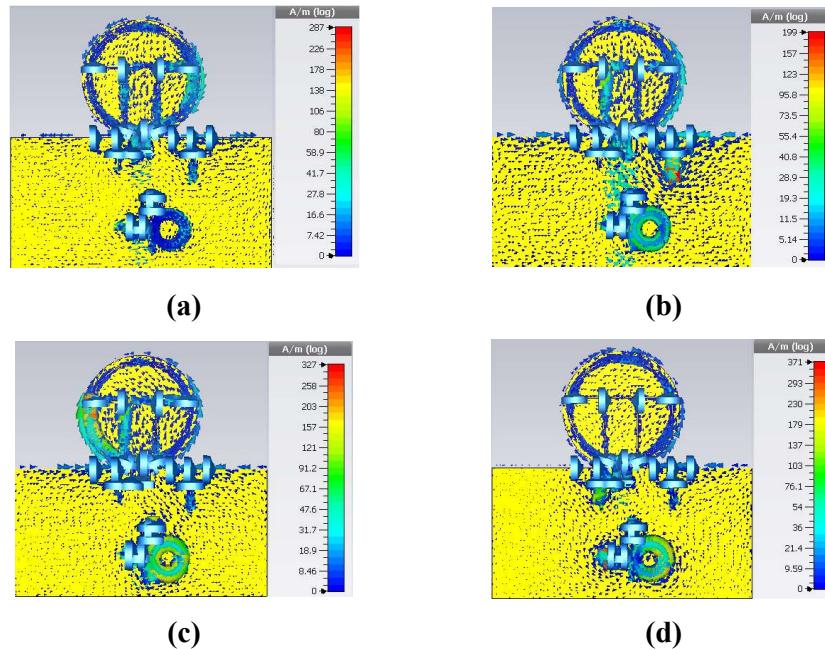
Fig. 5.16. Surface current distribution for different diode switching cases: (a) Case–I (UWB) at 6 GHz. (b) Case–II at 5 GHz. (c) Case–III and IV at 3.5 GHz. (d) Case–V at 8 GHz.

67
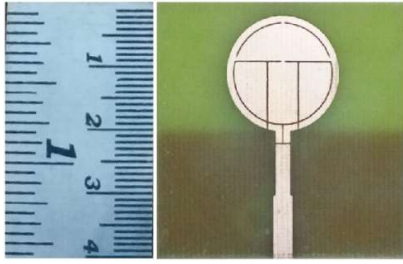
Fig. 5.17. Fabricated Antenna – Front view   **Fig. 5.18.** Fabricated Antenna – Back view
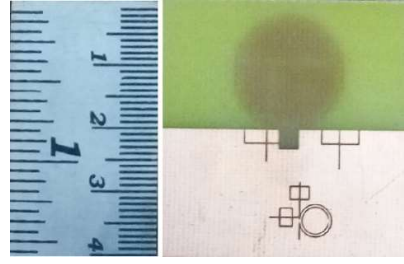
Fig.5.16 shows the surface current distributions for various cases of diode switching for LHCP radiation. Fig. 5.16 (a) represents the current distribution of case–I (UWB) where diode D1 is ON and hence CSRR is less coupled to feed line. Fig. 5.16 (b) represents current distribution of case-II. Here since D1 is OFF, it is shown that "Slot A" varies the current distribution and hence antenna resonates at 6GHz. The Ω-CSRR resonates. Also, it is shown that, since, D3 is OFF, "Slot 1" varies the current distribution and produces notch band at 5GHz. Fig.5.16 (c) represents current distribution of case-III and case-IV, which shows that, since D1 is OFF, antenna continues to resonate at 6GHz. In both these cases, either D2 is ON or OFF, Ω-CSRR resonates and produce notch band. Fig.5.16 (d) represents the current distribution for case-V. Here it is clearly shown that, since D4 is OFF, Slot 2 will vary the current distribution which results in shifting of upper band limit of the narrow band response, from 6.9GHz to 8.1GHz. Fabricated prototype of the antenna is shown in Fig. 5.17 and Fig. 5.18.

5.6   Summary

A compact bandwidth reconfigurable monopole antenna is designed, which can switch between UWB and narrow band responses. UWB response is obtained from 2.6GHz to 12GHz. The narrow band response obtained is centered at 6GHz and its impedance bandwidth of narrow band can be switched to 1GHz, 2.6GHz, 3.2GHz and 4.4GHz. Both the lower as well as upper band limits can be varied, whereby, the percentage impedance bandwidth is tuned from 16% to 73.3%, showing an increase in percentage bandwidth by a factor of 4.58. In addition to this, the antenna exhibits circular polarization which can be switched between LHCP and RHCP, with a fractional AR bandwidth of 16.7%. Bandwidth reconfigurable antennas are useful in applications which needs a change in bandwidth according to the varying data rate. The antenna can be used in Cognitive Radio as well as WiMAX and WLAN applications.

CHAPTER 6

ANTENNA GAIN ENHANCEMENT AND BEAM STEERING USING METASURFACE

One of the drawbacks of microstrip patch antenna is its low gain due to its low profile nature. There are various techniques to improve the gain of the antenna. One such method is to use zero phase reflection metasurface as reflector to the back scattered radiation, thereby achieving constructive interference of incident and reflected wave at far-field. For muti-resonant antennas, it is advantageous to use multi-band reconfigurable AMCs for the design of metasurface.

Antenna Beam steering can be achieved by using phase gradient metasurface as reflector for the back scattered radiation. This requires the integration of reconfigurability feature to the AMC unit cell in order to switch the reflection phase at the designed resonant frequency of antenna. Hence, the reflected waves at resonant frequency will have a linear phase gradient along the metasurface, resulting in tilting of the antenna beam at far field.

 The gain of the bandwidth reconfigurable circularly polarized antenna discussed in chapter 5 is found to be very low due to the low profile nature of the antenna. In this work, the gain of this antenna is enhanced by integrating a zero reflection phase metasurface. The design of zero phase metasurface is presented in section 3.4.1, using the AMC unit cell presented in section 3.2. In addition to this, a tunable phase gradient metasurface presented in section 3.4.2, using the same AMC unit cell is integrated with monopole antenna to obtain beam steering ability.

6.1 Gain Enhancement using Zero Phase Metasurface

From the simulation results, of circularly polarized monopole antenna shown in the Fig.5.7, it is clear that the gain is very low, since the back scattering is very high due to partial ground plane. In order to reflect the back scattered radiation and thereby

increasing the overall gain of antenna, a zero phase reflection metasurface is used as reflecting plane. The zero reflection phase unit cell, shown in Fig.3.3 is used to form 5x5 array AMC metasurface, shown in Fig.3.10.

For gain enhancement, radiated and reflected waves, should have identical phase. For this, the phase difference between them should be $2n\pi$, or distance, "d" between the antenna and metasurface should be "$n\lambda/2$", where "n" is an integer. Hence, metasurface is placed below the ground plane at a distance $d=\lambda/2$, which is 25mm here (resonant frequency is 6 GHz), as shown in Fig.6.1. The back scattered wave will thus undergo a total phase shift of 2π, between antenna and metasurface. All unit cells of the metasurface will give 0^0 reflection phase at 6 GHz. Thus the reflected wave will be in-phase with radiated wave, which will undergo constructive phase addition at far field resulting in enhanced gain. The overall size is 55mm x 55mm. The side and back view of antenna with AMC surface is shown in Fig. 6.2 and Fig.6.3.

Maximum gain of 6 dB is achieved due to the presence of metasurface. An increase of 4.5 dB gain achieved, compared to antenna without metasurface as shown in Fig.6.4. Radiation efficiency is plotted in Fig.6.5. The radiating beam direction is $+10^0$ to the normal for LHCP and -12^0 to the normal for RHCP switching conditions, as shown in Fig.6.7, Fig.6.8. Measured values are shown in Fig 6.9 and Fig. 6.10.
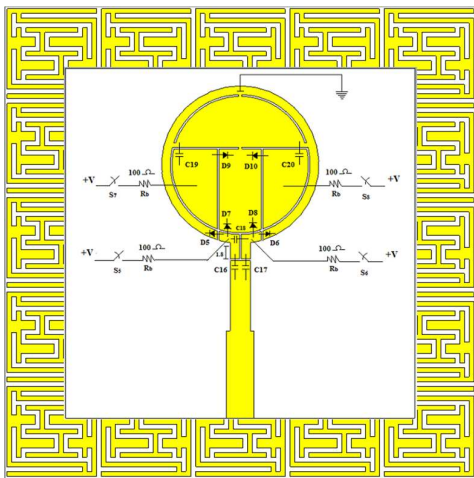
Fig. 6.1. Antenna backed by Zero Reflection Phase Metasurface - Front View.
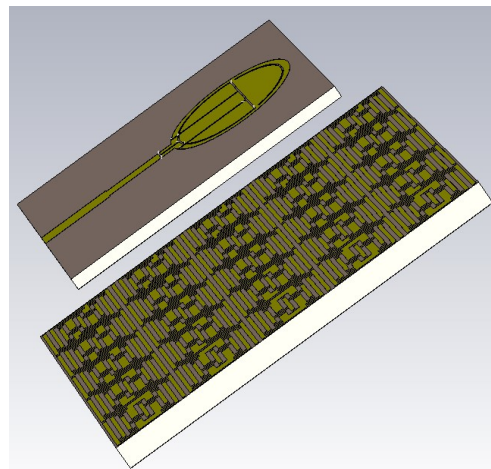
Fig. 6.2. Antenna backed by Zero Reflection Phase Metasurface - Side View
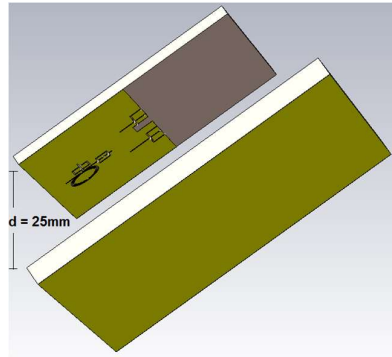
Fig. 6.3. Antenna backed by Zero
Reflection Phase Metasurface –Back View
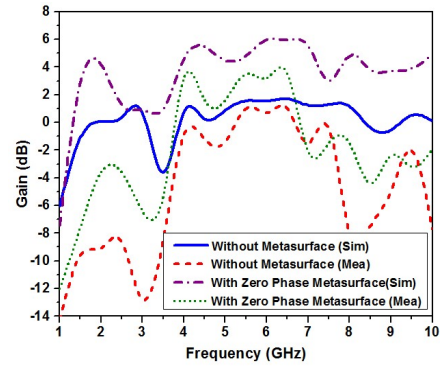
Fig. 6.4. Gain of the antenna
with & without AMC Metasurface
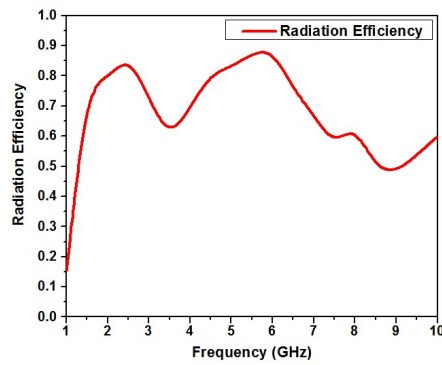
Fig. 6.5. Radiation Efficiency of the antenna

6.2   Antenna Beam Steering using Phase Gradient Metasurface

A linear phase gradient $(d\phi/dx)$ will reflect a normally incident microwave beam to an angle θr that depends on the magnitude of the gradient, given by the equation 1.8.
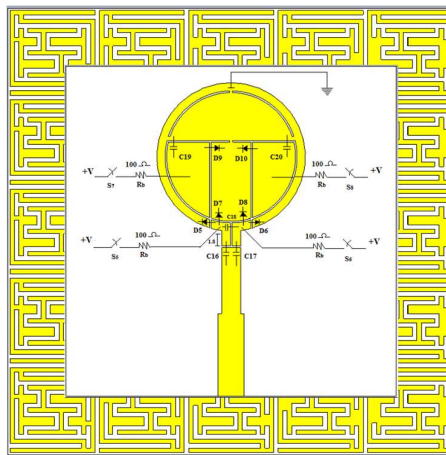
Fig. 6.6. Antenna backed by Phase Gradient Metasurface –Front View

As explained in section 3.4.2, five unit cells of different reflection phases, -120^0, -60^0, 0^0, $+60^0$ and $+120^0$, are selected and arranged in an array to design phase gradient metasurface. Its overall size is 55mm x 55mm, as shown in Fig. 3.15. It is then placed below the antenna ground plane at a distance d=λ/2, which is 25mm here, as shown in Fig.6.6.The beam of the antenna can be steered to $+23^0$ for LHCP and -27^0 for RHCP radiations, at frequency 6GHz, as shown in the Fig.6.7, Fig.6.8. Measured values are shown in Fig.6.9 and Fig.6.10.
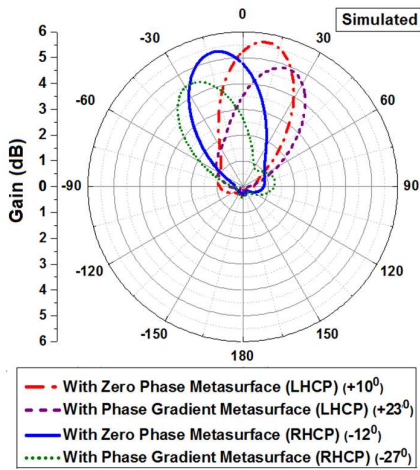
Fig. 6.7. Simulated steered beam
for LHCP and RHCP at 6 GHz
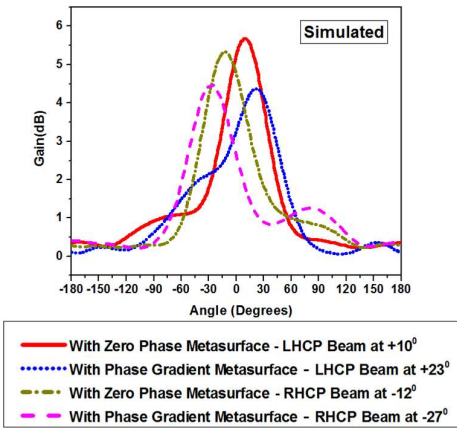
Fig. 6.8. Simulated steered beam (2D)
for LHCP and RHCP at 6 GHz
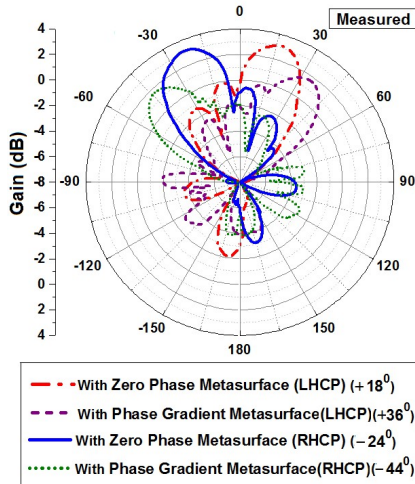
Fig. 6.9. Measured steered beam
for LHCP and RHCP at 6 GHz
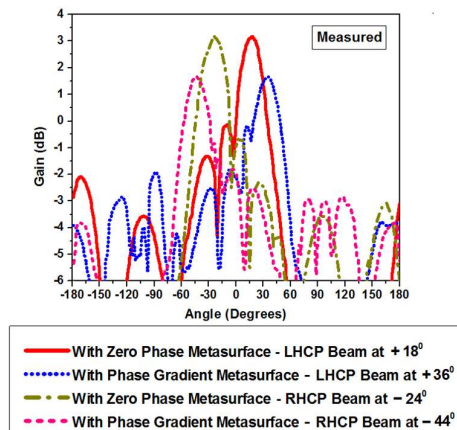
Fig. 6.10. Measured steered beam (2D)
for LHCP and RHCP at 6 GHz
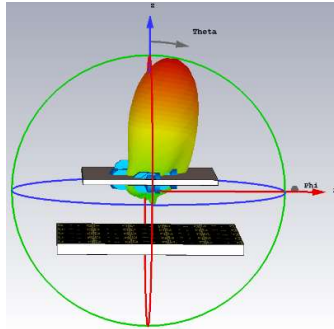
Fig. 6.11: LHCP Beam, with
Zero Phase Metasurface (3D) (+10^0)
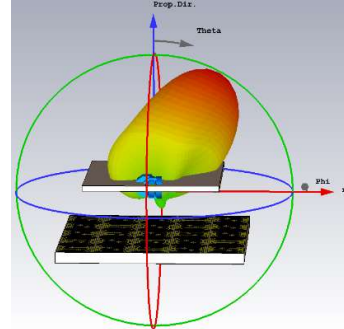
Fig. 6.12: LHCP tilted beam with
Phase Gradient Metasurface (3D) (+23^0)
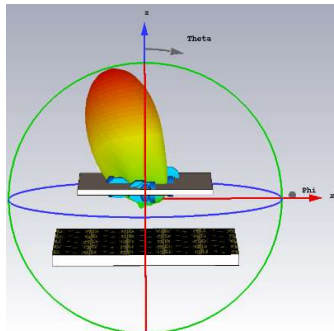
Fig. 6.13: RHCP Beam with
Zero Phase Metasurface (3D) (-12^0)
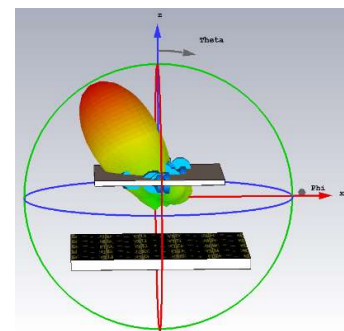
Fig. 6.14: RHCP tilted beam with
Phase Gradient Metasurface (3D) (-27^0)

The 3D radiation patterns are shown in Fig.6.10, Fig.6.11, Fig.6.12 and Fig.6.13. With zero reflection phase metasurface, placed at, d=25mm, below ground pane, the radiation has maximum gain and the beam direction is +10^0 to the normal for LHCP and -12^0 for RHCP switching conditions. Corresponding measured values are +18^0 and -24^0. On replacing the zero phase metasurface with phase gradient metasurface, the beam gets tilted to +23^0 for LHCP and -27^0 for RHCP, sense of polarizations, depending upon the switching condition. Corresponding measured values are +36^0 and -44^0. Thus a total range of 50^0 beam steering is achieved during simulation.

The distance "d", between antenna and metasurface can also be varied to change the phase of reflected wave for obtaining different set of beam angles for different sense of polarizations Unit cell slot dimensions of the metasurface can be varied for tuning the reflection phase and thereby beam steering angle.

A comparative study of this work, with similar previous works is shown in Table 6.1. It shows that proposed antenna exhibits better performance than other works.

6.3 Fabricated Antenna and Metasurface

Fabricated antenna is shown in Fig.6.14 and Fig.6.15. Fabricated AMC metasurfaces (zero phase and phase gradient) are shown in Fig.6.16 and Fig.6.17 respectively. Antenna with biasing circuit and the measurement setup inside anechoic chamber are shown in Fig.6.19 and Fig.6.19 respectively.
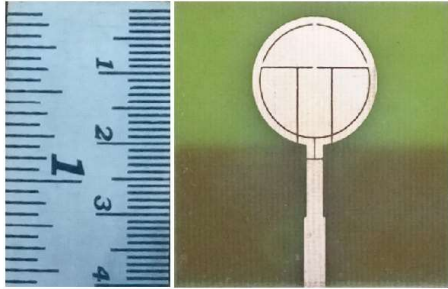
Fig. 6.15: Fabricated Antenna – Front view
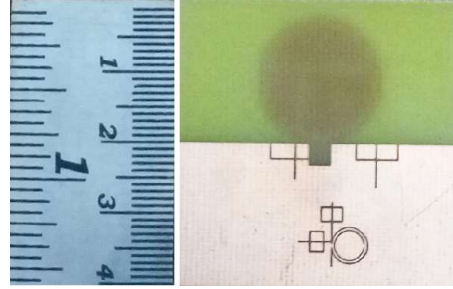
Fig. 6.16: Fabricated Antenna – Back view
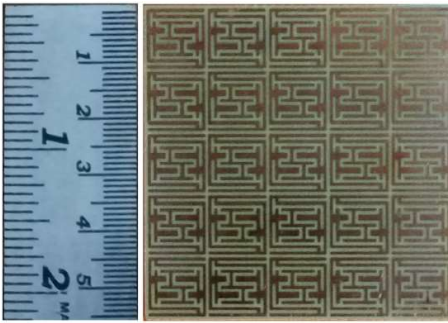
Fig. 6.17: Fabricated Zero Phase Metasurface
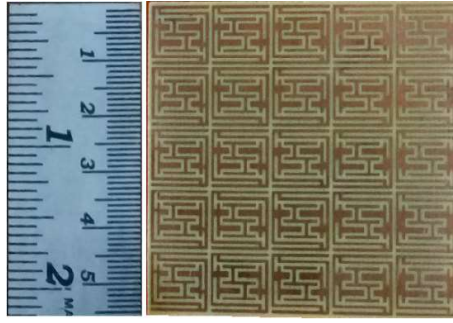
Fig. 6.18: Fabricated Phase Gradient Metasurface

Fig. 6.19: Biasing circuit for antenna backed by metasurface

74
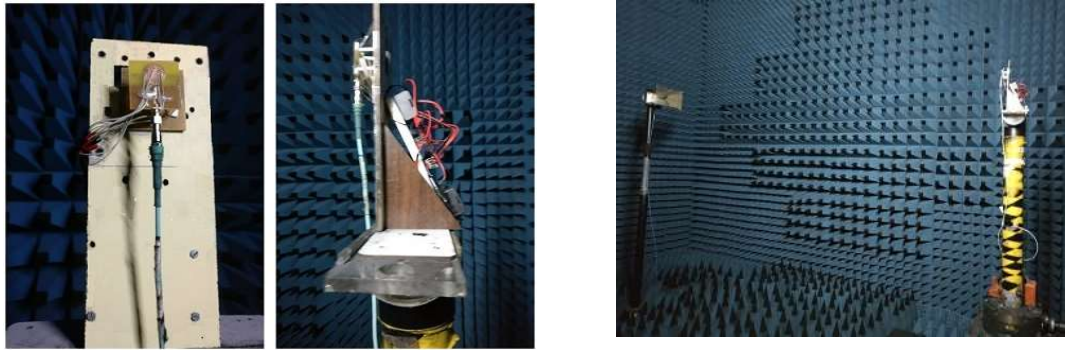
Fig. 6.20: Antenna measurements inside Anechoic Chamber

Table 6.1: Comparative study of this work with similar works on bandwidth reconfigurable antennas

References	Parameters				
	Antenna Dimensions (mm) and technique used	Bandwidth ranges and percentage bandwidth variation $[(F_h - F_l) / F_c]$ x 100	Switchable Polarization Sense	Beam Steering ability	Factor by which % bandwidth increased
Ali Mansoul et al. [2016]	Electronically reconfigurable antenna, Size : 56 x 54	810 MHz to 1870 MHz (43% – 76%)	Nil	Nil	1.77
Mohamed Alibakshi-Kenari et al. [2015]	"F" and "T" shaped antennas loaded with/without SRR, Size : 30 x 22	"F"antenna – 1.5GHz and 3.5GHz (31.5% – 75.4%)	Nil	Nil	2.39
Sasmitha Pahadsingh et al. [2017]	Electronically reconfigurable antenna, Size : 20 x 25.32	700 MHZ and 1200 MHz (7.2 % – 12.2%)	Nil	Nil	1.69
D. E. Anagnostou et al. [2017]	Chemically reconfigurable antenna loaded with VO_2 strips	380 MHz and 470 MHz (8% – 10%)	Nil	Nil	1.25
Linglong Meng et al. [2017]	Electronically reconfigurable antenna, Size : 70 x 30	600 MHz, 690 MHz and 1030 MHz (30.9% – 47.6%)	Nil	Nil	1.54
This work	**Electronically reconfigurable circular monopole antenna, loaded with Ω-CSRR, Size : 40 x 40**	**UWB (2.6–12 GHz) Narrow bands (1GHz, 2.6GHz, 3.2GHz and 4.4GHz) (16% –73.3%)**	**Switchable LHCP and RHCP**	**Yes**	**4.58**

6.4 Summary

A circularly polarized compact bandwidth reconfigurable monopole antenna is designed, which can switch between UWB (2.6-12 GHz) and narrow band responses centered at 6GHz, using PIN diodes. The impedance bandwidth of the narrow-band can be switched to 1GHz, 2.6GHz, 3.2GHz and 4.4GHz. A zero phase metasurface and a phase gradient metasurface are designed using the reconfigurable AMC unit cell and

integrated with the monopole antenna. Due to this, the back scattering is reduced and hence the gain is enhanced up to 4.5 dB more than that in the case of antenna without metasurface. Also, using the phase gradient metasurface, the beam of the antenna gets tilted, $+23^0$ to the normal for LHCP and -27^0 to the normal for RHCP resulting in a total beam steering range of 50^0. The antenna can be used in Cognitive Radio as well as WiMAX and WLAN applications.

CHAPTER 7

CONCLUSIONS AND SCOPE FOR FUTURE WORK

There is an increased demand for antennas that could be reconfigured, on the fly, for various applications and that could operate over a wide range of frequencies is urgently required in various fields such as cognitive radio services, industry, satellite communication, military, medical applications etc. This research focuses on designing novel, miniaturized antenna structures of low profile with desirable characteristics such as multiband and wideband reconfigurability features. In addition to this, the antenna should be capable of steering its beam in any desired direction with considerable gain, to increase its radiation performance. For this, the resonant properties of metamaterial and their ability to aid in configuring compact structures, along with tunable features using PIN diodes, are utilized.

7.1 Research Contributions

The research work primarily focuses on the design of a compact reconfigurable microstrip antenna, which is capable of switching the parameters such as frequency, bandwidth, polarization and radiation pattern with considerably high gain. Aim of this work is to integrate all these characteristics into a single, compact, antenna, which should be capable of switching / tuning, the desired characteristics, on the fly, depending upon the application requirements. For this, a reconfigurable microstrip patch antenna is designed, in which the technology of metamaterial / metasurfaces are smartly employed.

- ❖ Antenna is very compact, having size, 40 mm x 40 mm x 1.6mm
- ❖ Antenna is capable of switching and fine tuning between UWB as well as, 36 narrow-band frequencies, which can be used for cognitive radio services.
- ❖ Antenna is capable of reconfiguring the bandwidth of an individual narrow-band, which can be used for cognitive radio services.

- ❖ Antenna is capable of exhibiting circular polarization at designed frequency with reconfigurable sense of LHCP and RHCP.
- ❖ AMC unit cell is very compact of size, 11mm x 11mm x 3.2mm and capable of simultaneously resonating up to 6 bands between 2 to 12 GHz, so that it can be used with multi resonant antennas.
- ❖ AMC unit cell reflection phase at a single frequency, 6 GHz is independently tunable to achieve any phase between -180^0 and $+180^0$, without altering the reflection phase of other frequencies.
- ❖ Antenna is capable of enhancing its gain to about 4.5 dB more, by integrating the metasurface.
- ❖ Antenna is capable of steering the beam using the phase gradient metasurface, designed using the compact reconfigurable AMC unit cell.
- ❖ Antenna beam steering angle can be varied to significantly wide range by tuning the reflection phase of unit cell as well as varying the gap between the antenna and metasurface.

7.2 Scope for Future Work

Due to the rapid increase of communication devices and requirement of high speed communication of bulk data, the future generation of wireless communication requires increased coverage and capacity. This can be achieved by using Advanced Antenna Systems (AAS), which consists of smart/active antenna array and Multiple Input Multiple Output (MIMO) techniques, integrated with hardware and software to achieve adaptability, spatial multiplexing, beam forming and steer-ability. Hence, the future work includes increasing the features of the designed antenna such as incorporating multiband polarization switching agility and tuning of phase gradient metasurface using active elements to enable adaptive beam forming capability for the antenna, which suits for operating frequencies used for cognitive radio, IoT and other 5G applications. Also, applications that uses higher operating frequency bands faces big hurdles in the conventional antenna design methodologies and fabrication techniques, in terms of size and properties of material used for design. Future work can be directed to remove these barriers to realize efficient and compact antennas for the benefit of mankind.

LIST OF PUBLICATIONS BASED ON THESIS

Journals

1) Naveen Jacob, Muralidhar Kulkarni, Krishnamoorthy K., "An Electronically Switchable UWB to Narrow Band Antenna for Cognitive Radio Applications", *Microwave and Optical Technology Letters*, 2020, Vol.62, Issue 9, Pages: 2989-3001, wileyonlinelibrary.com/journal/mop, ©2020 Wiley Periodicals, Inc., DOI:https://doi.org/10.1002/mop.32417

2) Naveen Jacob, Muralidhar Kulkarni, Krishnamoorthy K., "Omega Shaped Complementary Split Ring Resonator Loaded Bandwidth Reconfigurable Antenna for Cognitive Radio Applications", *Elsevier, Science Direct: Procedia Computer Science Journal*, 2020, Vol:171, Pages 1279–1285. DOI:https://doi.org/10.1016/j.procs.2020.04.136

Conferences

1) Naveen Jacob, Prabhanjan Mannari, Krishnamoorthy K. & Muralidhar Kulkarni (2018), "A compact Reconfigurable Penta-Band Artificial Magnetic Conductor for WiFi Applications", *Proceedings of IEEE – INAE Workshop on Electromagnetics (IIWE), Trivandrum, India,* December 2018.

2) Naveen Jacob, Krishnamoorthy K. & Muralidhar Kulkarni (2019), "A Compact Frequency Reconfigurable Antenna for Cognitive Radio Applications", *International Engineering Symposium (IES 2019), Kumamoto University, Japan,* March 2019.

REFERENCES

[1] A. Mansoul, F. Ghanem, Mohamad Rijal & Mohamed Trabelsi (2014), "A Selective Frequency-Reconfigurable Antenna for Cognitive Radio Applications", *IEEE Antennas and Wireless Propagation Letters*, 13, 515-518.

[2] Adeel Afridi, Sadiq Ullah, Imad Ali, Shahbaz Khan and James A. Flint (2014), "Design and Parametric Analysis of a Dual-Band Frequency Reconfigurable Planar Dipole Using a Dual-Band Artificial Ground Plane", *IETE Journal of Research*, 60(1), 3-11.

[3] Adil Zaman Babar and Abdulla Zaman Babar (2017), "Design and Simulation of Dual Band EBG", *IEEE 14th International Bhurban Conference on Applied Science and Technology (IBCAST)*, 727-731.

[4] Ali Mansoul, Farid Ghanem, Mohamed R Hamid, Erkki Salonn & Marcus Berg (2016), "Bandwidth Reconfigurable Antenna with a Fixed Lower and a Variable Upper Limit" *IET Microwaves Antenna and Propagation*, 10(15), 1725–1733.

[5] Amin Tayebi, Junyan Tang, Pavel Roy Paladhi, Lalita Udpa, Sathish S. Udpa and Edward J. Rothwell (2015), "Dynamic Beam Shaping Using a Dual Band Electronically Tunable Reflectarray Antenna", *IEEE Transactions on Antennas and Propagation*, 63(10), 4534-4539.

[6] Ankam Laxman Kumar, Alok Ranjan, Monica Chauhan, Vinay Kumar Killamsetty & Biswajeet Mukherjee (2018), "Circular SRR Shaped UWB Antenna with WiMAX Band Notch Characteristics", *IEEE Radio and Antenna Days of the Indian Ocean (IEEE RADIO 2018)*.

[7] B. Majumder, and J. Mukherjee, K. Krishnamoorthy & K. P. Ray (2017), "A Novel Beam Steering Dipole Antenna using Phase Varying Metasurface as Reflector", *IEEE International Conference on Antenna Innovations & Modern Technologies for Ground, Aircraft and Satellite Applications (iAIM)*.

[8] Basudev Majumder, K. Krishnamoorthy, Jayanta Mukherjee and K. P. Ray (2016), "Frequency Reconfigurable Slot Antenna Enabled by Thin Anisotropic Double Layer Metasurfaces", *IEEE Transactions on Antennas and Propagation*, 63(4), 1218-1225.

[9] Beeresha R. S, A. M. Khan & Manjunath Reddy H. V. (2016), "Design and Optimization of Interdigital Capacitor", *International Journal of Research in Engineering & Technology*, 5(21), 73-78.

[10] Biplab Bag, Priyabrata Biswas, Sushanta Biswas & Partha Pratim Sarkar (2018), "Wide Bandwidth Multifrequency Circularly Polarized Monopole Antenna for Wireless Communication Applications", *International Journal of RF and Microwave Computer-Aided Engineering,* 29(3), 1-11.

[11] Biswajeet Mukherjee, Pragati Patel & Jayanta Mukherjee (2015), "A Novel hemispherical Dielectric Resonator Antenna with Complimentary Split Rings Shaped Slots and Resonator for Wideband and Low Cross-Polar Applications", *IEEE Antenna and Propagation Magazine*, 57(1), 120 – 128.

[12] Boyon Kim, Bo Pan, Symeon Nikolaou, Young-Sik Kim, John Papapolymerou and Manos M. Tentzeris (2008), "A Novel Single-Feed Circular Microstrip Antenna With Reconfigurable Polarization Capability", *IEEE Transactions on Antennas and Propagation*, 56 (3), 630–637.

[13] Bushra Faroq,Tahira Parveen, Imad Ali & Sadiq Ulla (2016), "Antenna Design for Advanced Wireless Systems using Metamaterial Surfaces", *Proceedings of IEEE International Bhurban Conferenceon Applied Sciences and Technology (IBCAST)*, 641-646.

[14] Chao Gu, Benito Sanz Izquierdo, Steven Gao, John C. Batchelor, Edward A. Parker, Fan Qin, Gao Wei, Jianzhou Li, and Jiadong Xu (2017), "Dual-Band Electronically Beam-Switched Antenna Using Slot Active Frequency Selective Surface", *IEEE Transactions on Antennas and Propagation*, 65(3), 1393-1398

[15] Chinmoy Saha & Jawad Y. Siddiqui (2011), "A Comparative Analysis for Split Ring Resonators of Different Geometrical Shapes", *Proceedings of IEEE Applied Electromagnetics Conference (AEMC)*.

[16] Chinmoy Saha & Jawad Y. Siddiqui (2012), "Theoretical Model for Estimation of Resonance Frequency of Rotational Circular Split-Ring Resonators", *Electromagnetics, Taylor & Francis*, 32(6), 345–354.

[17] Chinmoy Saha, Jawad Y. Siddiqui & Yahia M. M. Antar (2011), "Square Split Ring Resonator Backed Coplanar Waveguide for Filter Applications", *XXXth URSI General Assembly and Scientific Symposium, Istambul, Turkey*.

[18] Constantine A. Balanis (2005), "Antenna Theory Analysis and Design", *3rd Edn., John Wiley & Sons Inc*.

[19] D. E. Anagnostou, D. Torres, & N. Sepulveda (2017), "Vanadium Dioxide Switches for a Reconfigurable Bandwidth Antenna", *Proceedings of Loughborough Antennas & Propagation Conference*, IET.

[20] D. Hamzaoui, T. P. Vuong, F. Djahli and G. I. Kianiv (2014), "Novel Compact Dual Band Artificial Magnetic Conductors for Wi-Fi Applications", *IEEE 8th European Conference on Antenna and Propagation (EuCAP)*, 2397-2400.

[21] D. J. Kern, J. A. Bossard and D. H. Verner (2006), "Design of reconfigurable electromagnetic band gap surfaces as artificial magnetic conducting ground planes and absorbers", *IEEE Antennas and Propagation Society International Symposium*, 197-200.

[22] Dan Sievenpiper, Lijun Zhang, Romulo F. Jimenez Broas and Nicholas G. Alexopolous (1999), "High-Impedance Electromagnetic Surfaces with a Forbidden Frequency Band", *IEEE Transactions on Microwave Theory and Techniques*, 47(11), 2059-2074.

[23] Daniel F. Sievenpiper, James H. Schaffner, H. Jae Song, Robert Y. Loo, and Gregory Tangonan (2003), "Two-Dimensional Beam Steering Using an Electrically Tunable Impedance Surface", *IEEE Transactions on Antennas and Propagation*, 51(10), 2713-2722.

[24] Deshuang Zhao, Litao Lan, Yifei Han, Feng Liang, Qiaoli Zhang & Bing-Zhong Wang (2014), "Optically Controlled Reconfigurable Band-Notched UWB Antenna for Cognitive Radio Applications", *IEEE Photonics Technology Letters*, 26(21), 2173–2176.

[25] Dongxu Chen, Wanchen Yang, Wenquan Che, Quan Xue & Lizheng Gu (2019), "Two-Pair Slots Inserted CP Patch Antenna for Wide Axial Ratio Beamwidth", *IEEE Access*, 7, 77792-77803.

[26] Douglas J Kern, Douglas H. Verner, Agostino Monorchio, Luigi Lanussa and Michael J. Wilhelm (2005), "The Design Synthesis of Multiband Artificial Magnetic Conductors Using High Impedance Frequency Selective Surfaces", *IEEE Transactions on Antennas and Propagation*, 53(1), 8-17.

[27] Eko Tjipto Rahardjo, Fitri Yuli Zulkifli & Anne Widiastri (2011), Printed Antenna Design for Cognitive Radio Application at 1.8 GHz and 2.35 GHz Spectrum Allocation", Proceedings of Asia Pacific Microwave Conference, 1881-1884.

[28] Fan Yang & Yahya Rahmat Samii (2009), "Electromagnetic Band Gap Structures in Antenna Engineering", *Cambridge University Press*.

[29] Fan Yang & Yahya Rahmat-Samii (2003), "Reflection Phase Characterizations of the EBG Ground Plane for Low Profile Wire Antenna Applications.", *IEEE Transactions on Antennas and Propagation*, 51(10), 2691-2702

[30] Fan Yang and Yahya Rahmat-Samii (2002), "A Reconfigurable Patch Antenna Using Switchable Slots for Circular Polarization Diversity", *IEEE Microwave and Wireless Components Letters*, 12(3), 96-98.

[31] Farzana Khanam, Sathi Rani Mitra, Md. Asadur Rehman & Md. Selim Hossain (2013), "Design and Performance Analysis of Ultra Wide Band Double Inverted-FL Microstrip Antenna sor WiFi, WLAN, WiMAX and UMTS Applications", in Proc. IEEE International Conference on Electrical Information and Communication Technology (EICT), 1-6.

[32] G. P. Jin, D. L. Zhang & R. L. Li (2011), "Optically Controlled Reconfigurable Antenna for Cognitive Radio Applications", *Electronic Letters*, 47(17), 948-950.

[33] Gary D. Alley (1970), "Interdigital Capacitors and Their Applications to Lumped-Element Microwave Integrated Circuits", *IEEE Transactions on Microwave theory and Techniques*, 18(12), 1028-1033.

[34] Georgina Roses, Roberto Murphy & Wilfrido Moreno (2010), "Smart Antenna using MTMS-MEMS", *IEEE 11th AnnualWireless and Microwave Technology Conference(WAMICON)*, 1-5.

[35] H. Lalj, H. Griguer & M. Drissi (2014), Reconfigurable Multi Band Notches Antenna for Cognitive Radio Applications, *Wireless Engineering & Technology*, 5(3), 99-105.

[36] H. Zahra, S. Rafique, M. Farhan Shafique & Karu P. Esselle (2015), "A Switchable Frequency Selective Surface Based on a Modified Jerusalem-Cross Unit Cell", *IEEE 9th European Conference on Antennas and Propagation (EuCAP)*, 1-2.

[37] Hamid Boudaghi, Mohammadnaghi Azarmanesh & Mehdi Mehranpour (2012), "A Frequency Reconfigurable Monopole Antenna Using Switchable Slotted Ground Structure", *IEEE Antennas and Wireless Propagation Letters*, 11, 655-658.

[38] Harish Rajagopalan, Joshua M. Kovitz & Yahya Rahmat-Samii (2014), "MEMS Reconfigurable Optimized E-Shaped Patch Antenna Design for Cognitive Radio", *IEEE Transactions on Antennas and Propagation*, 62(3), 1056-1064.

[39] Huy Hung Tran, Cong Danh Bui, Nghia Nguyen-Trong & Truong Khang Nguyen (2021), "A Wideband Non-Uniform Metasurface-Based Circularly Polarized Reconfigurable Antenna", *IEEE Access*, 9, 42326-42332.

[40] J. D. Baena, J. Bonache, F. Martin, R. M. Sillero, F. Falcone, T. Lopetegi, M. A. G. Laso, J. Garcia-Garcia, I. Gil, M. F. Portillo & M. Sorolla (2005), "Equivalent-Circuit Models for Split-Ring Resonators and Complementary Split-Ring Resonators Coupled to Planar Transmission Lines", *IEEE Transactions on Microwave Theory and Techniques*, 53(4), 1451–1461.

[41] James R. Kelly & Peter S. Hall (2010), "Integrated Wide-Narrow Band Antenna for Switched Operation", *Microwave & Optical Technology Letters*, 52(8), 1705-1707.

[42] Jawad Yaseen Siddiqui, Chinmoy Saha & Yahia M. M. Antar (2014), "Compact SRR Loaded UWB Circular Monopole Antenna With Frequency Notch Characteristics", *IEEE Transactions on Antennas and Propagation*, 62(8), 4015–4020.

[43] Jiaqing Chen , Yongjiu Zhao, Lei Xing, Huijuan Dai, Xiaofeng Chen, Yue Ge (2019), "Dual-Band Reflected Beam Steering with Single-Layered Focusing Anisotropic Metasurface", *IET Microwaves, Antennas and Propagation*, 13(9), 1498-1502.

[44] K. C. Gupta (1988), "Broadbanding Techniques for Microstrip Patch Antennas - A Review", *Scientific Report, University of Colorado*.

[45] K. K. A. Devi, Ng Chun Hau, C. K. Chakrabarty & Norashidah Md. Din (2014), "Design of Patch Antenna using Metamaterial at GSM1800 for RF Energy Scavenging", *Proceedings of IEEE Asia Pacific Conference on Wireless and Mobile*, 157-161.

[46] K. Kandasamy, B. Majumdaar, J. Mukherjee & K. P. Ray (2015), "Low-RCS and Polarisation-Reconfigurable Antenna using Cross-Slot-Based Metamaterial", *IEEE Transactions on Wireless Propagation*, 14, 1638-1641.

[47] K. Kandasamy, B. Majumder & J. Mukherjee (2015), "Design of SRR Loaded Reconfigurable Antenna for UWB and Narrow Band", *IEEE International Symposium on Antennas and Propagation & USNC/URSI National Radio Science Meeting*, 1192-1193.

[48] K. Kandasamy, B.Majumder, J.Mukherjee & K. P. Ray (2015), "Beam-Tilted and Wide Beam Antennas using Hybrid Electromagnetic Band Gap Structures", *Proceedings of the 45th European Microwave Conference*.

[49] Kin-Fai Tong and Ting-Pong Wong (2007), "Circularly Polarized U-Slot Antenna", *IEEE Transactions on Antennas and Propagation*, 55(8), 2382–2385.

[50] Krishnamoorthy Kandasamy, Basudev Majumder, Jayanta Mukherjee & Kamla Prasan Ray (2016), "Dual-Band Circularly Polarized Split Ring Resonators Loaded Square Slot Antenna", *IEEE Transactions on Antennas and Propagation*, 64(8), 3640–3645.

[51] Krishnamoorthy Kandasamy, Basudev Majumder, Jayanta Mukherjee, and K. P. Ray (2014), "A Circular Polarization Reconfigurable Antenna Based on Reconfigurable Electromagnetic Band-Gap Structures", IEEE *8th International Congress on Advanced Electromagnetic materialsin Microwaves and Optics, Copenhagen, Denmark*.

[52] Linglong Meng, Weimin Wang, Jinchun Gao & Yuanan Liu (2017), "Bandwidth Reconfigurable Antenna with Three Step-Shaped Slots", *Proceedings of IEEE 6th Asia-Pacific Conference on Antennas and Propagation*.

[53] Liping Han, Gen Cheng, Guorui Han, Runbo Ma, and Wenmei Zhang (2019) "Electronically Beam-Steering Antenna With Active Frequency-Selective Surface", *IEEE Transactions on Antennas and Propagation*, 18(1) , 108-112.

[54] Lu-Yang Ji , Zhi-Ya Zhang and Neng-Wu Liu (2019), "A Two-Dimensional Beam-Steering Partially Reflective Surface Antenna Using a Reconfigurable FSS Structure", *IEEE Antennas and Wireless Propagation Letters*, 18(6), 1076-1080.

[55] M. Abu, M. K. A. Rahim, O. Ayop and F. Zubir (2011), "Design of Tripple-Band Dipole-Type Antenna with Dual-Band Artificial Magnetic Conductor Structure", *IEEE 5th European Conference on Antennas and Propagation (EUCAP)*, 1514-1517.

[56] M. Ameen, O. Ahmad & R.K. Chaudhary (2019), "Wideband Circularly-Polarised "High-Gain Diversity Antenna Loaded with Metasurface Reflector for Small Satellite Applications", *Electronic Letters*, 55(15), 829-831.

[57] M. Karmugil and K. Anusudha (2016), "Design of Circular Microstrip Antenna for Ultra Wide Band Applications", *IEEE International Conference on Control, Instrumentation, Communication and Computational Technologies*, 304-308.

[58] Mahmoud Niroo-Jazi and Tayeb A. Denidni (2011), "Reconfigurable Dual Band Frequency Selective Surfaces Using a New Hybrid Element", *Proceedings of IEEE International Symposium on Antennas and Propagation (APSURSI)*, 2673-2676.

[59] Mandana Mehrparvar & Farrokh Hodjat Kashani (2012), "Microstrip Antenna Miniaturization using Metamaterial Structures", *Proceedings of IEEE Iranian Conference on Electrical Engineering (ICEE)*, 1243–1246.

[60] Mansour Nejatijahromi, Mahdi Naghshvarianjahromi & Muhib Ur Rahman (2018), "Switchable Planar Monopole Antenna Between Ultra-Wideband and Narrow Band Behavior", *Progress in Electromagnetics Research Letters*, 75, 131-137.

[61] Minakshi Tewari, Ajay Yagav & R. P. Yadav (2016), "Frequency Reconfigurable Antenna: Using Pixel Ground", *Proceedings of IEEE International Conference on Recent Advances and Innovations in Engineering (ICRAIE)*, 1-6.

[62] Mohamed Alibakshi-Kenari, Mohamed Naser-Moghadasi & R. A. Sadeghzadeh (2015), "Bandwidth and Radiation Specifications Enhancement of Monopole Antennas Loaded with Split Ring Resonators", *IET Microwaves Antenna and Propagation*, 9(14), 1487–1496.

[63] Moufida Bouslama, Ali Gharssalah, Moubarek Traii and Tayeb Denidni (2015), "Reconfigurable New Unit Cell Frequency Selective Surface for Beam Switching Applications", *IEEE 5th National Symposium on Information Technology: Towards New Smart World*, 1-4.

[64] Muhammed Umar Khan, Muhammad Said Sharavi & Raj Mittra (2015), "Microstrip Patch Antenna Miniaturization Techniques:A Review", *IET Microwaves, Antenna & Propagation*, 9(9), 913-922.

[65] N.A. Abbasi & R.J. Langley (2010) "Multiband-Integrated Antenna/Artificial Magnetic Conductor", *IET Microwaves, Antennas & Propagation*, 5(6), 711-717.

[66] Nader Behdad & Kamal Sarabandi (2004), "Bandwidth Enhancement and Further Size Reduction of a Class of Miniaturized Slot Antennas", *IEEE Transactions on Antennas and Propagation*, 52 (8), 1928–1935.

[67] Nader Engetha & Richard W. Ziolkowski (2006), "Metamaterials – Physics and Engineering Explorations", *John Wiley & Sons Inc*.

[68] Ning Liu, Xianjun Sheng, Jingjing Fan, Yongquing Wang and Dongming Guo (2017), "Reconfigurable Frequency Selective Surface with multiband characteristic", *IEEE International Conference on Electromagnetics in Advanced Applications (ICEAA)*, 897-899.

[69] Paritosh Peshwe and Ashwin Kothari (2018), "Performance Enhancement of Millimeter Wave Antenna with Integrated Inter-Digital Capacitor Structure", *Radio Engineering*, 27(3), 651-661.

[70] Pei-Yuan Qin, Andrew R. Weily, Y. Jay Guo, and Chang-Hong Liang (2010) "Polarization Reconfigurable U-Slot Patch Antenna", *IEEE Transactions on Antennas and Propagation*, 58 (10), 3383-3388.

[71] Pratap N. Shinde & Jayashree P. Shinde (2015), "Design of Compact Pentagonal Slot Antenna with Bandwidth Enhancement for Multiband Wireless Applications", *International Journal of Electronics & Communication (AEU)*, 68-71.

[72] Princy Maria Paul, Krishnamoorthy Kandasamy and Mohammad S. Sharawi (2017), "A Tri-Band Slot Antenna oaded with Split Ring Resoators ", *Microwave and Optical Technology Letters*, 59(10), 2638-2643.

[73] Princy M. Paul, Krishnamoorthy Kandasamy and Mohammad S. Sharawi (2019), "A Corner Expanded Slot Antenna Loaded with Copper Strips for Dual-Band Circular Polarization Characteristics", *Microwave and Optical Technology Letters*, 62(1), 491 – 497.

[74] Princy Maria Paul, Krishnamoorthy Kandasamy and Mohammad S. Sharawi (2018), "A Triband Circularly Polarized Strip and SRR-Loaded Slot Antenna", *IEEE Transactions on Antennas and Propagation*, 66(10), 5569-5573.

[75] Princy Maria Paul, Krishnamoorthy Kandasamy and Mohammad S. Sharawi (2020), "A Multi-Band U-Strip and SRR Loaded Slot Antenna withCircular Polarization Characteristics", *Advanced Electromagnetics*, 9(1), 41-48.

[76] Puneeth Kumar Tharehalli Rajanna et al. (2019), "Compact triband circularly polarized planar slot antenna loaded with split ring resonators", *International Journal of RF and Microwave Computetr Aided Engineering*, 29(12), 1-9.

[77] Puneeth Kumar, Tharehalli Rajanna, Karthik Rudramuni, Krishnamoorthy Kandasamy (2019), "A Wideband Circularly Polarized Slot Antenna Backed by a Frequency Selective Surface", *Journal of Electromagnetic Engineering and Science*, 19(3), 166-171.

[78] Puneeth Kumar T. R, Karthik R., Krishnamoorthy K. (2020), "Compact Wideband Circularly Polarized SRR Loaded Slot Antenna for Soil MoistureSensor Application", *Microwave Review*, 26(2), 8-13.

[79] R. Saad and K. L. Ford (2012), "Miniaturized Dual-Band Artificial Magnetic Conductor with Reduced Mutual Coupling", *Electronic Letters*, 48(8).

[80] Rajni & Anupma Marwaha (2016) "An Accurate Approach of Mathematical Modelling of SRR and SR for Metamaterials", *Journal of Engineering Science and Technology Review*, 9 (6), 82–86

[81] Reshmi Dhara (2021) "A Compact Dual Band Dual Polarized Monopole Antenna with Enhanced Bandwidth for C, X, and Ku Band Applications", *Progress In Electromagnetics Research Letters*, 96, 65–72.

[82] S. F. Shi, B. Zeng, H. L. Han, X. Hong. H. Z. Tsai, H. S. Jung, A. Zettl, M. F. Crommie & F. Wang (2015), "Optimising Broadband Tera Hertz Modulation with

Hybrid Graphine/Metasurface Structures", *Nano Letters, ACS Publication*, 372-377.

[83] Sarang Patil & Vandana Rohokale(2015), "Multiband Smart Fractal Antenna Design for Converged 5G Wireless Networks", *Proceedings of IEEE International Conference on Pervasive Computing (ICPC)*, 1-5.

[84] Sarin V. Pushpakaran, Rohit K. Raj, Vineah P. V., Dinesh R., P. Mohanan & K. Vasudevan (2014), "A Metaresonator Inspired Dual Band Antenna for Wireless Applications", *IEEE Transactions on Antenna and Propagation*, 62(4), 2287-2291.

[85] Sasmita Pahadsingh, Sudhakar Sahu and Satyadeep Das (2017), "Compact Ultrawideband-Reconfigurable Antenna for Cognitive Radio Platforms", *Proceedings of IEEE International Conference on Wireless Communications, Signal Processing and Networking (WiSPNET)*, 2735–2738.

[86] Soumik Dey, Ankita Indu, Santanu Mondal, Partha P. Sarkar (2020), "Diagonalliy Asymetric CSRRs Loaded Circularly Polarized Antenna with Frequency Selective Surface", *Progress in Electromagnetic Research*, 92, 43-54.

[87] Tu Tuan Le , Han-Young Park and Tae-Yeoul Yun (2019), "Simple Reconfigurable Circularly Polarized Antenna at Three Bands", *Sensors*, 19(10), 2316-2328.

[88] Tu Tuan Le and Tae-Yeoul Yun (2019) "A Quad-Band Dual-Sense Circularly-Polarized Square-Ring Antenna for Multi-Functional Wireless Applications", *IEEE Access*, 7, 149634 – 149640.

[89] Venkateshwar V. Reddy and N. V. S. N. Sarma (2015), "Reconfigurable Koch Antenna for GSM/WI-FI Applications", *Microwave and Optical Technology Letters*, 57(12), 2895-2898.

[90] Vivek Kumar Pandit and A. R. Harish (2016), "Design of Dual Band CPW-Fed Monopole Antenna with Dual Band AMC Surface for WLAN", *IEEE Annual India Conference (INDICON)*, 1-4.

[91] Weiping Cao, Beibei Li, L. Shafai, Simin Li, Xi Gao & Xinhua Yu (2015), "A Smart Antenna Based on Metamaterial", *Procedimgs of IEEE International Symposium on Antennas and Propagation & UNSNC/URSI National Radio Science Meeting*, 2301-2302.

[92] Weiyang Yin, Hou Zang, Tao Zhong and Xueliang Min (2018), "A Novel Compact Dual Band Frequency Selective Surface for GSM Shielding by Utilizing a 2.5-Dimensional Structure", *IEEE Transactions on Electromagnetic Compatibility*, 60(6), 2057-2060.

[93] Xue-Xia Yang, Bing Cheng Shao, Fan Yang, Atef Z. Elsherbeni and Bo Gong (2012), "A Polarization Reconfigurable Patch Antenna with Loop Slots on the Ground Plane", *IEEE Antennas and Wireless Propagation Letters*, 11, 69-72.

[94] Y. M. Pan, P. F. Hu, X. Y. Zhang & S. Y. Zeng (2016), "A Low-Profile High-Gain and Wideband Filtering Antenna with Metasurface", *IEEE Transactions on Antennas and Propagation*, 64(5), 68-71.

[95] Y. Tawk, J. Constantine, K. Avery & C. G. Christodoulou (2011), Implementation of a Cognitive Radio Front-End Using Rotatable Controlled Reconfigurable Antennas, *IEEE Transactions on Antenna and Propagation*, 59(5), 1773-1778.

[96] Yeu Li, Zhijun Zhang, Jianfeng Zheng & Zhenghe Feng (2011), "Compact Heptaband Reconfigurable Loop Antenna for Mobile Handset", *IEEE Antennas and Propagation Letters*, 10, 1162–1165.

[97] Yuandan Dong & Tatsuo Itoh (2012), "Metamaterial Based Antennas", *Proceedings of the IEEE*, 100(7), 2271-2285.

[98] Yun Fei Cao, and Xiu Yin Zhang (2018), "A Wideband Beam-Steerable Slot Antenna Using Artificial Magnetic Conductors With Simple Structure", *IEEE Transactions on Antennas and Propagation*, 66(4), 1685-1694.

[99] Z. H. Hu, C. T. P. Song, J. Kelley, P. S. Hall & P. Gardner (2009), "Wide Tunable Dual Band Reconfigurable Antenna", *Electronic Letters*, 45 (22), 1109-1110.

[100] Zi-Xian Yang, Hong-Chun Yang, Jing-Song Hong & Yang Li (2014), "Bandwidth Enhancement of a Polarization-Reconfigurable Patch Antenna With Stair-Slots on the Ground", *IEEE Antennas and Wireless Propagation Letters*, 13, 579-582.

CURRICULUM VITAE

Name : Naveen Jacob

Address : Vadakkemuttappillil House,

Near KSRTC Bus Stand,

Muvattupuzha P. O.,

Kerala – 686661.

Email : naveenjacob@yahoo.com

Phone : 9947679397

Qualification : 1) M. Tech (Communication Engineering) – National Institute of Technology Karnataka, Surathkal, 2009.

2) B.Tech (Elecetronics & Communication Engineering) – Mar Athanasius College of Engineering, Kerala, 1999.

Experience : Associate Professor, Department of Electronics & Communiacation Engineering, Viswajyothi College of Engineering & Technology, Vazhakulam, Kerala. (29-01-2003 to till date).